AD-A038 724 STATE UNIV OF NEW YORK AT BUFFALO DEPT OF ELECTRICAL --ETC F/G 10/2
HIGH POWER STUDY - POWER CONDITIONING.(U)
JAN 76 A S GILMOUR F30602-75-C-0122

UNCLASSIFIED AFAPL-TR-76-101 NL

1 OF 2
AD A038724



AD A038724

AFAPL-TR-76-101

HIGH POWER STUDY - POWER CO

DEPARTMENT OF ELECTRICAL ENGINEERING
STATE UNIVERSITY OF NEW YORK AT BUFFALO,
BUFFALO, NY 14226

AU NO.
DDC FILE COPY

JANUARY 1976

TECHNICAL REPORT AFAPL-TR-76-101
FINAL REPORT FOR PERIOD JUNE 75 - JANUARY 76

Approved for public release; distribution unlimite

AIR FORCE AERO-PROPULSION LABORATORY
AIR FORCE WRIGHT AERONAUTICAL LABORATORIES
AIR FORCE SYSTEMS COMMAND
WRIGHT-PATTERSON AIR FORCE BASE, OHIO 45433

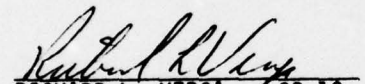
NOTICE

When Government drawings, specifications, or other data are used for any purpose other than in connection with a definitely related Government procurement operation, the United States Government thereby incurs no responsibility nor any obligation whatsoever; and the fact that the Government may have formulated, furnished, or in any way supplied the said drawings, specifications, or other data, is not to be regarded by implication or otherwise as in any manner licensing the holder or any other person or corporation, or conveying any rights or permission to manufacture, use, or sell any patented invention that may be related thereto.

This final report was submitted by the Department of Electrical Engineering of the State University of New York at Buffalo, under Contract F30602-75-C-0122. The effort was sponsored by the Air Force Aero-Propulsion Laboratory, Air Force Systems Command, Wright-Patterson AFB, Ohio under Project 3145, Task 32, and Work Unit 39 with Mr. Richard L. Verga, AFAPL/POD-1 as project engineer. Dr. A. S. Gilmour, Jr., of the Department of Electrical Engineering at the State University of New York at Buffalo was technically responsible for the work.

This report has been reviewed by the Information Office (ASD/OIP) and is releasable to the National Technical Information Service (NTIS). At NTIS, it will be available to the general public, including foreign nations.

This technical report has been reviewed and is approved for publication.



RICHARD L. VERGA / GS-13
Project Engineer

FOR THE COMMANDER



PHILIP E. STOVER
Chief, High Power Branch

Copies of this report should not be returned unless return is required by security considerations, contractual obligations, or notice on a specific document.

AIR FORCE - 16 MARCH 77 - 225

UNCLASSIFIED

SECURITY CLASSIFICATION OF THIS PAGE *(When Data Entered)*

REPORT DOCUMENTATION PAGE

READ INSTRUCTIONS BEFORE COMPLETING FORM

1. REPORT NUMBER: AFAPL-TR-76-101	2. GOVT ACCESSION NO.
3. RECIPIENT'S CATALOG NUMBER	
4. TITLE *(and Subtitle)*: HIGH POWER STUDY - POWER CONDITIONING	5. TYPE OF REPORT & PERIOD COVERED: FINAL REPORT Jun 75 - Jan 76
6. PERFORMING ORG. REPORT NUMBER	
7. AUTHOR(s): A. S. Gilmour, Jr	8. CONTRACT OR GRANT NUMBER(s): F30602-75-C-0122
9. PERFORMING ORGANIZATION NAME AND ADDRESS: Department of Electrical Engineering, State University of New York at Buffalo, 4232 Ridge Lea Rd. Buffalo NY 14226	10. PROGRAM ELEMENT, PROJECT, TASK AREA & WORK UNIT NUMBERS: Program Element 62203F, Project/Task 31453239
11. CONTROLLING OFFICE NAME AND ADDRESS: Air Force Aero-Propulsion Laboratory, Wright-Patterson Air Force Base OH 45433	12. REPORT DATE: Jan 1976
	13. NUMBER OF PAGES: 183
14. MONITORING AGENCY NAME & ADDRESS *(if different from Controlling Office)*: 3145 32	15. SECURITY CLASS. *(of this report)*: UNCLASSIFIED
	15a. DECLASSIFICATION/DOWNGRADING SCHEDULE

16. DISTRIBUTION STATEMENT *(of this Report)*

Approved for public release; distribution unlimited

174 p.

17. DISTRIBUTION STATEMENT *(of the abstract entered in Block 20, if different from Report)*

18. SUPPLEMENTARY NOTES

19. KEY WORDS *(Continue on reverse side if necessary and identify by block number)*

Power Conditioning	Transformers
High Power	Solid State Switches
Inverter	Capacitors
Converter	Inductors
Light Weight Components	Adiabatic Components

20. ABSTRACT *(Continue on reverse side if necessary and identify by block number)*

This paper summarizes the power conditioning portion of the high power study that was performed for the Air Force Aero-Propulsion Laboratory by the State University of New York at Buffalo. This effort defines the power conditioning system and critical component developments which will be required to interface the airborne 10 MW to 50 MW sources defined under separate study efforts with certain loads. Power conditioning systems are considered for use with magnetohydrodynamic generators and turbine driven alternators, both conventional and superconducting. The critical components required for each of the

DD FORM 1 JAN 73 1473 EDITION OF 1 NOV 65 IS OBSOLETE

UNCLASSIFIED

SECURITY CLASSIFICATION OF THIS PAGE *(When Data Entered)*

470 160

power conditioning systems are identified and then analyzed. The component analyses include estimations of development efforts necessary and of specific weights and volumes of components. The primary components considered are transformers (for alternator as well as for inverter use), switches, capacitors and inductors. Weight algorithms are developed for each of the components. Following the component analyses, subsystems such as inverters and rectifier and filter packages are considered. The data for the various components and subsystems are then utilized for a comparison of the power conditioning techniques to be used with the various power sources. The weights and volumes of power conditioning systems for 8 point designs (8 variations of power, voltage, duty cycle and total run time) are derived. Finally a development program is outlined for the critical components and subsystems.

PREFACE

In the course of performing this study, it was necessary to interact with and obtain information from a large number of individuals and organizations. In particular, the assistance of Dr. D. L. Lockwood and Mr. R. McNall of Thermal Technology Laboratory, Inc. and of Dr. Francisc C. Schwarz of Power Electronics Associates, Inc. are greatly appreciated. Significant discussions are also acknowledged with personnel from Maxwell Laboratories Inc., Capacitor Specialists Inc., Component Research, Inc., Westinghouse, General Electric, Westcode, Rocketdyne, Garrett and International Rectifier. Throughout the course of this study, guidance and assistance was provided by personnel from the Air Force Aero-Propulsion Laboratory of the Air Force Systems Command, Wright Patterson Air Force Base, Ohio.

ACCESSION for
NTIS White Section
DDC Buff Section
UNANNOUNCED
JUSTIFICATION
BY
DISTRIBUTION/AVAILABILITY CODES
Dist. AVAIL. and/or SPECIAL
A

CONTENTS

		Page
I.	INTRODUCTION	1-1
II.	IDENTIFICATION OF POWER CONDITIONING TECHNIQUES	
	A. Alternator Power Source	2-1
	B. MHD Power Source	2-3
	C. Pulsed Load	2-5
III.	IDENTIFICATION OF CRITICAL COMPONENTS	3-1
IV.	CRITICAL COMPONENT ANALYSIS	
	A. Transformers	4-1
	1. Alternator Transformers	4-2
	2. Inverter Transformers	4-9
	B. Switches	
	1. Solid State	4-13
	2. Vacuum Arc	4-19
	C. Capacitors	
	1. Filter Capacitors	4-21
	2. Inverter Capacitors	4-21
	D. Inductors	4-30
V.	SUBSYSTEM ANALYSIS	
	A. Inverter	5-1
	B. Rectifier and Filter	5-6
	1. Alternator Power Rectification	5-6
	2. L-C Filter Analysis	5-7

		Page
	3. Inverter Power Rectification	5-13
	4. π Filter Analysis	5-19
	C. Load Protection	5-23
VI.	ANALYSIS AND COMPARISON OF POWER CONDITIONING TECHNIQUES	
	A. Algorithm Compilation	6-1
	B. Computer Program	6-9
	C. Results	6-23
VII.	RECOMMENDED DEVELOPMENT PROGRAM	
	A. Transformers	7-1
	B. Switches	7-1
	C. Capacitors	7-2
	D. Inverters	7-2
VIII.	SUMMARY	8-1
IX.	REFERENCES	9-1
X.	APPENDICES	
	A. Point Design Analysis of a DC-DC Converter	10-1
	B. Transformer Design Program	10-30
	C. Full-Wave Three-Phase Rectifier Voltage Waveforms	10-46
	D. The Interruption of Vacuum Arcs at High DC Voltages	10-55

I. INTRODUCTION

The following Statement of Work for the power conditioning effort of the High Power Study was provided at the outset of the study by AFAPL. This Statement of Work serves as an appropriate introduction for this report.

STATEMENT OF WORK
HIGH POWER STUDY - POWER CONDITIONING

1. GENERAL

The purpose of this effort is to define the power conditioning system and critical component developments which will be required to interface the power sources being defined under separate study efforts with certain loads. The power sources being considered are magnetohydrodynamic generators and turbine driven alternators, both conventional and superconducting. Although the power source studies are being tasked to produce point designs, no such requirement is imposed for this study. The load the power conditioning must interface with is not well defined and therefore a range of load parameters will be investigated. For purposes of this study, the load will either be continuous during the running time or will be pulsed at a 5 kHz to 10 kHz rate with a 15% duty cycle. The load is assumed to be self switched. This study shall provide the Air Force with technical information to make a decision on the type of systems to be considered in a subsequent system analysis, design, and critical component development program.

There are two general types of parameters to be considered:

a. External Parameters

Those which must be provided to a designer in numerical form in order for him to design a suitable system (e.g., input power, input voltage, frequency).

b. Internal Parameters

Those which must be selected by a designer in the course of his design activities, and which must be described numerically but are not of essential importance to a system integrator (e.g., conversion frequency, secondary voltages).

The general procedure to be followed in these studies is to treat weight and volume as dependent variables and to treat the external parameters and selected internal parameters as independent variables.

The contractor shall analyze possible power conditioning systems to identify all important internal parameters, and a final selection of internal parameters to be used in the study will be made at the working session. A simple computer program shall be written which will calculate the weight and volume of the power conditioning system.

This study and the power sources studies must address a compatible set of parameters. To insure this compatibility, two coordination meetings of all contractors and the Air Force will be held. The first will be an orientation briefing, scheduled as soon as practical after contract award (6 June 1975). The second will be a working session held approximately four weeks later (2 July 1975), at which time each contractor will suggest any revisions he deems appropriate to the lists of parameters and to the study structure.

2. EXTERNAL PARAMETERS

In performing the parametric analysis, the contractor shall, as a minimum, determine the dependence of weight and volume on the following quantitative external parameters: power, input voltage, output voltage, input frequency, run time, duty cycle, regulation, and efficiency. Where a range is given in Table 1 for a parameter, the dependence over the entire range will be determined. For the remaining parameters, the contractor shall choose a range appropriate to the type of power conditioning system being considered. In addition, the contractor shall identify and include any additional parameters he deems important to the system. The study may be truncated to exclude any systems for which the power conditioning specific weight exceeds 1 pound per kilowatt of average power. The following external parameters are not necessarily quantitative but are of significant importance in assessing the advisability of system development. The contractor shall treat each of the following parameters as appropriate for each type of power conditioning system being considered and shall assess each relative to its impact on the system: physical configuration, reliability, control, protection (load and source), logistics support, complexity, sophistication, expendables, cost (development, initial, unit, life cycle) installation characteristics, flexibility, efficiency characteristics, thermal characteristics (cooling and heating requirements), safety, electromagnetic compatibility, development confidence, altitude effects, orientation limitations (if any), temperature, maintenance (repair and replacement), noise (acoustic), emissions, "g" loading.

3. INTERNAL PARAMETERS

There are certain internal parameters that the designer must fix for a given power conditioning system configuration; the more important of these shall be included as parameters in the study. These principal internal parameters for the power conditioning system include but are not limited to:

conversion frequency, number of transformer primaries and secondaries, primary and secondary voltages, rectifier and switch module P.I.V., switch control power requirements.

4. ANALYSIS TASKS

The analysis of the power conditioning system can be subdivided into three tasks. The parameter ranges from Table 1 will be used in the performance of these tasks.

a. The first of these tasks is the analysis of the transformer. Two types shall be considered; polyphase sinusoidal and inverter. Various tradeoffs between the transformer and the rest of the system shall be performed. For example, can rectifier weight be minimized by using multiple secondaries on the transformer, thus obviating the need for rectifier balancing networks without sacrificing transformer efficiency and specific weight.

b. In the second task, the contractor shall analyze the switching technique appropriate for the cases in which an inverter is applicable, and the rectification technique in all cases. Any necessary controls for the switches and rectifiers as well as filters shall be considered. It is most important that the availability of required switches be treated in detail.

c. In the third task, the contractor shall examine the various power conditioning techniques and determine their areas of applicability within the parameter ranges in Table 1. For example, one might consider immediate rectification of the alternator output with subsequent chopping at a relatively high frequency followed by voltage adjustment, rerectification, filtering, regulation, etc. A simple algorithm computer program will be written to permit weight and volume to be calculated as a function of the important parameters.

TABLE 1

SYSTEMS PARAMETERS

PARAMETER	UNITS	RANGE
Power	MWE	10-50
Voltage	KV	20-250
Duty Cycle		
On Time	Sec	1-120
Off Time		2-300
No. of Cycles/Mission		
Total Run Time	Sec	30-120
Start-Up Time	Sec	
Idle Time	Min	5-120

NOTE 1: The subsystem shall be designed for a 100 mission life (total life - 100 x number of cycles above).

NOTE 2: Electrical sources shall be designed to produce 60 KV, if possible. If the source cannot achieve 60 KV directly, design for minimum weight and volume regardless of voltage.

Although point designs were excluded in the above Statement of Work, these were later requested as listed in Table II during the course of the study.

The parameter lists provided by AFAPL in the Statement of Work were found to be very nearly complete. Only one additional external parameter is suggested and that is the ripple percentage that can be tolerated in the load voltage. Additional internal parameters that have been considered are interconnection techniques, harmonic effects, heat distribution and the packaging techniques for the switches and rectifiers.

TABLE II

SUBSYSTEM PARAMETERS

PARAMETER	UNITS	RANGE	1	2	3	4	5	6	7	8
Power	MWE	10-50	10	10	25	25	25	25	50	50
Voltage	KV	20-250	60	60	60	60	60	60	200	200
Duty Cycle										
On Time	Sec	1-120	21	21	4	120	21	21	25	12
Off Time		2-300	30	300	4	N/A	30	300	N/A	78
No. of Cycles/Mission			3	3	16	1	3	3	3	10
Total Run Time	Sec	30-120	63	63	64	120	63	63	75	120
Start-Up Time	Sec		1	1	1	1	1	1	1	1
Idle Time	Min	5-120	0	0	0	0	0	0	0	0

NOTE 1: The subsystem shall be designed for a 100 mission life(total life = 100 x number of cycles above).

NOTE 2: Electrical sources shall be designed to produce 60 KV directly, design for minimum weight and volume regardless of voltage.

NOTE 3: The subsystem shall be designed for 1 second start-up time, if possible. If one second start-up is not possible, design for minimum start-up time. If start-up time is greater than 3 seconds, provide for 10 minutes idle.

II. IDENTIFICATION OF POWER CONDITIONING TECHNIQUES

During the course of this study, analyses have been performed that permit the evaluation of power conditioning techniques that may be used with ac or with dc power sources. Both continuous loads and loads pulsed at a 5 kHz to 10 kHz rate with a 15% duty cycle have been considered. In addition, the power conditioning techniques that might be used with an auxiliary load requiring an order of magnitude less power than the primary load have been analyzed. The particular power conditioning techniques that have been considered are classified according to the type of power source (alternator or MHD) and are as follows:

A. Alternator Power Source

Shown in Figure 2-1 are the various power conditioning techniques that have been evaluated for use with an alternator power source. The symbols used in Figure 2-1 have the meanings listed below:

ALT	alternator
R & F	rectifier and filter
T	transformer
I	inverter
LP	load protection device
AUX	auxiliary load

The various techniques shown in Figure 2-1 are described in the following paragraphs.

In the first technique, the output from a high voltage alternator is rectified and filtered for direct application to the load. Although no information has been provided concerning the load protection that may be required in case of a load fault, it is probable that some sort of a load protection device will be required. Load regulation, switching, etc. could be accomplished by using thyristors in the rectifier and controlling their conduction time.

In the second technique, one or more transformers are used to boost the voltage output of a relatively low voltage alternator. The output of the transformer is rectified and filtered and the required load protection is provided.

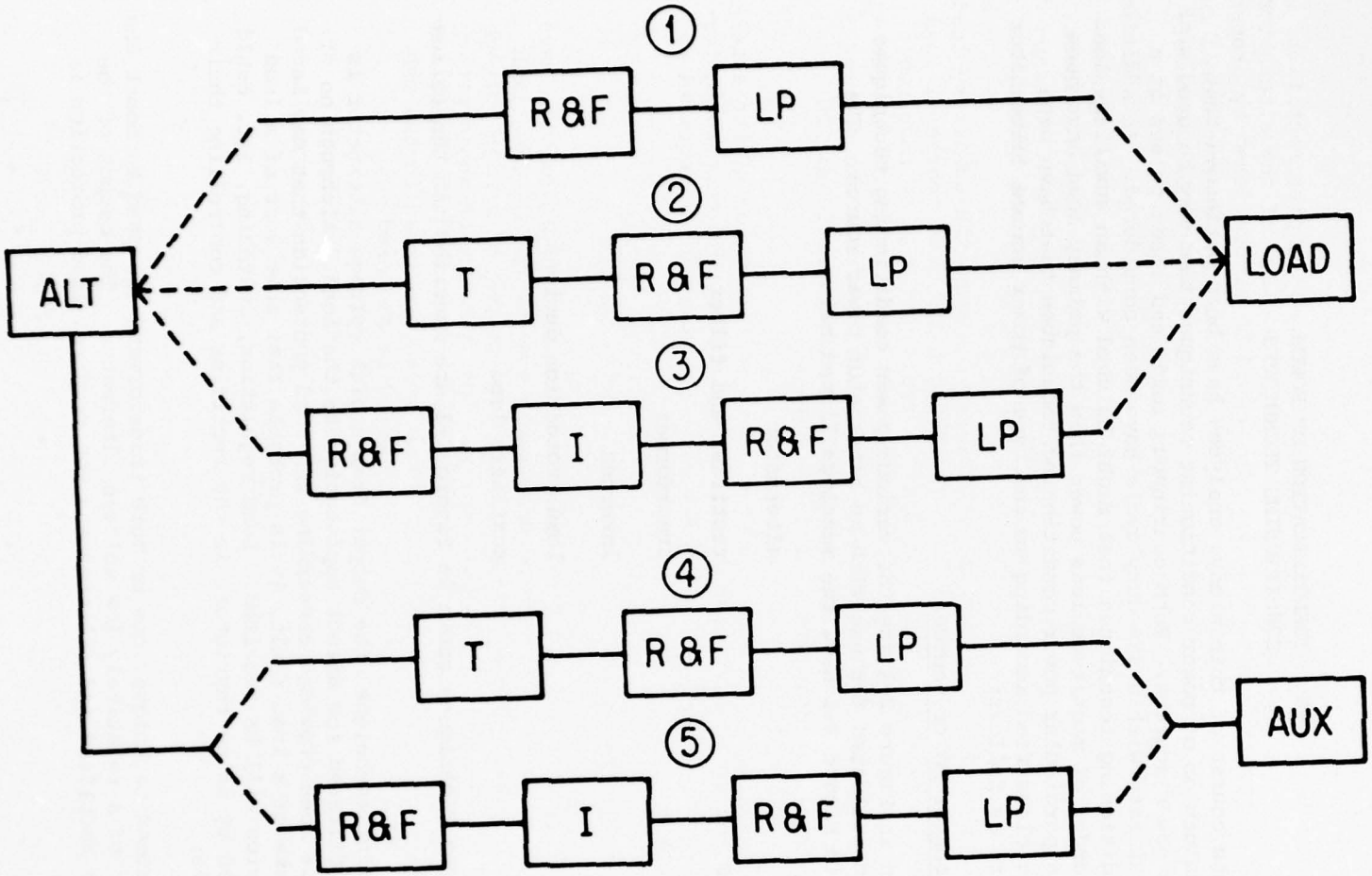


Figure 2-1 Power conditioning techniques considered for use with an alternator power source and a continuous load.

In the third technique, a dc to dc converter (inverter plus rectifier and filter) is used to step up the rectified output voltage of the alternator. In this case load regulation, switching, etc. could be accomplished by proper control of the inverter. At high inversion frequencies, the energy stored in the inverter output filter would be relatively small and there is the possibility that no load protection device would be required.

The fourth and fifth techniques would be used at a power level approximately an order of magnitude below the second and third techniques. There may also be differences in the degree of load protection required. Conceptually however techniques four and five are identical to two and three.

It should be pointed out that if the primary load and the auxiliary load can both be operated at the same voltage level, with the same degree of load regulation, then techniques 2 and 4 or 3 and 5 could probably be combined. There may also be the possibility of combining some but not all of the functions of techniques 2 and 4 or 3 and 5. For example, a single transformer could be used to drive two separate rectifier and filter sections. This would permit independent regulation of the two loads.

The powering of the auxiliary load by direct rectification of the alternator output is not shown in Figure 2-1 because it is assumed that the alternator will not be capable of producing the 200 KV voltage level required by the auxiliary load.

B. MHD Power Source

Shown in Figure 2-2 are the power conditioning techniques that have been evaluated for use with a magnetohydrodynamic power source. The sixth technique is conceptually the simplest of all. The output of a high voltage MHD source is used to power the load directly. Load protection would probably be required. Also, a switch would probably be required to connect and disconnect the load. If load regulation cannot be accomplished in the MHD source, then an additional regulation device would be required.

In the seventh and eighth techniques direct dc to dc conversion of the MHD output is performed. Regulation and switching would be accomplished by controlling the inverter.

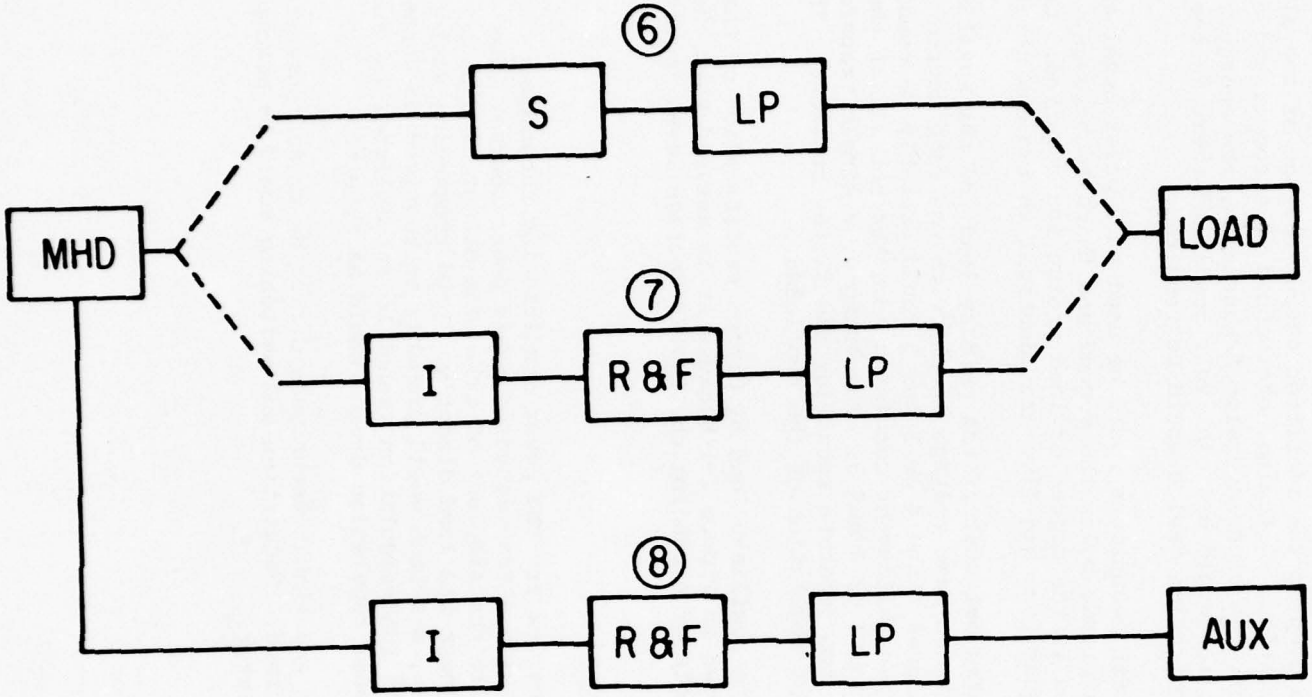


Figure 2-2 Power conditioning techniques considered for use with a magnethydrodynamic power source and a continuous load.

C. Pulsed Load

Figure 2-3 contains power conditioning techniques that have been considered for use with a pulsed load. It has been assumed that, even though the load is considered to be self pulsed, that energy will be delivered to it by a pulse forming network (PFN). Conceivably, a capacitor could be used rather than a PFN, however its size and the energy stored in it would probably have to be prohibitively large to prevent voltage droop during a pulse. For the purposes of this study, the PFN has been assumed to contain a charging inductor and any diodes that may be required. This study considers only the power conditioning elements leading up to the PFN.

Particular attention should be given to the use of an inverter to charge the PFN (as shown in the tenth and thirteenth techniques). The inverter is basically a variable-frequency pulsed current source that can be operated at the same repetition frequency as the load. Conceivably the inverter could be used to drive the PFN directly without a requirement for a charging inductor or diodes.

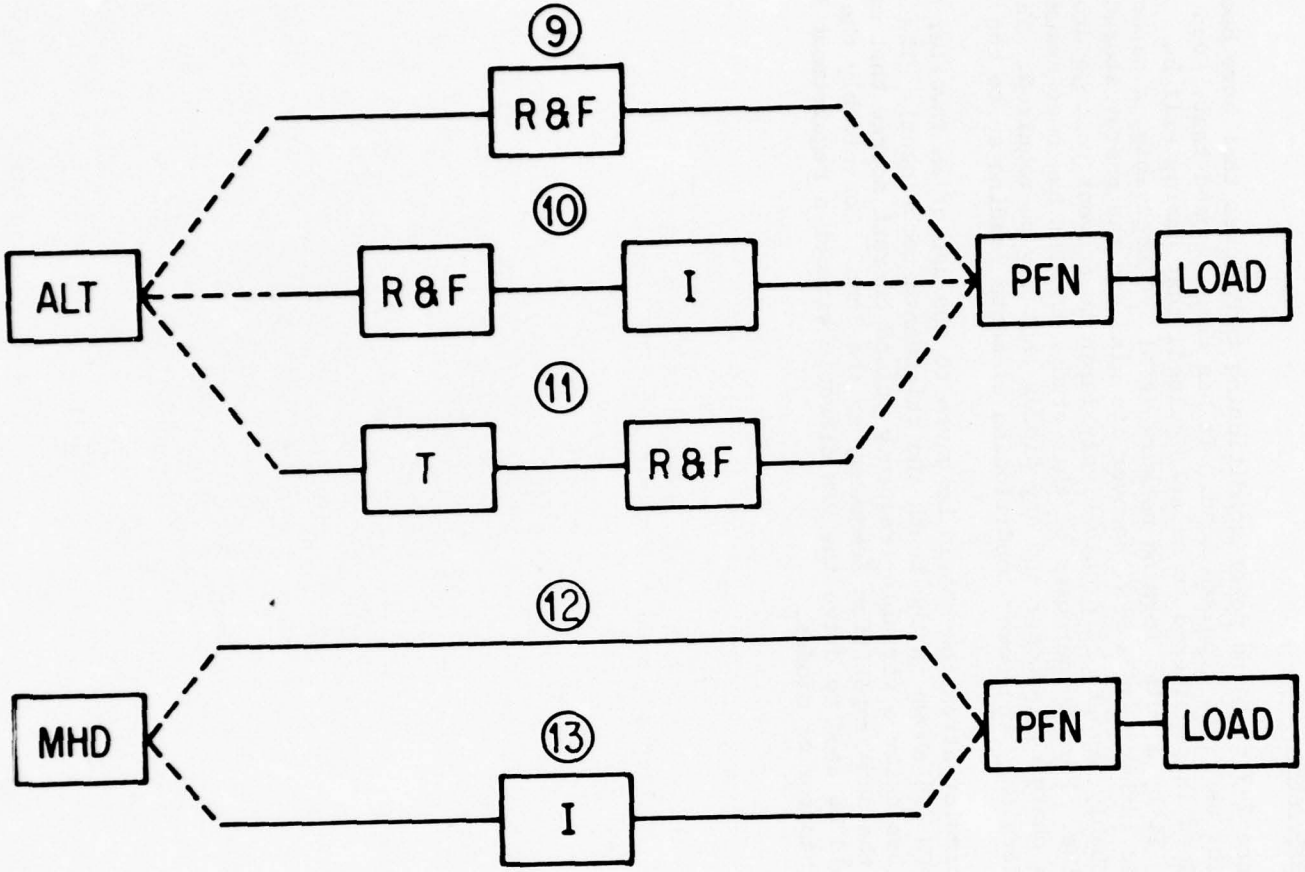


Figure 2-3 Power conditioning techniques considered for use with a pulsed load.

III. IDENTIFICATION OF CRITICAL COMPONENTS

Many of the critical components that may be required for the various power conditioning techniques shown in Figures 2-1, 2-2 and 2-3 are evident from these Figures. For example, in addition to the obvious need for transformers, switching devices are required in the rectifiers, and capacitors and inductors may be required in the filters. The inverter may also contain these elements, as is indicated by the circuit diagram in Figure 3-1 for one of the inverter configurations that was considered in this study. Of course, many of the elements in the inverter are required to operate under high frequency ac conditions.

The protection device indicated in Figures 2-1 and 2-2, if it is required, will probably contain only one critical component and that is a fast high-current switch. There will be detection and control circuitry, however this will probably not require a component development.

In Figure 2-2, a switch is shown connecting the MHD source to the load. If this switch is required to open under loaded conditions, then a switch development effort may well be required.

Figure 3-2 contains a summary listing of critical components and of the functions in which they are used in Figures 2-1, 2-2 and 2-3.

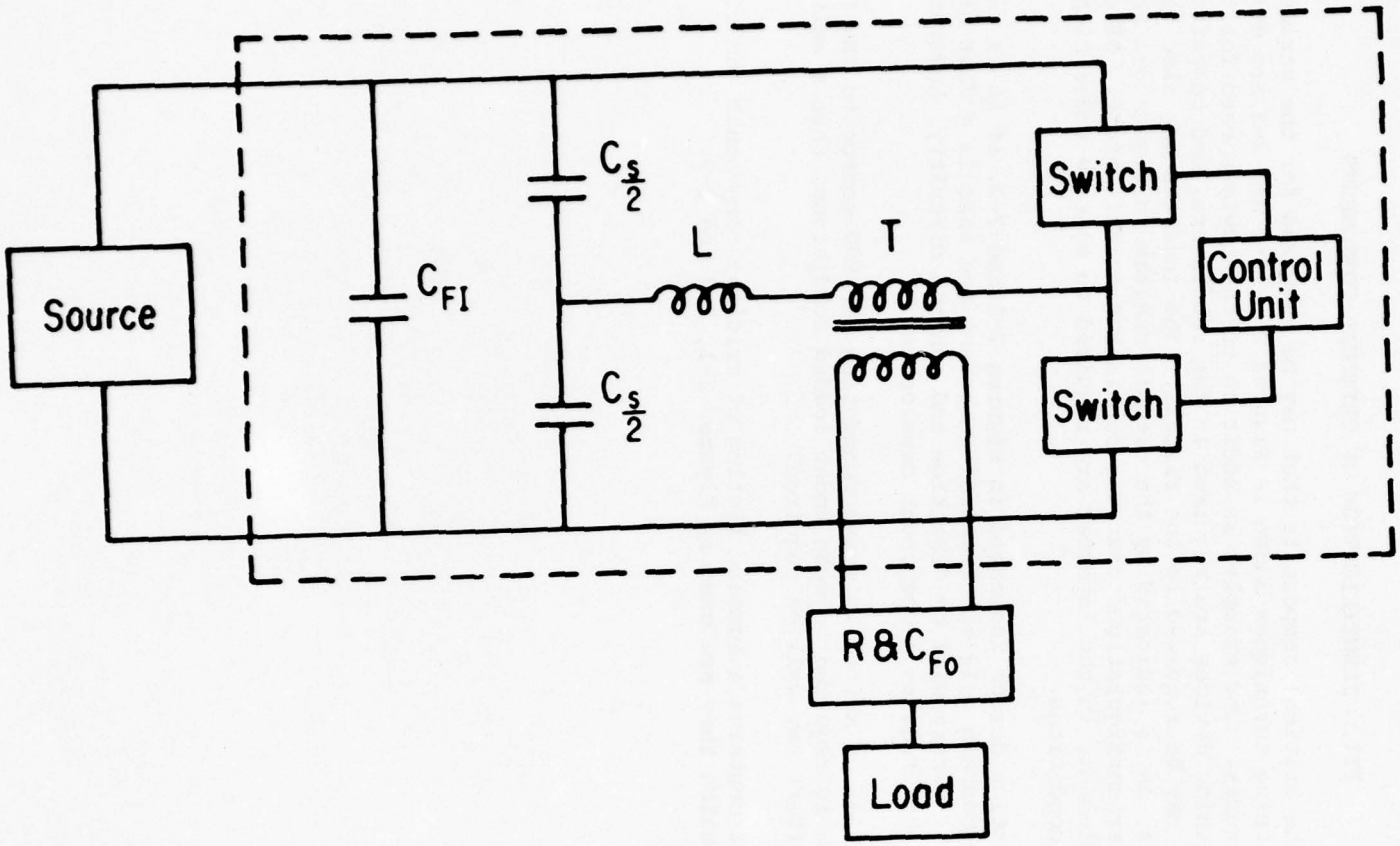


Figure 3-1 Possible inverter configuration

COMPONENT	WHERE USED
CAPACITOR	I, F, R & F
SWITCH	I, R & F, S, LP
TRANSFORMER	T, I
INDUCTOR	I, R & F

Figure 3-2 Critical component identification

IV. CRITICAL COMPONENT ANALYSIS

A. Transformers

Four classes of transformers were investigated in detail during this High Power Study. Two of these were at power levels in the 10 to 50 MW range and the other two were in the 1 to 5 MW range (for use with the auxiliary load). In each power range, three phase sinusoidal and single phase square wave transformers were analyzed in detail. The three phase sinusoidal transformers would be used to boost the output voltage of the alternator. The single phase transformers would be used in the inverters.

The transformer study was carried out with the assistance of Thermal Technology Laboratory, Inc. (TTL). Individual transformer designs were performed using the TTL transformer design computer program. This program (which is included as Appendix B) was used in a mode whereby it automatically minimized the weight of a transformer with any given set of operating parameters. Designs utilizing external cooling (by freon for example) and "adiabatic" (wherein the heat capacity of the transformer material is used to absorb the heat generated) were examined in detail. Also, the use of cryogenics was taken into consideration. For the operating periods under consideration (120 seconds maximum) the "adiabatic" designs were found to produce substantially lower specific weights than the designs utilizing external cooling. Thus, only the results of the "adiabatic" design studies are included in this report. An ambient temperature of 160°F (71°C) and a maximum wire temperature of 500°F (260°C) were assumed for these studies. If liquid nitrogen could be used for cooling the transformer prior to the start of a mission, the studies show that a weight reduction by a factor of at least four could be realized.

It should be pointed out that, for the transformer designs analyzed for this study, the current density in the conductors was about 13000 A/in^2 and it was assumed that all of the conductor losses were stored in the conductors. It was assumed that none of the heat diffused into the insulation. By comparison, it should be noted that in the Garrett thermal lag alternator designs, a current density in the conductors of 15000 to 16000 A/in^2 is used. The diffusion of heat into the insulation is taken into account and a temperature rise from 130°F to 400°F is found to occur. It appears, therefore, that if heat diffusion into the insulation was taken into account in the transformer design, that the maximum conductor temperature would probably be below 400°F.

Because of the high operating frequencies anticipated for the transformers, the conductors were assumed to be Litz wire. It was found that if no ac resistance effects occurred and if, as a result, solid conductors could be used, the reduction in transformer weight would be only six per cent. Thus, the use of Litz wire at all frequencies anticipated seems justified to eliminate unnecessary heating.

The use of multiple secondaries on transformers to eliminate the need for rectifier balancing networks was examined. While the use of multiple secondaries appears to be desirable from a circuit performance point of view, no reduction in the overall specific weight of the system is expected to result. The reason is that any weight reduction in the rectifier stacks is offset by an increase in the transformer weight.

1. Alternator transformers

As was pointed out previously, three phase sinusoidal transformers for use in boosting the output voltage of an alternator were analyzed in detail. In addition, single phase and polyphase sinusoidal transformers were very briefly examined. For a given set of operating conditions, the optimized weights of these transformers were found to be well represented by that of a three phase transformer.

Over sixty point designs for optimized weight were established to enable the development of transformer algorithms valid over the complete range of system parameters for the High Power Study. Each of these designs contains detailed specifications for a transformer for operation under the given set of operating conditions.

Figures 4-1 through 4-4 contain the specific weights of some of the optimized three phase transformers that were designed in the 10 MW to 50 MW power range. Also included in these figures are curves representing the specific weight predictions from the following algorithm:

$$S_{TA}(\text{main}) = .0505\left(\frac{\tau}{120}\right)^{0.337}\left(\frac{Vo}{100}\right)^{-.0413}$$

$$\times \left[.693 + .307\left(\frac{P}{25}\right)^{-.79}\right]$$

$$\times \left[.931 + .069\left(\frac{Vo}{100}\right)^{1.3}\right]$$

$$\times \left[.242 + .758\left(f_a\right)^{-.926}\right] \quad \text{lb/kW}$$

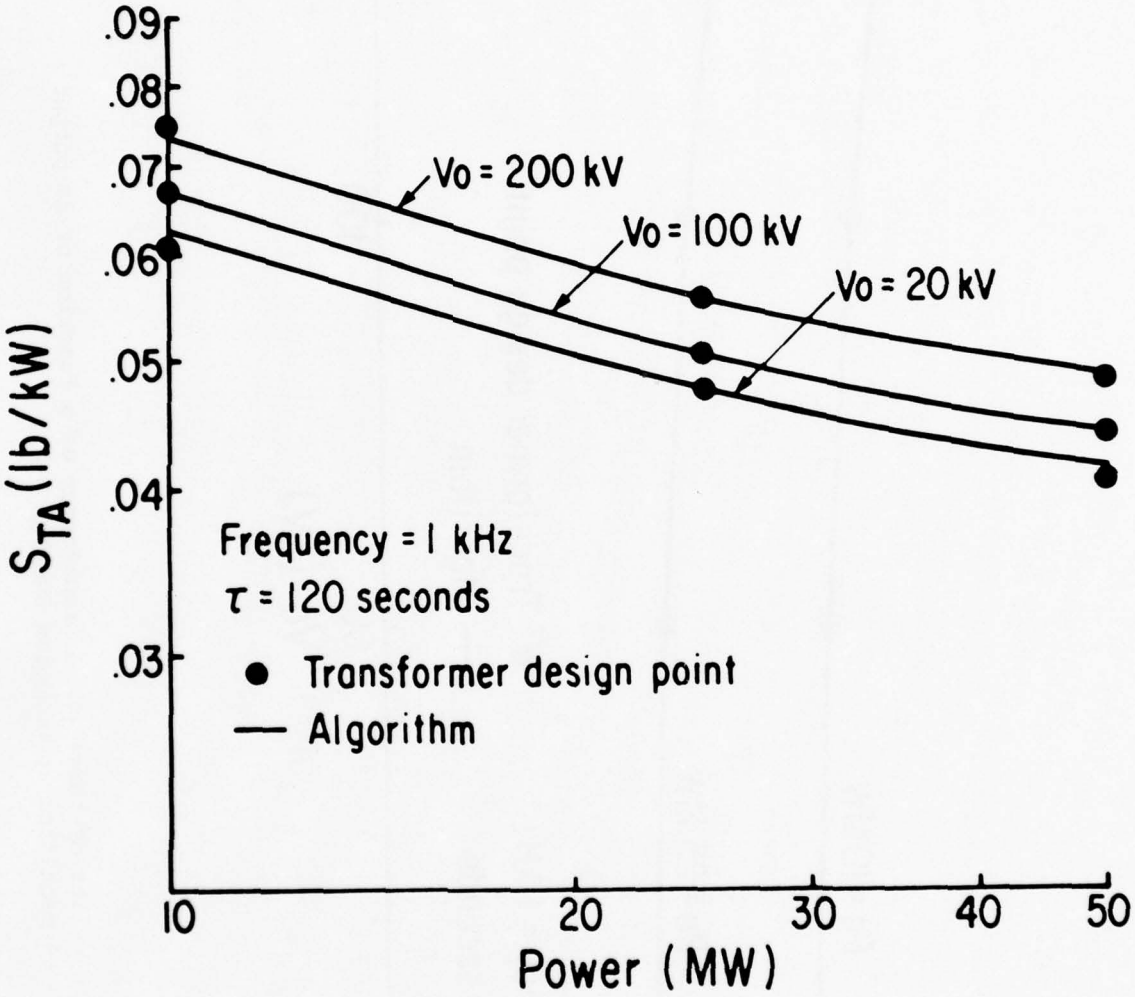


Figure 4-1 Specific weight of three phase transformer as a function of operating power level.

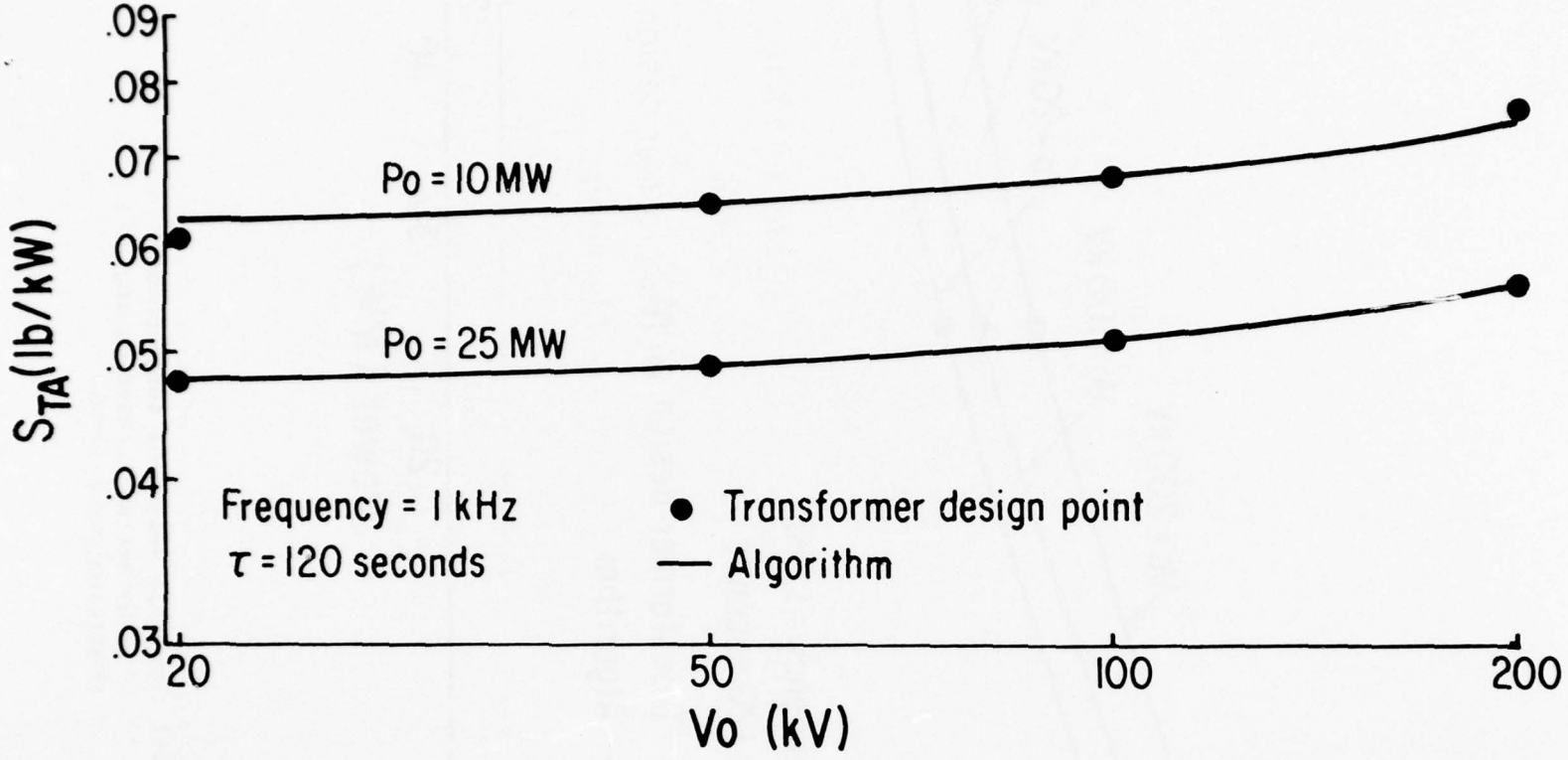


Figure 4-2 Sepcific weight of three phase transformer as a function of dc output voltage of rectifier (conduction overlap = 0).

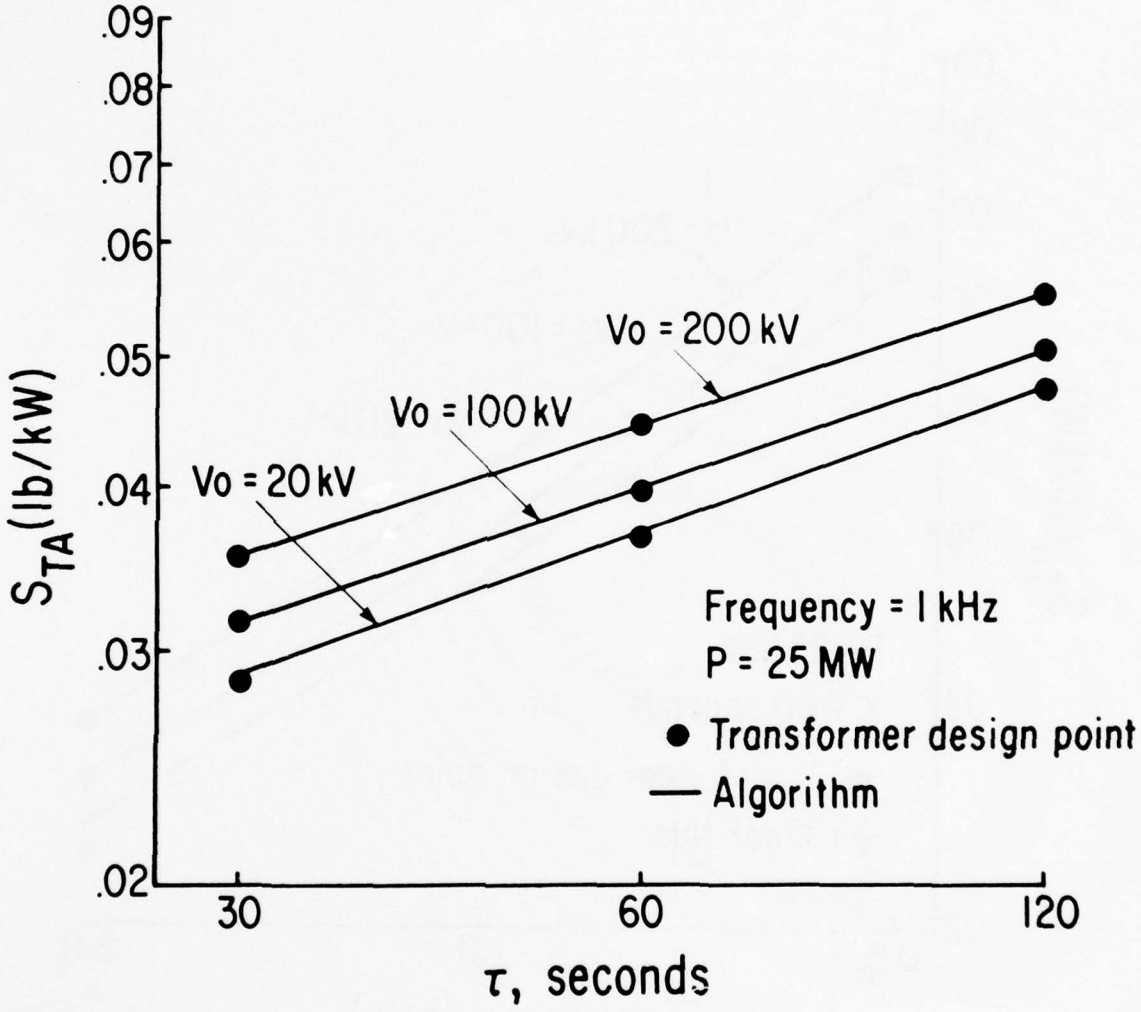


Figure 4-3 Specific weight of three phase transformer as a function of total operating time during a mission.

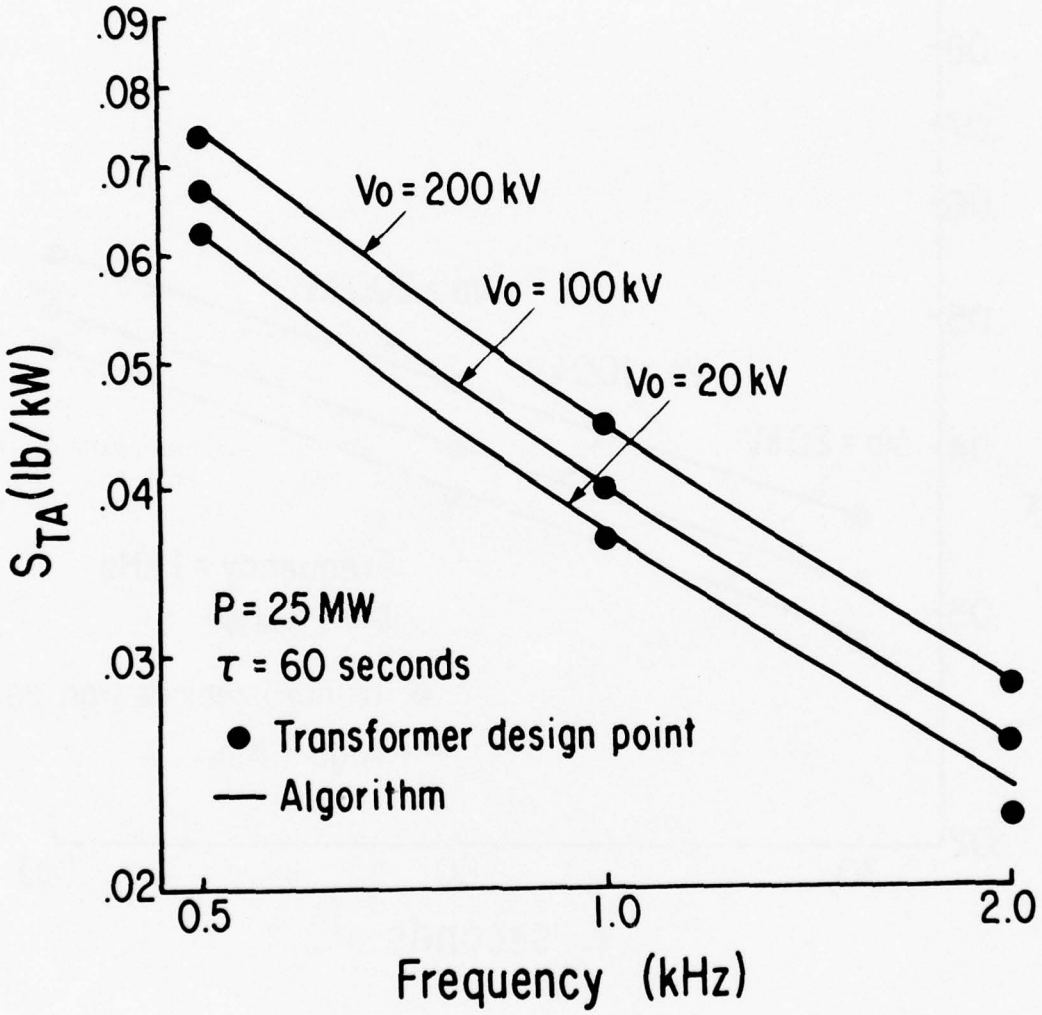


Figure 4-4 Specific weight of three phase transformer as a function of frequency.

where

τ = total run time during mission in seconds

P = power level in megawatts

V_o = dc load voltage in kilovolts assuming zero conduction overlap in rectifier

f_a = alternator frequency in kHz

This algorithm is designated S_{TA}(main) to differentiate if from S_{TA}(aux), which is given in a following paragraph. S_{TA}(main) is valid over the power range from 10 MW to 50 MW. It should be noted that the input voltage to the transformer is not a variable in the algorithm for S_{TA}(main). This is because the transformer weight was found to vary less than one percent as the input voltage (line to line, rms) was varied from 1 kV to 5 kV. It should also be noted that the factor .0505 gives the specific weight of this transformer when

τ = 120 seconds

P = 25 megawatts

V_o = 100 kV

f_a = 1 kHz

The algorithm that was derived to give the three-phase-sinusoidal transformer specific weights over the power range from 1 MW to 5 MW is

$$S_{TA}(aux) = .1275\left(\frac{\tau}{120}\right)^{.281} \times \left[.612 + .388\left(\frac{P}{2.5}\right)^{-.985}\right] \times \left[.608 + .392\left(\frac{Vo}{200}\right)^{.71}\right] \times \left(f_a\right)^{-.767}$$

The factor .1275 gives the specific weight of this transformer when

τ = 120 seconds

P = 2.5 megawatts

Vo = 200 kV

f = 1 kHz

2. Inverter transformers

Over sixty single phase, square wave transformers for use in series inverters at frequencies in the range from 5 kHz to 10 kHz were designed. Figures 4-5 and 4-7 contain the specific weights of some of these optimized transformers in the power range from 10 MW to 50 MW. Also included in these figures are curves representing specific weight predictions from the following algorithm:

$$S_{TI}(\text{main}) = .00940 \left(\frac{\tau}{120}\right)^{.302} \left(\frac{Vo}{100}\right)^{-.095} \times \left[.479 + .521\left(\frac{P}{25}\right)^{-.614}\right] \times \left[.880 + .120\left(\frac{Vo}{100}\right)^{1.33}\right] \times \left(\frac{f_i}{10}\right)^{-.754} \left(\frac{V_{in}}{5}\right)^{-.089} \quad \text{lb/kW.}$$

where τ, P, and V_o are as given for the alternator transformer, f_i is the inversion frequency and V_{in} is the input voltage to the transformer in kilovolts.

The algorithm that was derived to give the single-phase square-wave transformer specific weights over the power range from 1 MW to 5 MW is

$$S_{TI}(\text{aux}) = .0263 \left(\frac{P}{2.5}\right)^{-.426} \left(\frac{Vo}{200}\right)^{.274} \times \left(\frac{\tau}{120}\right)^{.219} \left(\frac{f_i}{10}\right)^{-.8} \quad \text{lb/kW.}$$

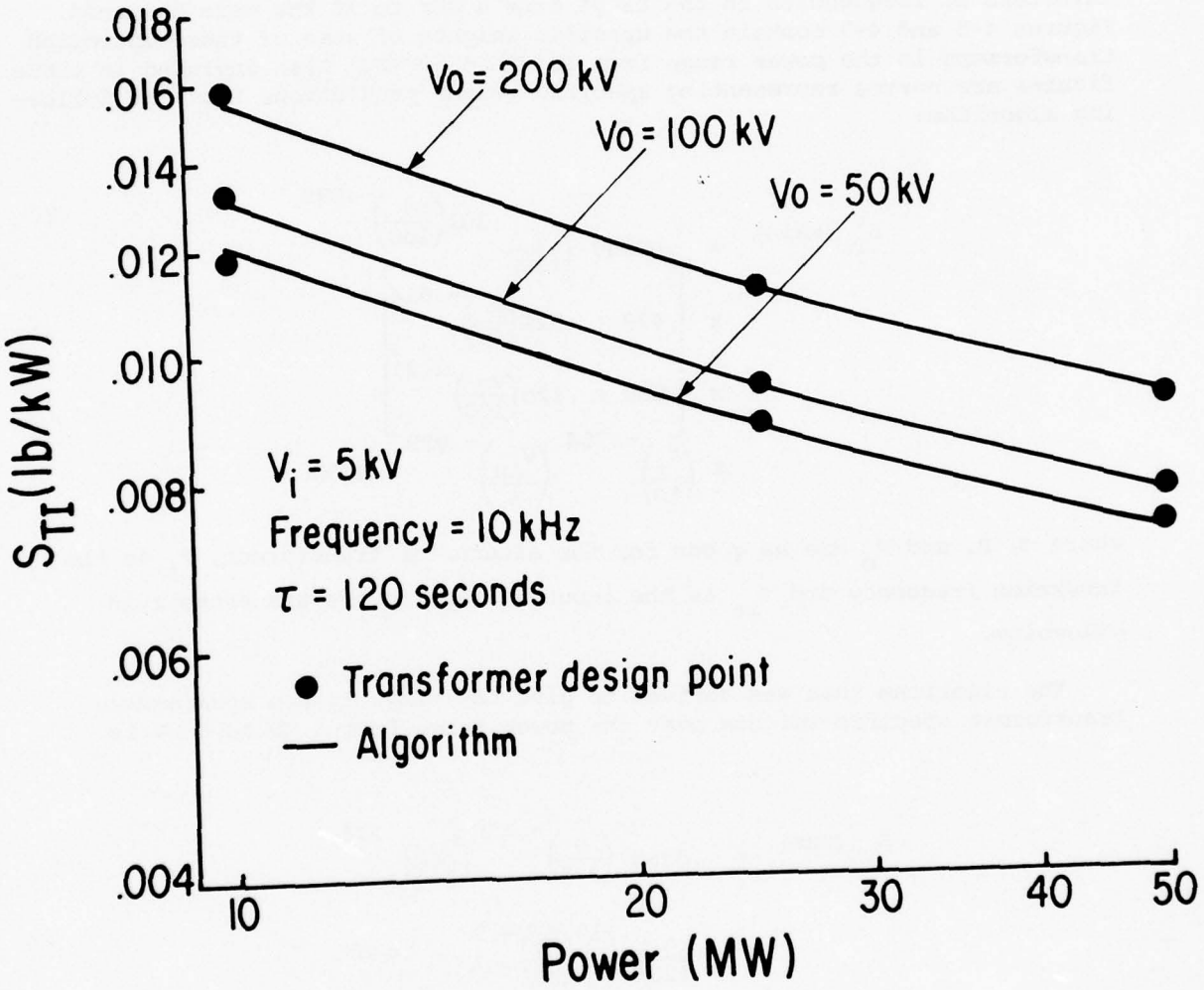


Figure 4-5 Specific weight of inverter transformer as a function of operating power level.

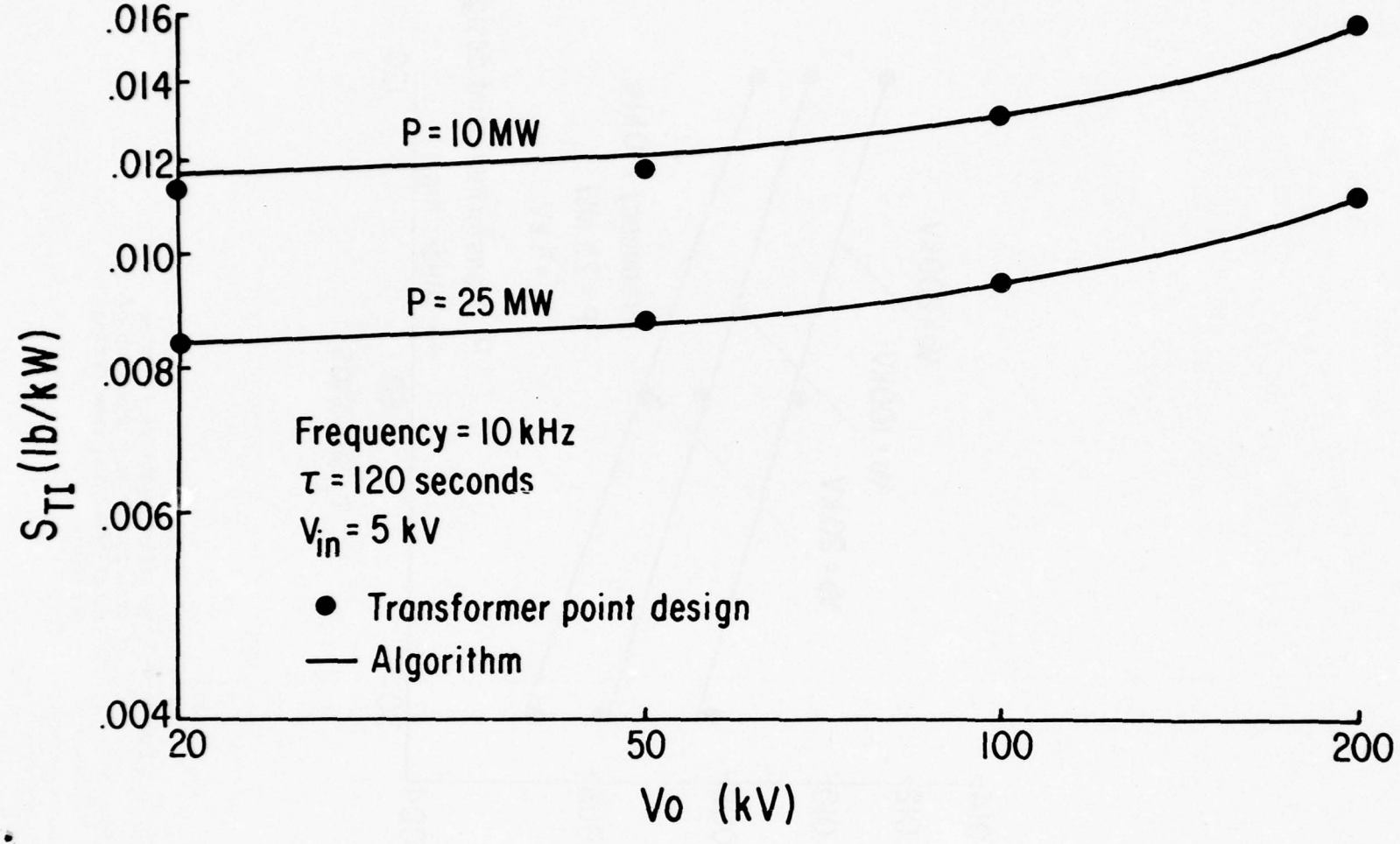


Figure 4-6 Specific weignt of inverter transformer as a function of dc output voltage of rectifier.

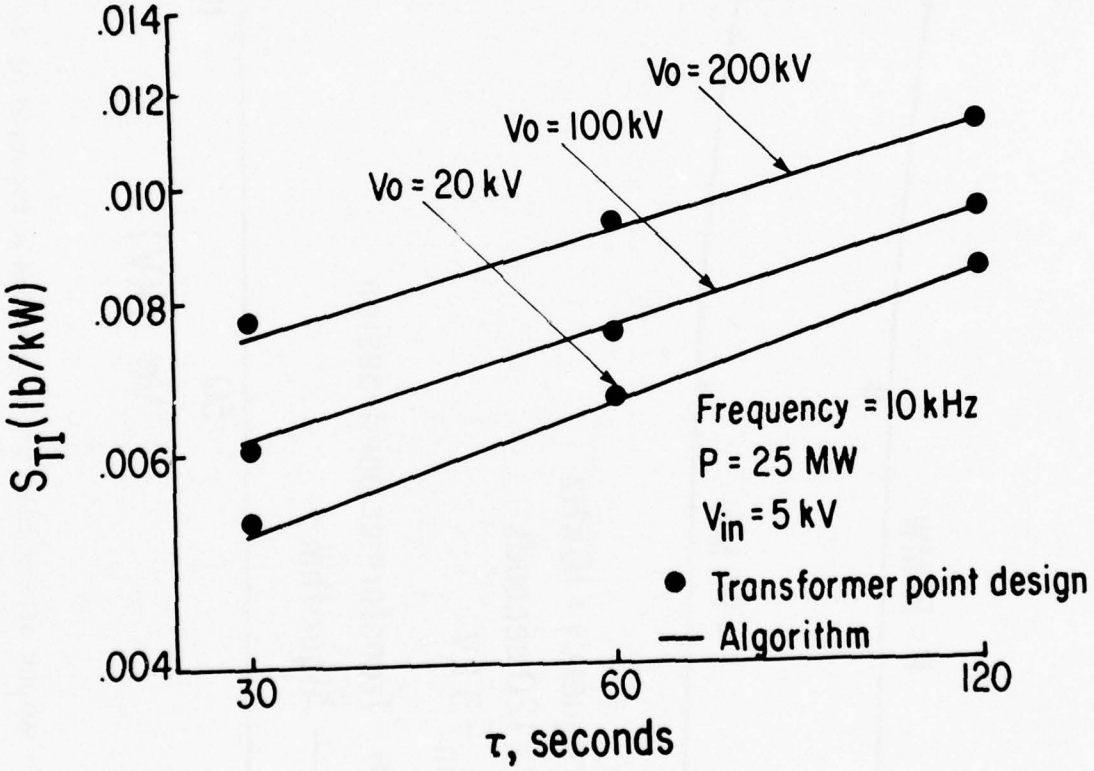


Figure 4-7 Specific weight of interter transformer as a function of total operating time during a mission.

B. Switches

Several types of switches have been investigated during the course of this study. As was pointed out previously in this report, switches are required in the three phase and single phase rectifiers as well as in the inverters. In addition, switches will be required in the load protection circuits and in the connecting link between the MHD source and the load.

1. Solid State

A conceptual design of an "adiabatic" rectifier stack is shown in Figure 4-8. In this case "hockey puck" rectifiers are shown sandwiched between heat sinks. The entire stack of rectifiers and heat sinks is housed in a cylindrical insulating sleeve. The required forces for the rectifiers would be applied using the appropriate compression fittings at the ends of the sleeves.

The average forward current capability of solid state devices is temperature dependent as is shown by the example given in Figure 4-9. The optimum operating current of an "adiabatic" rectifier stack is dependent on the amoung of heat the heat sinks can absorb. When rectifier losses as a function of average current are taken into account then the specific weight of a rectifier stack as a function of average current is as shown in Figure 4-10. Obviously, an average current value should be chosen that nearly minimizes the weight of the stack. When this is done, then the specific weight of the rectifier stack as a function of output voltage is found to be as shown in Figure 4-11. The specific weight as a function of operating period is shown in Figure 4-12. The resulting algorithms that describe the specific weight of three phase, $S_{3\phi r}$, and single phase, $S_{1\phi r}$, rectifier stacks are as follows:

$$S_{3\phi r} = .0073\left[.945 + .055\left(\frac{Vo}{100}\right)^{2.2}\right]\left(\frac{\tau}{60}\right)^{0.83} \quad \text{lb/kW}$$

$$S_{1\phi r} = .0042\left[.945 + .055\left(\frac{Vo}{100}\right)^{2.2}\right]\left(\frac{\tau}{60}\right)^{0.83} \quad \text{lb/kW.}$$

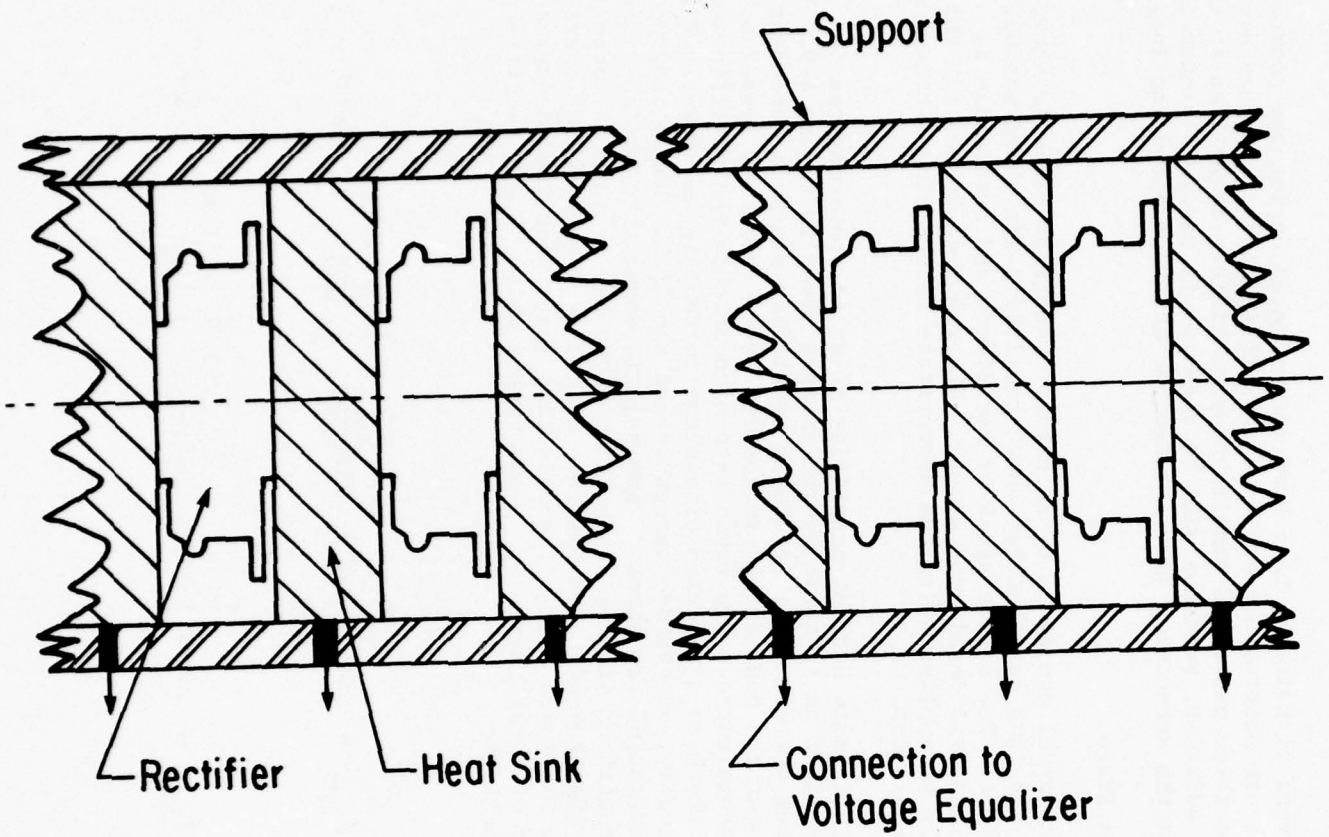


Figure 4-8 Conceptual design of "adiabatic" rectifier stack

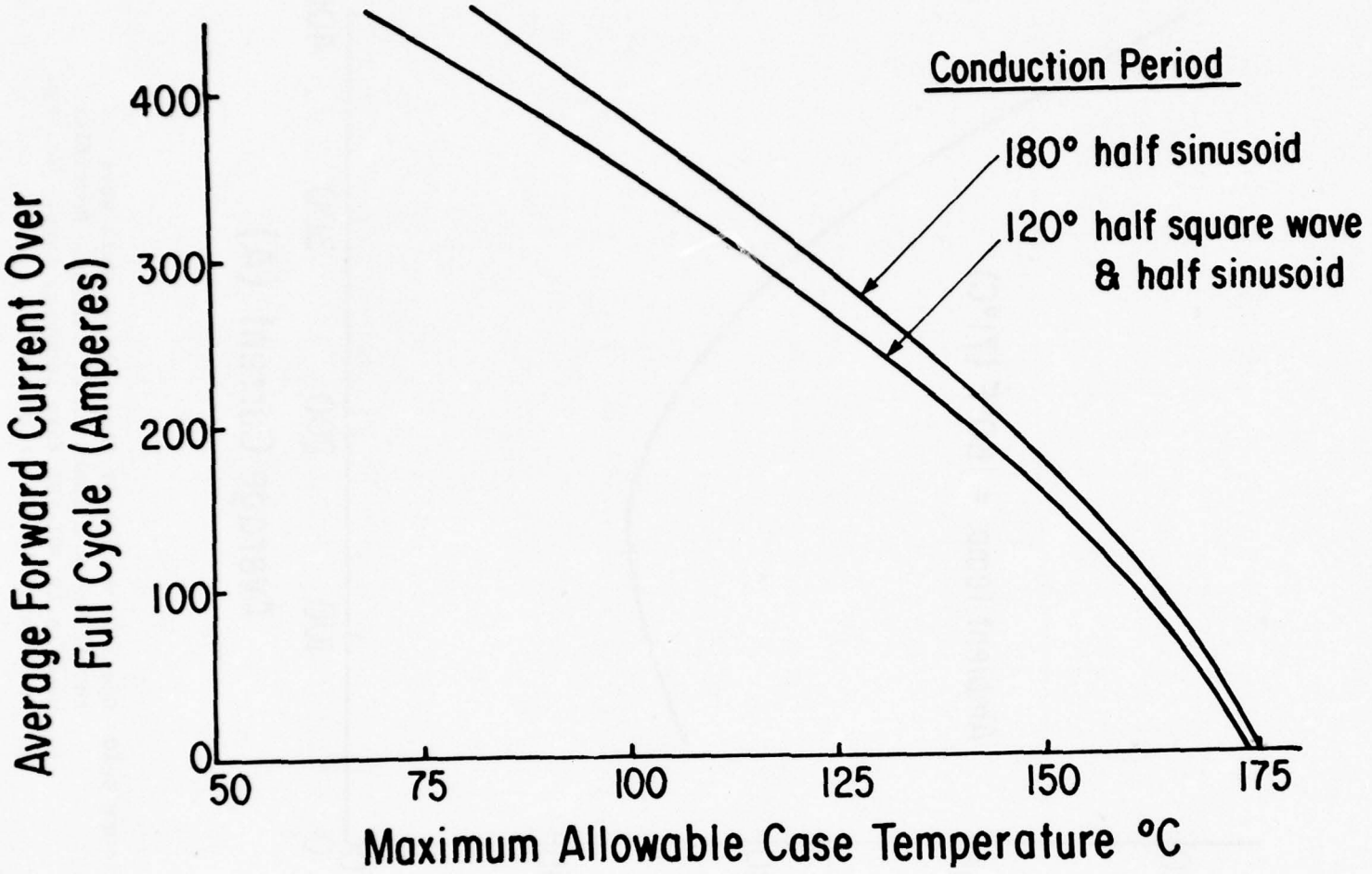


Figure 4-9 Average forward current as a function of case temperature for International Rectifier 401 PDL series fast-recovery rectifiers.

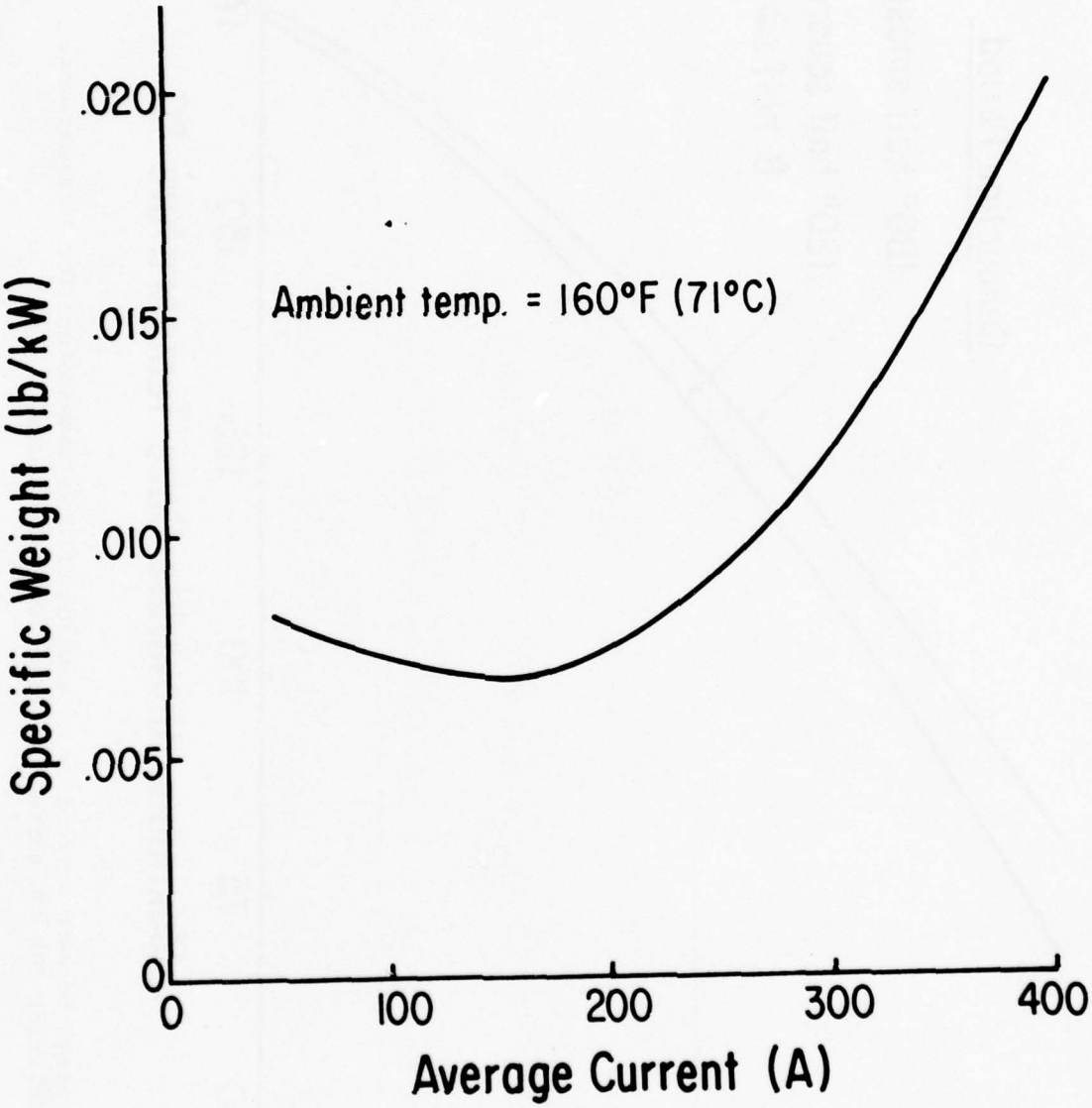


Figure 4-10 Specific weight of three phase, full wave rectifier as a function of current. Rectifier used is IR 401 PDL fast recovery type. Voltage is derated by factor of two.

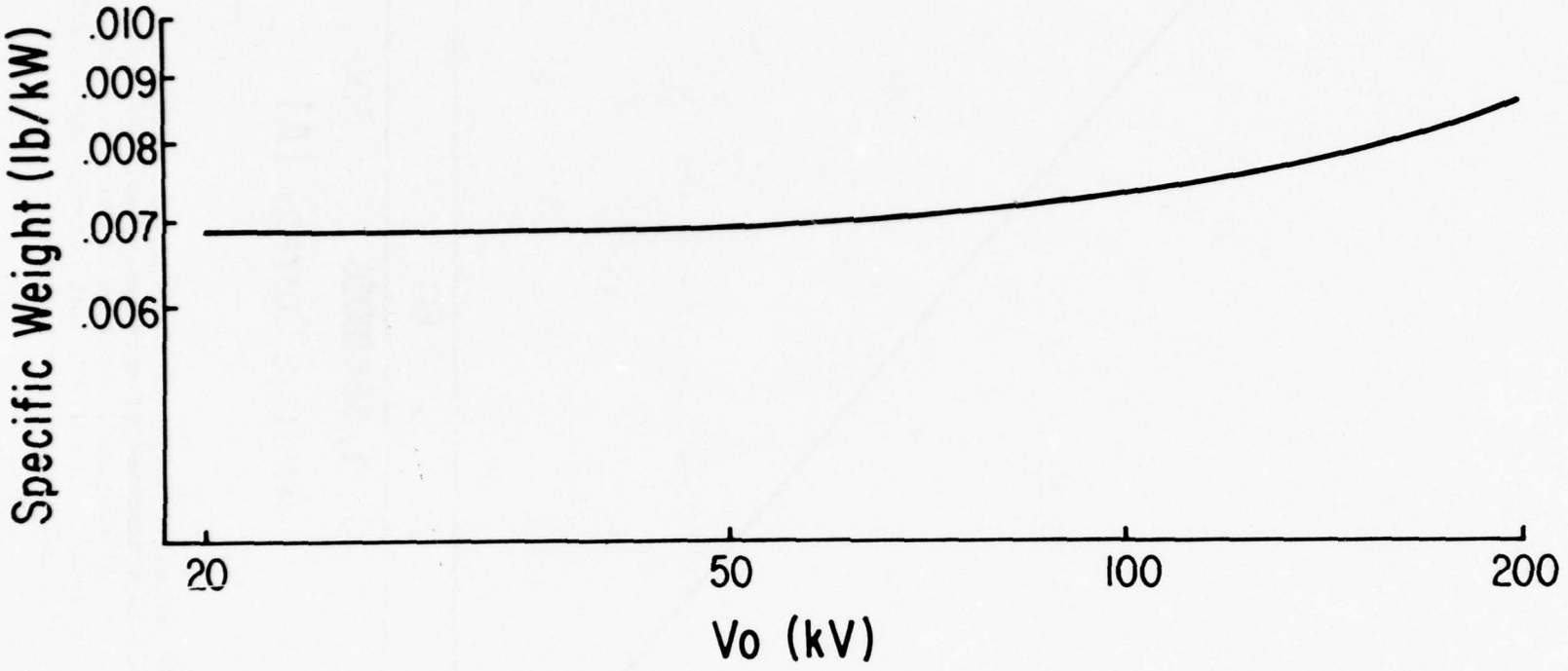


Figure 4-11 Specific weight of three phase, full wave rectifier as a function of output voltage.

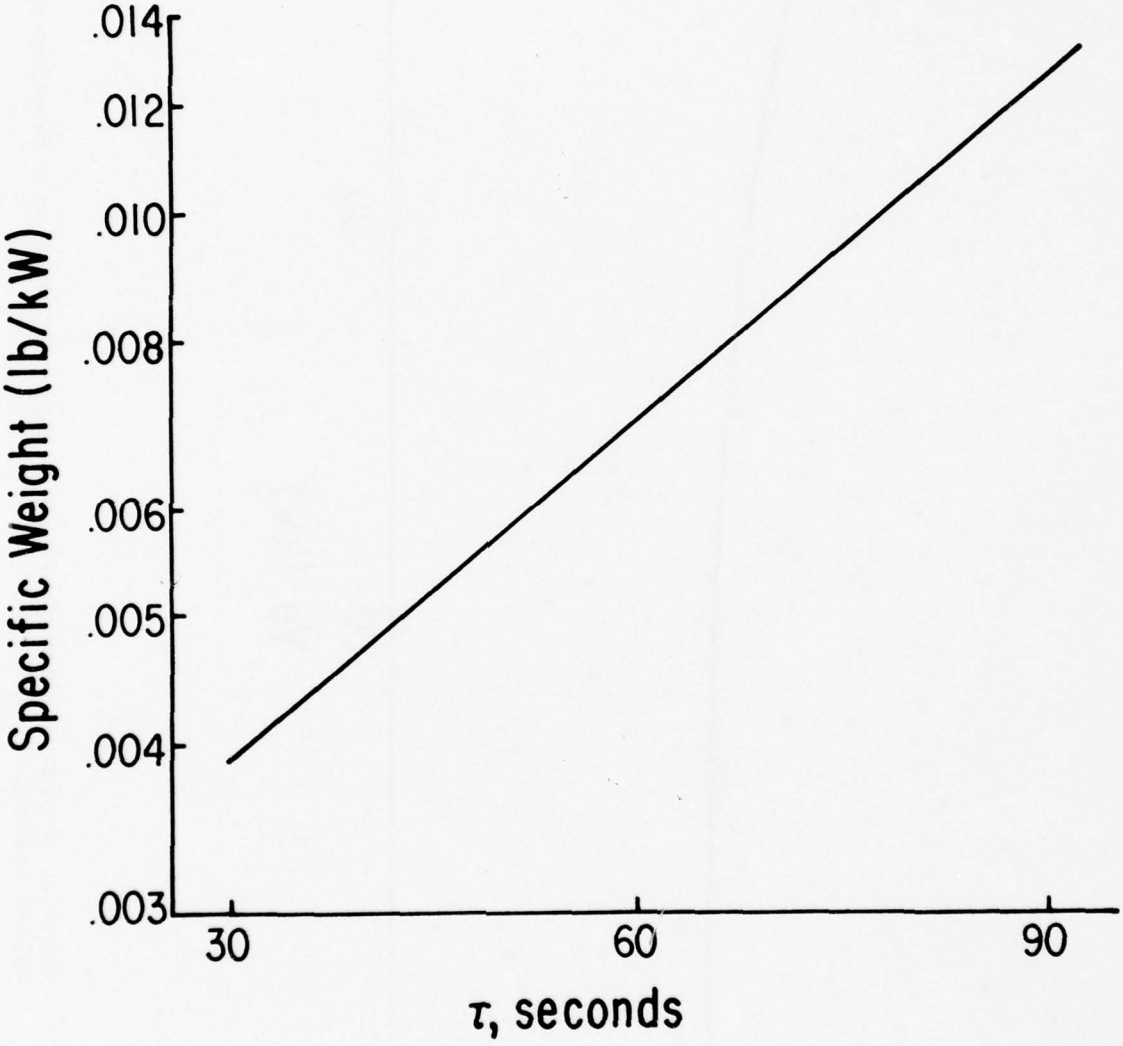


Figure 4-12 Specific Weight of three phase rectifier as a function of operating time

When a similar analysis is performed for the SCR's for the inverter the algorithm is found to be

$$S_{scr}(\text{inverter}) = .024\left(\frac{\tau}{60}\right)^{0.83} \quad \text{lb/kW.}$$

There is no appreciable voltage dependence because the inverter SCR stacks operate at a relatively low voltage (near the alternator voltage).

2. Vacuum Arc

20-22 A brief examination was made of the weights of vacuum arc switches for use in rectifier and inverter circuits. Appendix D contains a paper describing the basic operating principles of these vacuum arc switches. For use in phase controlled rectifiers and in series resonant inverters, the magnetic-field control of conduction is not necessary. Thus, an outline drawing of the controlled vacuum arc rectifiers would be as is shown in Figure 4-13. For "adiabatic" designs, the cathode assembly would have twice the mass of the anode assembly since studies performed under AFAPL sponsorship have shown that two thirds of the switch losses are deposited in the cathode and the other one third are deposited in the anode. The specific weight of a switch of this type is estimated to be .002 lb/kw.

If a magnetically controlled vacuum arc switch was used in the connecting link between an MHD source and the load, the specific weight would be somewhat larger than that for controlled rectifier service, but certainly no larger than .004 lb/kw.

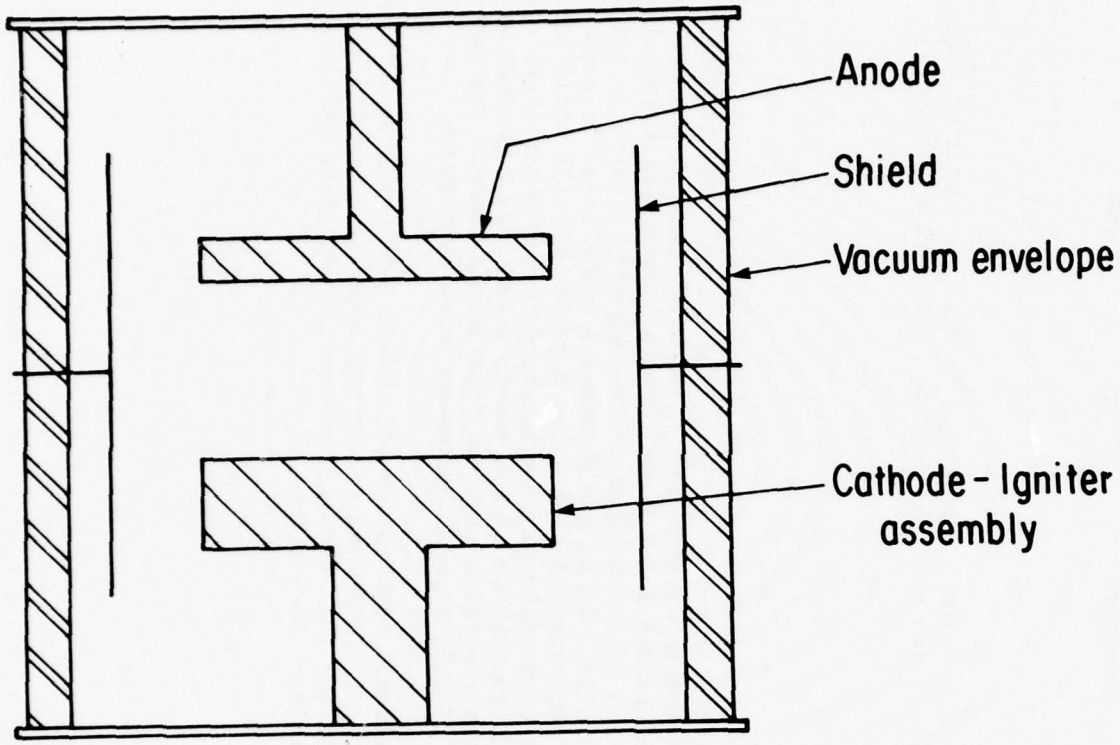


Figure 4-13 Outline drawing of controlled vacuum arc rectifier

C. Capacitors

1. Filter Capacitors

Filter capacitors are used for ripple reduction purposes in the filter sections used with the rectifiers for the alternator or the inverter. Except for system start-up and shut-down cycles and load fault conditions, these capacitors have a dc voltage with a small (few percent) ripple component applied to them. Capacitors are available (Maxwell and General Electric for example) which are suitable for this application and which have energy densities in the neighborhood of 100 joules/lb.

Capacitors using polyvinylidine flouride[16] may become available. These have energy densities in the 300 to 500 joule/lb range but have a high dissipation factor (on the order of one percent). Thus, they are suitable for filtering applications at reasonable ripple amplitudes.

Because 100 joule/lb capacitors are available at the present time, the use of these will be assumed in the filter analyses sections of this report.

2. Inverter Capacitors

An inverter capacitor is used in a series resonant circuit operating at a frequency that may range from 1 kHz to 20 kHz. The most probable frequency range is from 5 kHz to 10 kHz. The total number of cycles of operation that this capacitor may experience is the product of the frequency of operation, the missing duration and the number of missions. This product may be as high as

$$20 \times 10^3 \text{ Hz} \times 120 \text{ seconds} \times 100 \text{ missions}$$

or

$$2.4 \times 10^8 \text{ cycles.}$$

If this capacitor is examined from a pulse capacitor point of view then the number of reversals is extremely high, in fact, beyond the range normally considered for pulse capacitors. If, on the other hand, this capacitor is examined from an ac capacitor point of view, then the life is short compared to that normally considered (several years at 60 Hz or on the order of 2×10^9 cycles).

Discussions were held with many capacitor manufacturers in an effort to determine the characteristics (most importantly, the minimum specific weight and volume) that could be expected for a capacitor being used for this (series inverter) application. No manufacturer was found which had actually built a capacitor for use under these conditions. The information contained in the following paragraphs is a composite of that obtained from several manufacturers and represents the best estimate, at the present time, of the achievable capacitor characteristics. It is clear that a research and development program containing a substantial testing task will be required to substantiate and/or correct this estimate.

The two primary factors that must be considered in designing and fabricating high energy density, high frequency ac capacitors are:

1. heating effects
2. corona effects.

When considering heating effects, the most weight and volume effective way to accomodate heat losses in a capacitor that must operate for a short period (like 120 seconds) is to utilize the heat capacity of the capacitor material. For a given energy content, externally cooled capacitors (such as those that are manufactured by the Westinghouse Corp. in Bloomington, Ind. for induction heater use at 10 kHz) are typically at least an order of magnitude heavier than those utilizing only heat capacity.

The heating of a capacitor can be determined directly from the capacitor dissipation, the energy density of the capacitor and from the number of voltage reversals to which the capacitor is subjected. Thus, if the energy density of the active storage elements of a capacitor is D joules/lb and the dissipation factor is δ then the energy lost per discharge cycle is δD joules/lb. The total number of discharge cycles at a frequency of f kHz and a mission duration of τ seconds is $2\tau f \times 10^3$ and so the total energy deposited in the capacitor during a mission is $2\tau f \delta D \times 10^3$ joules/lb. The average heat capacity of the active storage elements is about 0.35 cal/gm/^{o}C or 665 joules/lb/^{o}C. Thus, the temperature rise, ΔT, of the active storage elements is

$$\Delta T = \frac{2\tau f \delta D}{0.665} \quad {}^{o}C$$

This is the "worst case" temperature rise. It has been assumed that no cooling occurs during the mission. This assumption is very nearly valid because of the poor thermal conductivity of the dielectric materials used in the active storage elements. If the allowable temperature rise is known, then D can be readily calculated from

$$D = \frac{0.665\ \Delta T}{2\tau f \delta} \quad \text{joules/lb.}$$

The dissipation factors for the various dielectric systems that might be considered for use are given in Figure 4-14. The maximum operating temperature for each of these systems is given below:

dielectric system	maximum temperature
p-ppl-p-ppl-p castor oil	75°C
ppl-p-ppl - aroclor	100°C
ppl - silicone oil	125°C
ppl	125°C

Now, Figure 4-15 shows the maximum active element energy density possible for each of the above listed dielectric systems based on heating effects only. The ambient temperature and starting temperature of the capacitor has been assumed to be 160°F (71°C) and the operating period has been chosen as 120 seconds.

In ac capacitors operating at 60 Hz, corona effects and the voltage at which they occur are documented. For very long life applications of ac capacitors, corona effects are completely avoided by operating at a voltage level well below (by a factor of about 3) that at which corona effects occur.

For the limited life application under consideration in this study, the importance of corona effects is not at all clear. To permit the derivation of an algorithm for the inverter capacitor, it will be assumed that operation at the corona extinction voltage should be permissible. This is the voltage at which a corona discharge, once initiated, extinguishes. It should be noted that operation at a somewhat higher or lower voltage may be permissible and/or desirable, however, this decision must be made on the basis of additional information which is not available at this time.

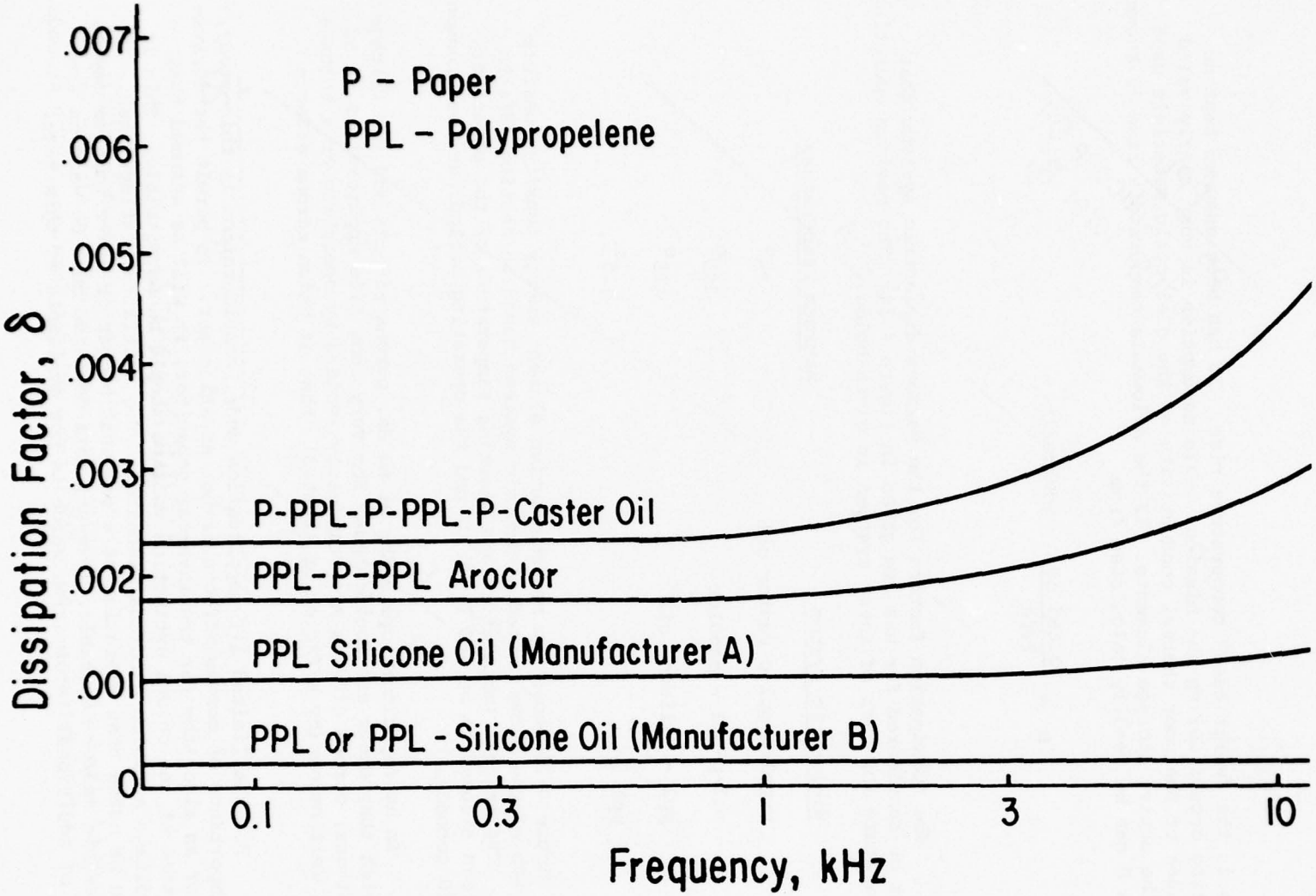


Figure 4-14 Frequency Coefficient of Dissipation Factor

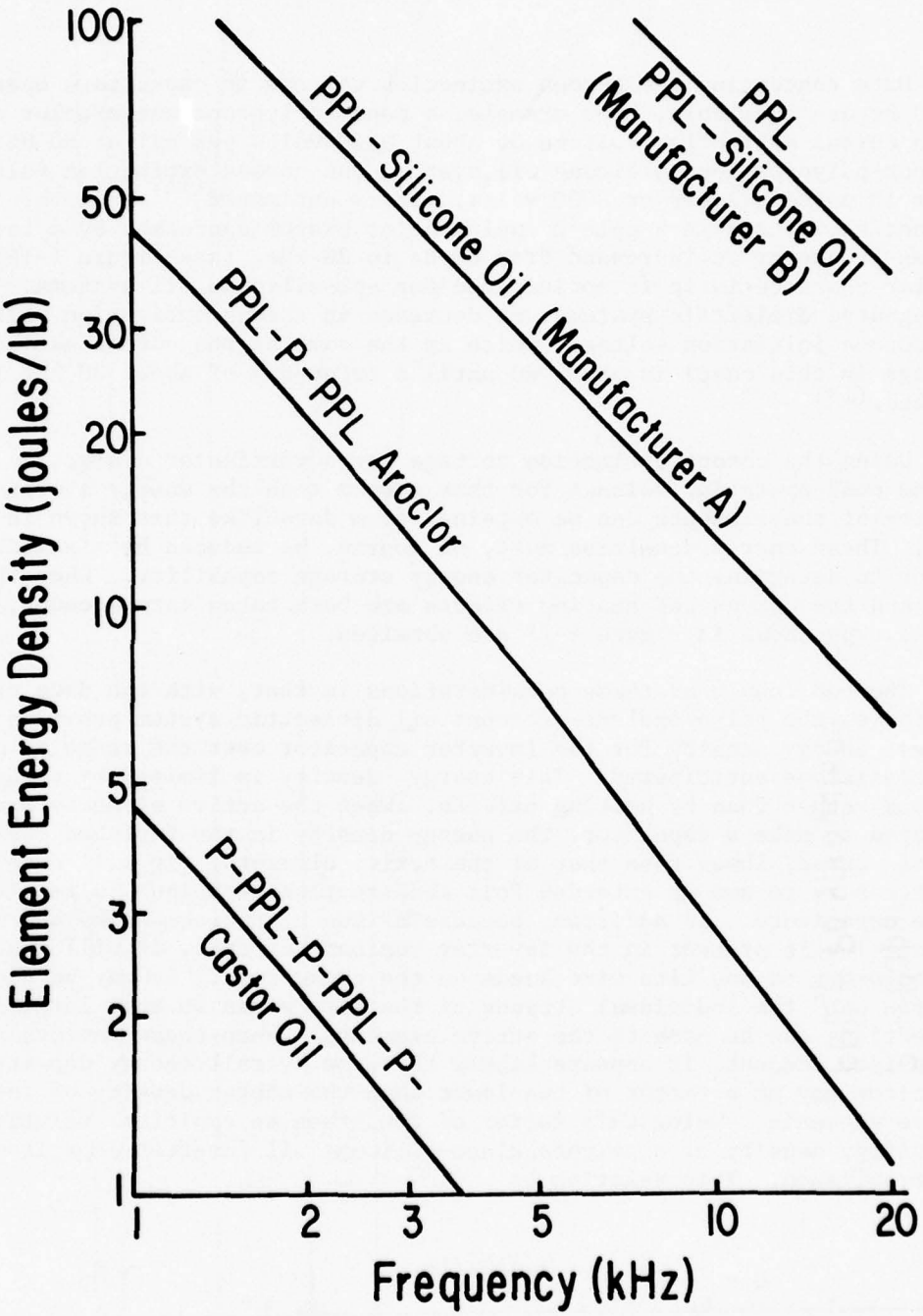


Figure 4-15 Maximum energy density (of active elements) based on heating effects only as a function of frequency for air ambient temperature of 160°F(71°C) and a mission duration of 120 seconds.

Data concerning the corona extinction voltage in capacitors operating at 60 Hz are available. For example, a paper-polypropelene-aroclor system has a corona extinction voltage of about 3600 volts per mil at 60 Hz. For a paper-polypropelene silicone oil system, the corona extinction voltage is about 15 percent lower or 3000 volts. It is estimated[14] that the corona extinction voltage in a ppl- p -ppl aroclor system decreases by a factor of two as frequency is increased from 60 Hz to 20 kHz. (see Figure 4-16). A similar characteristic is anticipated for ppl-silicone oil systems. For gas impregnated dielectric systems, no decrease in corona extinction voltage (or corona initiation voltage, which is the same as the corona extinction voltage in this case) is observed until a frequency of about 30 kHz is reached.[15]

Using the corona extinction voltage for a particular dielectric system as the peak operating voltage for that system then the energy storge capability of the elements can be obtained from data like that shown in Figure 4-17. These energy densities must, of course, be reduced by a suitable factor to determine the capacitor energy storage capability. When this is done and the corona and heating effects are both taken into account, results of the type shown in Figure 4-18 are obtained.

The end result of these considerations is that, with the data presently available, the polypropelene-silicone oil dielectric system provides the highest energy density for the inverter capacitor over the range of operating conditions anticipated. This energy density is limited by corona effects rather than by heating effects. When the active elements are packaged to make a capacitor, the energy density in the finished capacitor is, of course, lower than that of the active elements. It will undoubtedly be necessary to use an extended foil construction technique in fabricating these capacitors. In addition, because of the high frequencies and high current levels present in the inverter resonant circuit, it will probably be necessary to use Litz wire leads on the capacitors. It may be necessary to "fan out" the individual strands of the Litz wires so that large-area connections can be made to the active elements. When these factors are taken into account, it appears likely that the overall energy density of a capacitor may be a factor of two lower than the energy density of the active elements. Using this factor of two, then an empirical relation for the energy density of a polypropelene-silicone oil inverter capacitor can be established. This relation is

$$D = \frac{15.5}{f_i^{0.28}} \quad \text{joules/lb.}$$

Once more, it is pointed out that this energy density is limited by corona effects rather than by heating elements. The above relation for the inverter capacitor energy density will be used to determine the specific weights of the inverter capacitors after the capacitor energy storage requirements have been determined.

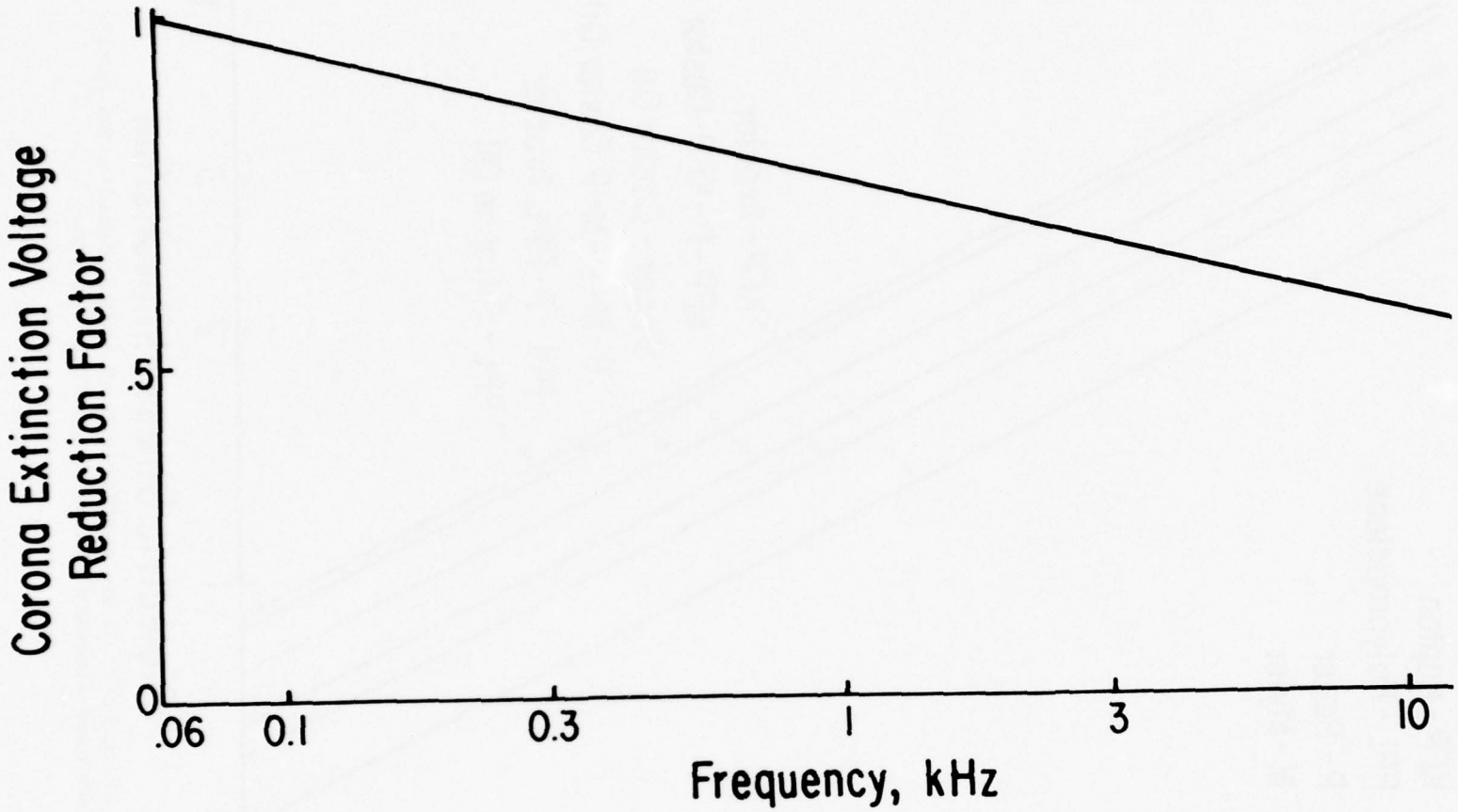


Figure 4-16 Factor by which corona extinction voltage is decreased (relative to value at 60Hz) as a function of frequency

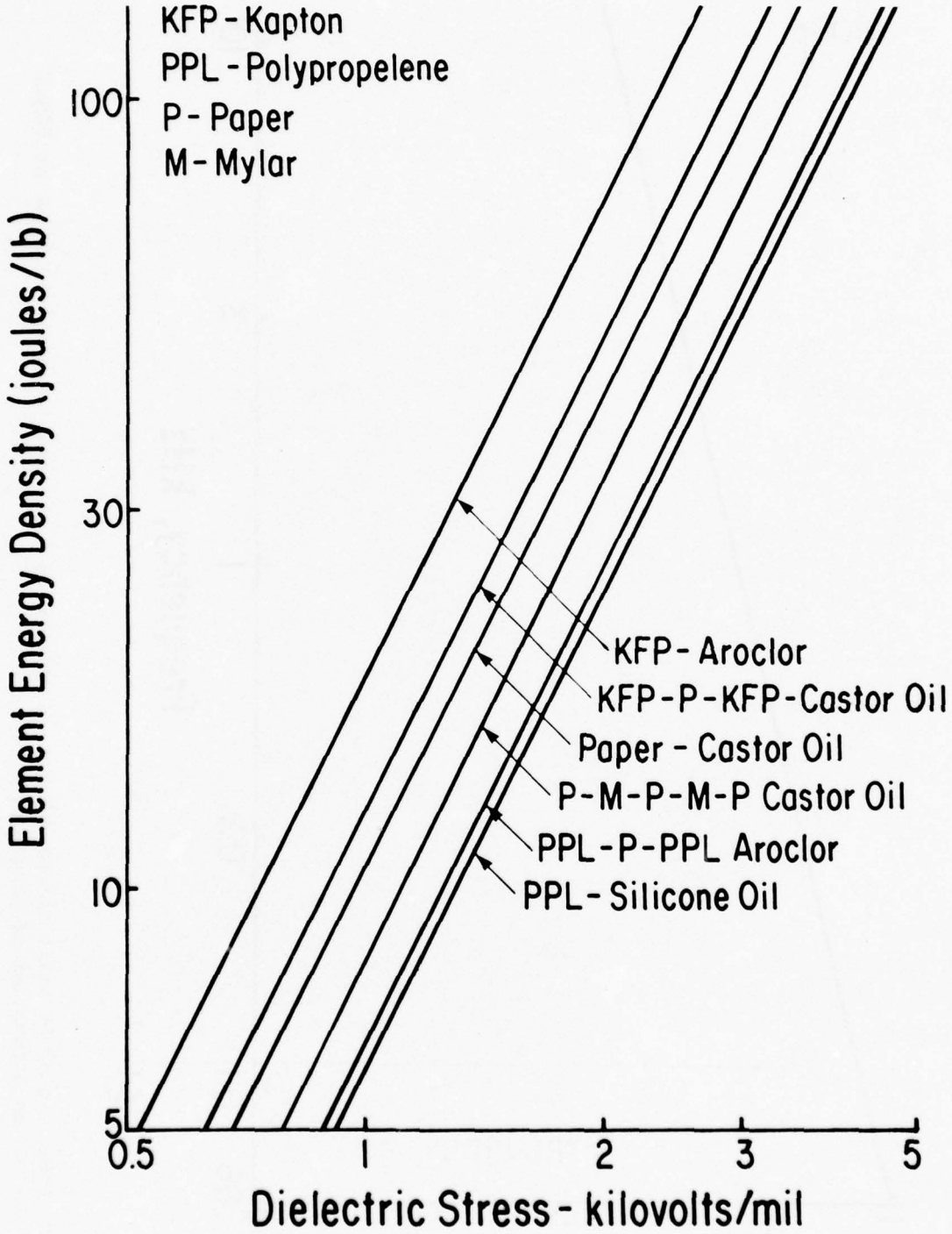


Figure 4-17 Dielectric stress coefficient of energy density (of active storage elements) Maxwell Laboratories Inc.

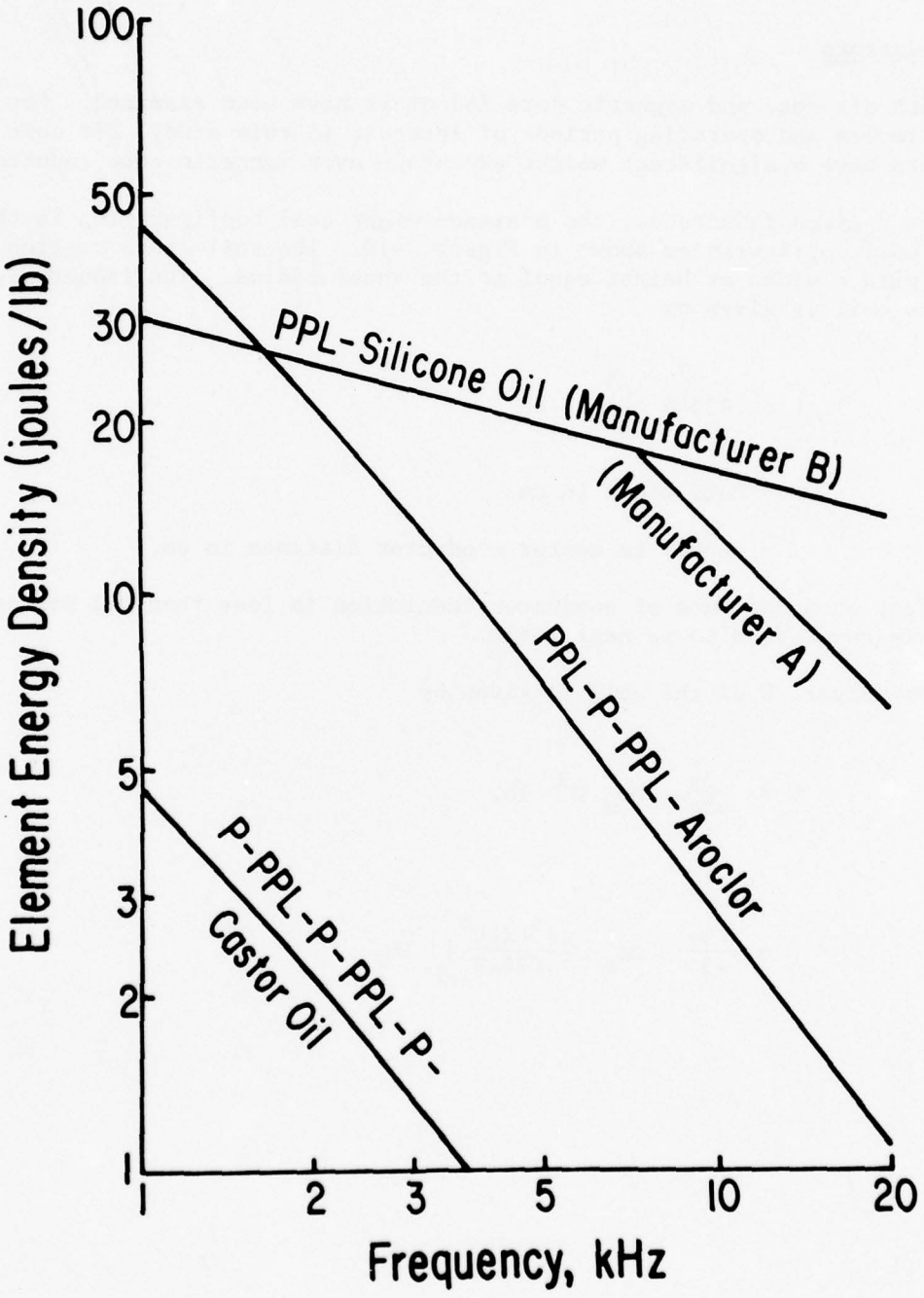


Figure 4-18 Composite maximum energy density (of active elements) as a function of frequency for an ambient temperature of 160°F (71°C) and a mission duration of 120 seconds.

D. Inductors

Both air-core and magnetic core inductors have been examined. For the energy levels and operating periods of interest in this study, air core inductors have a significant weight advantage over magnetic core inductors.

For a given inductance, the minimum-weight coil configuration is the Brooks coil configuration shown in Figure 4-19. The coil cross section is square with a width or height equal to the inner radius. The inductance of a Brooks coil is given by

$$L = .02549 \frac{C^5}{\delta^4} \quad \mu H$$

where C = coil width in cm

δ = center to center conductor distance in cm.

The effect on inductance of conductor insulation is less than 0.1 per cent and so is considered to be negligible.

The weight, W of the coil is given by

$$W = \frac{3\pi}{454} m\rho_m C^3 \quad lb.$$

$$= \frac{3\pi}{454} m\rho_m \left[\frac{\delta^4 L x 10^6}{.02549}\right] \quad lb.$$

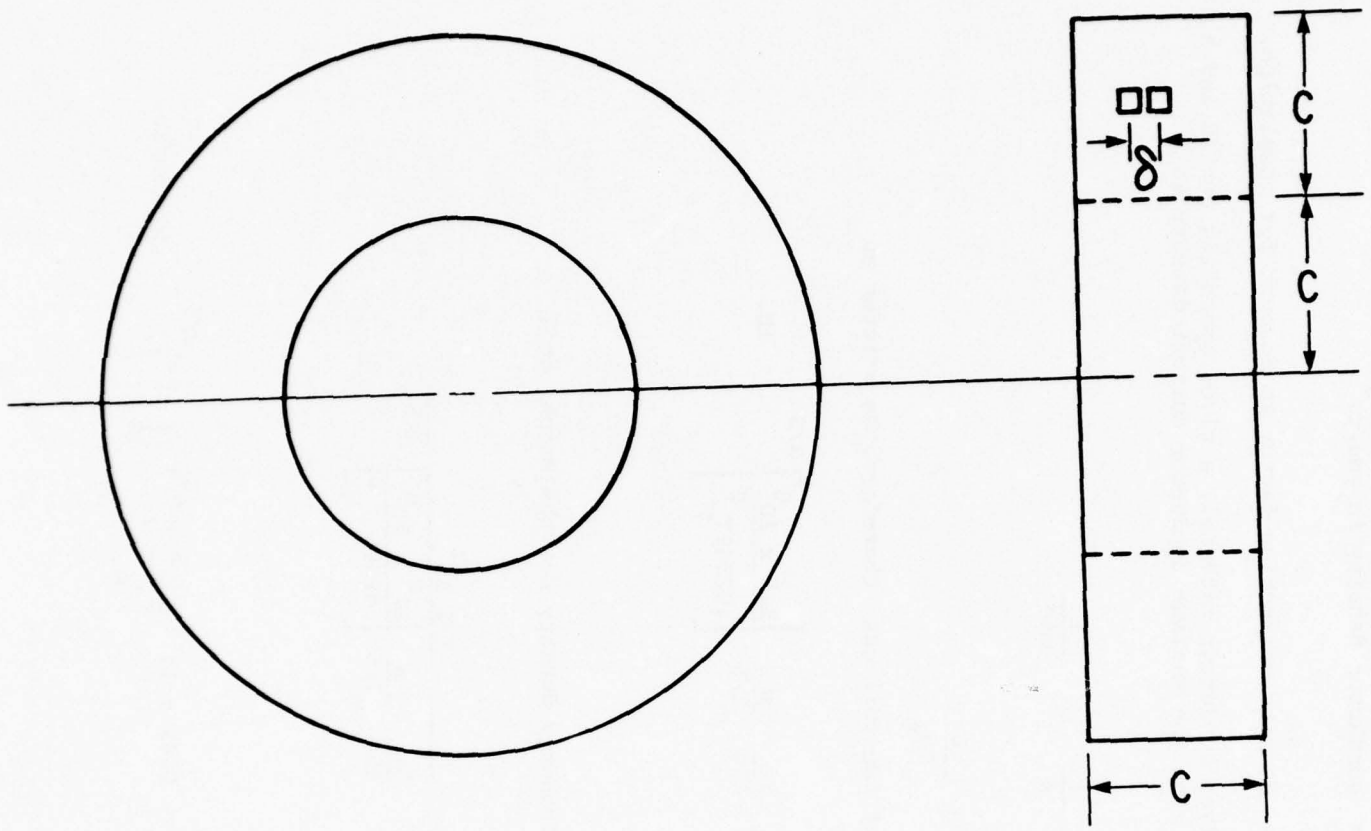


Figure 4-19 Brooks coil[19] configuration for minimizing weight of inductor.

where ρ_m = conductor density in gms/cm^3

and m = density correction factor to account for insulation.

For a given conductor material, a given operating period and a given temperature rise the maximum conductor current density is

$$J_m = \frac{I}{A} = \frac{I}{m\delta^2}$$

so $$\delta^2 = \frac{I}{mJ_m}$$

The weight of the coil can, therefore, be written as

$$W = \frac{3\pi}{454} \frac{\rho_m}{m^{1/5}} \left[\frac{LI^2 \times 10^6}{.02549 J_m^2}\right]^{3/5} \quad \text{lb.}$$

Now, the energy density for the Brooks coil is

$$D_L = \frac{1/2\ LI^2}{\frac{3\pi}{454} \frac{\rho_m}{m^{1/5}} \left[\frac{LI^2 \times 10^6}{.02549\ J_m^2}\right]^{3/5}}$$

or

$$D_L = 8.83 \times 10^{-4} \frac{m^{1/5}}{\rho_m} J_m^{6/5} \left(\frac{1}{2} LI^2\right)^{2/5} \quad \text{joules/lb.}$$

For an ambient temperature of 160°F(71°C) and a final conductor temperature of 500°F(260°C) the maximum current densities, J_m, for aluminum and copper are shown in Figure 4-20 and are given by

$$J_m \text{ (copper)} = 2080 \left(\frac{\tau}{60}\right)^{-\frac{1}{2}} \text{ A/cm}^2$$

and $$J_m \text{ (aluminum)} = 1336 \left(\frac{\tau}{60}\right)^{-\frac{1}{2}} \text{ A/cm}^2$$

The ratio of the 1.2 power of current density to conductor density required for the energy density calculation is

$$\frac{J_m^{6/5}}{\rho_m} \text{ (copper)} = 1070 \left(\frac{\tau}{60}\right)^{-3/5}$$

$$\frac{J_m^{6/5}}{\rho_m} \text{ (aluminum)} = 2087 \left(\frac{\tau}{60}\right)^{-3/5}$$

Thus, to maximize energy density, aluminum conductors should be selected. With aluminum, the energy density of the Brooks coil is

$$D_L = 1.84\, m^{1/5} \left(\frac{\tau}{60}\right)^{-3/5} \left(\frac{1}{2} LI^2\right)^{2/5} \text{ joules/lb.}$$

This equation is plotted in Figure 4-21 for a value of m of 0.9. (The actual value of m, as long as it is near unity makes little difference because of the one fifth power exponent). Note that the energy density for an operating time of 60 seconds and an energy content of 1000 joules is about 25 joules/lb.

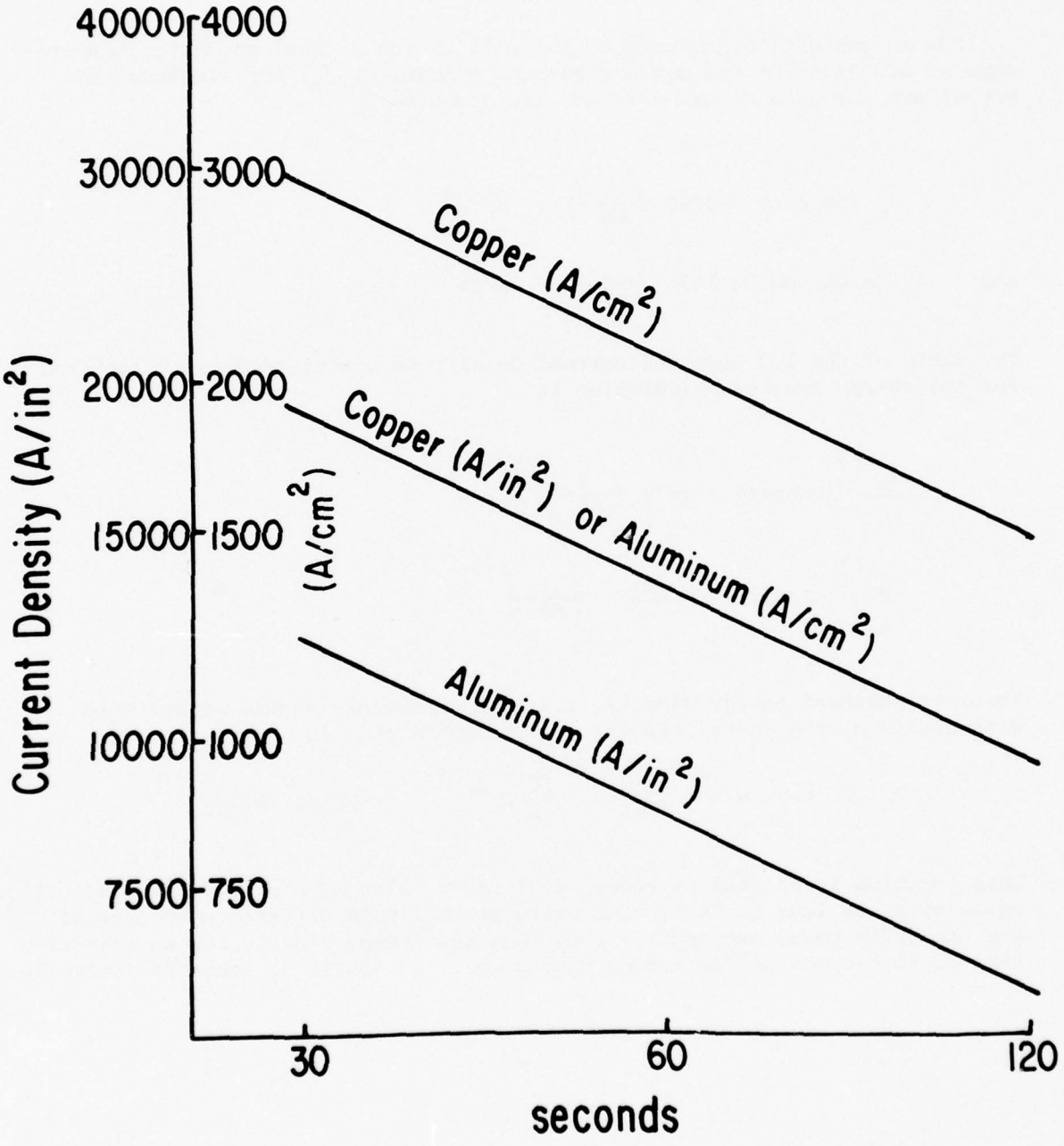


Figure 4-20 Allowable current density in copper or aluminum as a function of operating time for an ambient temperature of 160°F(71°C) and a final conductor temperature of 500°F (260°C).

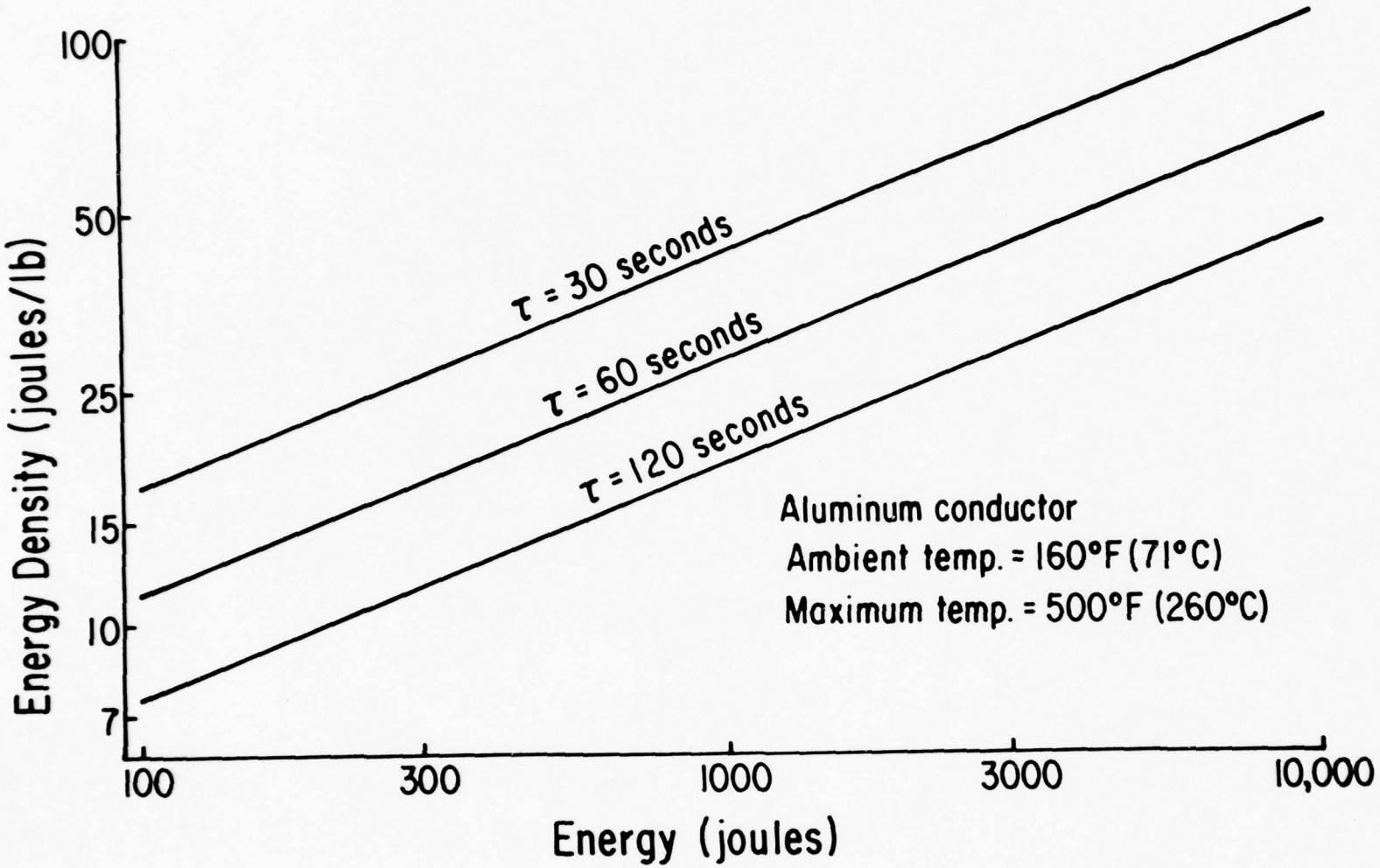


Figure 4-21 Maximum energy density as a function of energy content for an aluminum Brooks coil operating for 30, 60 or 120 seconds.

V. SUBSYSTEM ANALYSES

A. Inverter

Inverters of both the parallel and the series type were investigated. Series inverters were selected for final detailed analysis because of their anticipated high efficiency and light weight. The two types of series inverters given primary consideration were the full bridge transformer type shown in Figure 5-1 and the full bridge transformerless type (23) shown in Figure 5-2. For the inverter circuit shown in Figure 5-1 the series inductance for the resonant circuit is assumed to be distributed between the leakage inductance of the transformer and that of the dv/dt limiting coils.

To provide a basis for comparing, consideration must be given to the circuit voltages and currents and to the energy stored in the various circuit components.

To insure oscillation of the transformer-type inverter circuit, the peak value of the ac voltage across the capacitor must be above a certain minimum value. This is

$$V_p \geqslant \frac{1}{2} \text{ Vs.}$$

Thus, the minimum value for the peak energy stored in the capacitors of the transformer-type inverter is

$$\frac{1}{2} \text{ C } \left(\frac{V_s}{2}\right)^2 = \frac{1}{8} \text{ C } V_s^2$$

Now, the specific weight of the capacitor in the transformer-type inverter can be determined by examining the energy per half cycle E_L of inverter operation that must be delivered to the load.

This is

$$E_L = \frac{V_s I_s}{2f_i}$$

$$= \frac{1}{\pi} \quad \frac{V_s I_p}{f_i}$$

$$= \frac{1}{\pi} \quad \frac{V_s V_p}{f_i} \sqrt{\frac{C}{L}}$$

$$= 2 \text{ C } V_s V_p$$

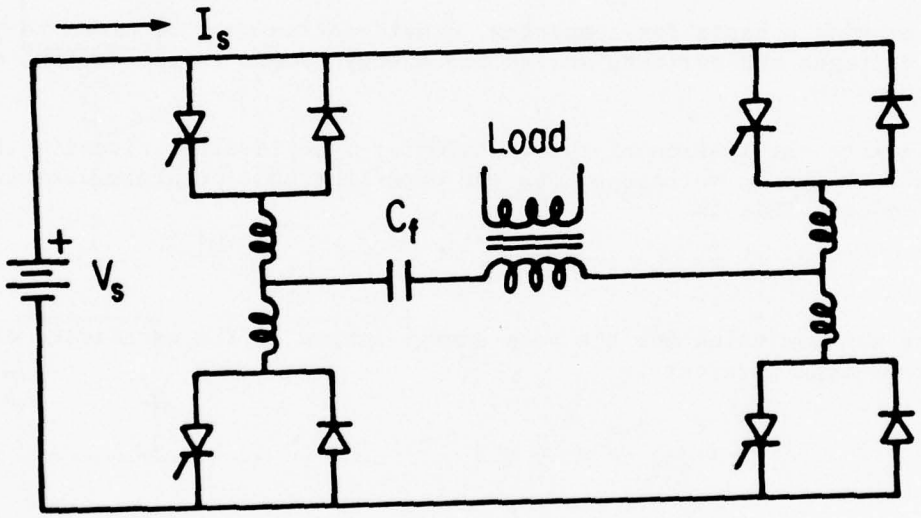


Figure 5-1 Series resonant inverter containing a transformer.

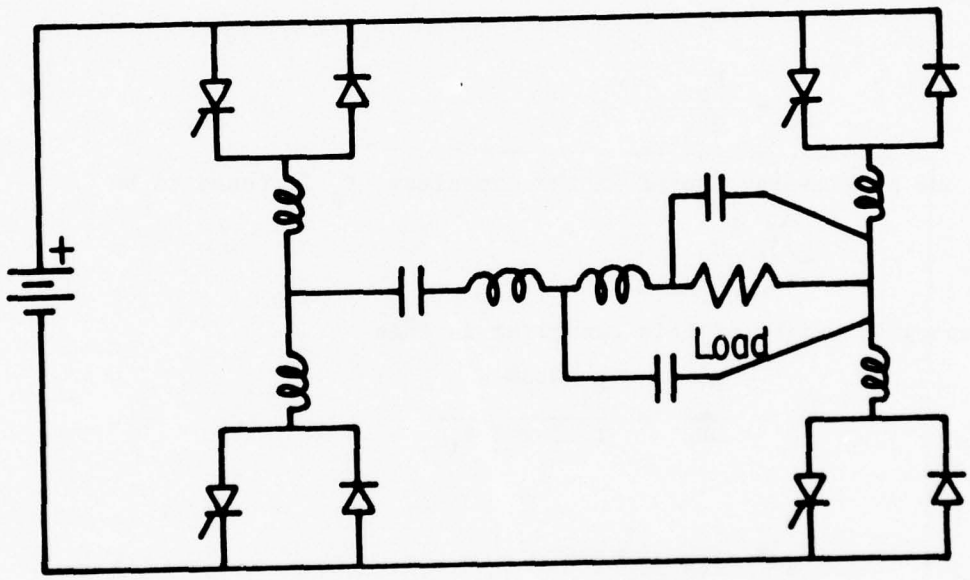


Figure 5-2 Full bridge transformerless Inverter

So

$$E_L \geq CV_s^2.$$

The specific weight of this capacitor may be determined by examining the peak energy stored in it and by using the energy density for the inverter capacitor. The minimum peak energy was found to be $1/8\ C\ V_s^2$. Increasing this by a factor of two to account for voltage transients and using

$$C = \frac{E_L}{V_s^2}$$

Where

$$E_L = \frac{P_o}{2f_i}$$

Then the peak energy stored in the capacitor, E_p is found to be

$$E_p = \frac{P_o}{8f_i}$$

The specific weight of this capacitor is then

$$S_c = \frac{E_p}{DP_o} = \frac{f_i^{0.28}}{15.5 \times 8\ f_i}$$

or

$$S_c = \frac{1}{124\ f_i^{0.72}}$$

where f_i is the inversion frequency in kHz.

The only other element of significance in the transformer inverter shown in Figure 5-1 is the transformer.

Next, a comparison between the full bridge transformer-type and transformerless inverters must be made. The difference between the two is obvious from Figures 5-1 and 5-2. The transformer in one is replaced by capacitors and inductors in the other. From an operational point of view, there appears to be no substantial difference between the two units. It should be pointed out, however, that the transformer-type inverter has been under development for several years and the analysis of its operation including its ability to achieve precise load regulation has been reported in the literature.[1-13] Because of these factors its adaption to high power levels may be more readily accomplished than the development of the transformerless type.

Judging from the information available concerning the transformerless inverter, the specific weight of this unit is essentially the same as that of the transformer-type unit. This is demonstrated by comparing the specific weight of the capacitors and inductors of the transformerless inverter with the specific weight of the capacitor and transformer in the transformer-type unit. From reference 23 the peak energy stored in the capacitors of a 10 MW 10 kHz transformerless inverter would be 786 joules. The energy stored in the inductors would be 1130 joules. (These levels would vary slightly with voltage level and would scale directly with output power). Using an energy density for the capacitor of 8 joules/lb and for the inductor of 25 joules/lb (estimated in a previous section of this report) then the specific weight of the transformerless inverter reactive elements is .014 lb/kW. For a 10 kHz transformer-type inverter, the specific weight of the transformer and the series capacitor would be approximately .01 lb/kW. Thus, since the main part of the weight of either inverter is in the thyristor and diode packages, and these are the same for both inverters, the weights of the two inverters would be essentially the same.

In summary, at this point in time, because of development experience and analyses performed, it appears that the transformer-type inverter should be selected for development.

B. Rectifier and Filter

Before it is possible to define the filtering requirements of a power conditioning system it is necessary, of course, to describe the waveform that must be processed by the filter and to define the load ripple requirement. At this point in this power conditioning study, the load ripple requirement has not been defined and so it must be left as an input parameter to be supplied by the high power system designer.

On the other hand, the waveforms that must be processed by the filter can be described reasonably well. The waveforms resulting from the rectification of the outputs of three phase alternators and of inverters are described in the following sections. Then, the specific weights and the energy contents of L-C and π filters are analyzed. Some attention is paid to the minimization of weight or of energy and the penalties that result from the minimization of one or the other.

1. Alternator Power Rectification

When the output of a three phase alternator (or three-phase alternator/transformer package) is full wave rectified the resulting average voltage (divided by the line to line rms voltage) can be expressed by the following empirical relations (from Appendix C).

When $\alpha < \beta$

$$\frac{V_{avg}}{V_{l\text{-}lrms}} = 1.350 \cos (.660\,\alpha + 2 \times 10^{-5}\alpha^3) \cos (.692\beta + .07\alpha)$$

and when $\alpha \geq \beta$

$$\frac{V_{avg}}{V_{l\text{-}lrms}} = 1.350 \cos (.660\,\alpha + 2 \times 10^{-5}\alpha^3) \cos (.699\alpha)$$

where α is the firing angle of the SCR's in the rectifier and β is the conduction overlap angle.

Similarly, the 6th harmonic ripple factor (the rms value of the 6th harmonic voltage divided by the average voltage) can be expressed by the following empirical relations (from Appendix C).

when $\alpha < \beta$

$$r_6 = .01 \left\{ .217\beta - .04\alpha + \left[2 + 3.3\left(\frac{\alpha}{30}\right)^2\right] \sin \left[\left(6.32 + \alpha^{.15}\right) (\beta-\alpha)\right] \right.$$

$$\left. + \left[4.1 + 38.8\left(\frac{\alpha}{60}\right)^2 - .217\beta + 1.5 \sin 5\beta + .04\alpha\right] e^{-\frac{\beta-\alpha}{8.5+\frac{\sqrt{\alpha}}{1.5}}} \right.$$

and when $\alpha \geq \beta$ then

$$r_6 = .01 \left[4.1 + 38.8 \left(\frac{\alpha}{60}\right)^2 + 1.5 \sin 5\alpha\right] .$$

These empirical relations for V_{AVG} and r_6 provide an excellent characterization of the waveform to be processed by the filter used with the bridge.

When the load regulation requirement is limited to a few percent and the conduction overlap angle is 45°, the value of r_6 is approximately .08. Curves showing the amplitudes of the 12th and the 18th harmonic ripple factors are given in Appendix C. Empirical relations for these harmonics have not been developed because the amplitudes of these harmonics are substantially below that of the fundamental after filtering.

At this point it should be mentioned that if two three phase transformers are used with an alternator then some reduction in the ripple percentage can be achieved. This is done by using one of the transformers in a wye-wye configuration and the other in a wye-delta configuration. The ripple-voltage waveforms produced by three-phase full-wave rectifiers connected to these transformers will have a thirty degree phase difference. Thus, the 6th and 18th harmonic ripple voltages will cancel. Unfortunately, however, the 12th harmonic ripple voltages will add in phase. Now a filtering section (such as the L-C filter discussed in the following section) will have twice as much attenuation at the 12th harmonic as it has at the 6th harmonic. Thus, the 12th harmonic voltage level at the output of the filter will be the same for the two transformer system (one wye-wye and the other wye-delta) af for the single transformer system. The 6th and 18th harmonic voltage, will, however, be absent.

2. L-C Filter Analysis

The following section contains an analysis of the design of a simple L-C filter for use in attenuating the ripple voltages from the rectifier used with an alternator or alternator/transformer package. As is indicated in Figure 5-3, the rms load ripple factor, r_ℓ, is related to the ripple factor at the input of the filter, r_i, by

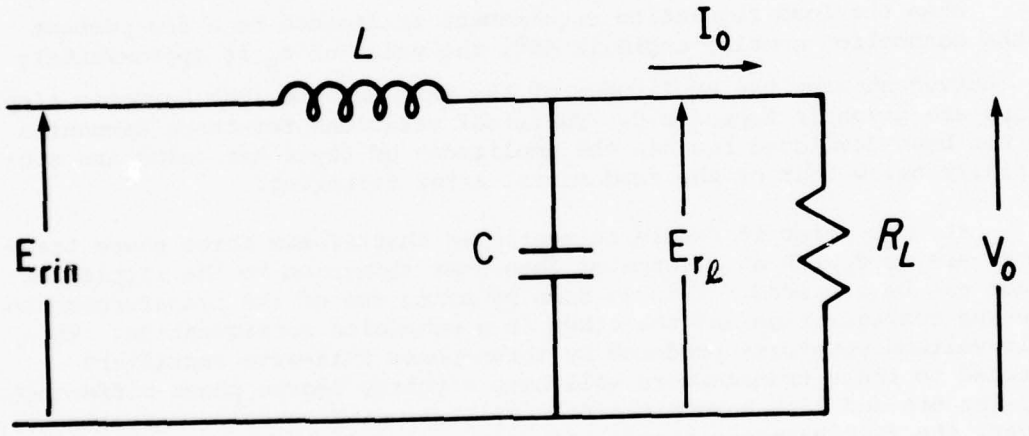


Figure 5-3 L-C Filter

$$r_\ell = \frac{E_{r\ell}}{V_o} \approx \frac{X_c}{X_L} \frac{E_{ri}}{V_o} = \frac{X_c}{X_L} r_i = r_r r_i$$

where V_o = dc load voltage

$E_{r\ell}$ = rms load ripple voltage

E_{ri} = rms input ripple voltage

r_r = ripple reduction factor

The above relations are approximately correct as long as the ripple frequency, f_r, does not coincide with the resonant frequency of the L-C section.

The specific weight of this filter may be determined by considering the energy stored and the energy density of each component. The energy stored in the capacitor is

$$E_c = \frac{1}{2} C V_o^2$$

and the energy stored in the inductor is

$$E_L = \frac{1}{2} LI^2 = \frac{1}{2} L \left(\frac{P_o}{V_o}\right)^2 \times 10^6 \quad (P_o \text{ in kW})$$

The total energy stored in the filter is

$$E = \frac{1}{2} C V_o^2 + \frac{1}{2} L \left(\frac{P_o}{V_o}\right)^2 \times 10^6 \text{ joules}$$

The energy density of C is D_c joules/lb. and the energy density of L is D_L joules/lb. The power delivered to the load is P_o kW so that the specific weight of the capacitor is

$$S_c = \frac{E_c}{P_o D_c} \text{ lb/kW}$$

and of the inductor is

$$S_L = \frac{E_L}{P_o D_L} \qquad \text{lb/kW}$$

The specific weight of the filter is

$$S_{Lc} = \frac{C V_o^2}{2 D_c P_o} + \frac{L P_o^2}{2 D_L V_o} \times 10^6 \qquad \text{lb/kW.}$$

For a given power and voltage level, and for given component energy densities, S_{Lc} is a function of L and C. Now L and C are related to r_r, the ripple reduction factor. That is

$$r_r \approx \frac{X_c}{X_L} = \frac{10^{-6}}{(2\pi f_r)^2 LC} \qquad (f_r \text{ in kHz}).$$

so that the specific weight of the filter can be written as

$$S_{Lc} = \frac{C V_o^2}{2 D_c P_o} + \frac{P_o}{2 D_L V_o^2 (2\pi f_r)^2 r_r C} \qquad \text{lb/kW.}$$

This specific weight can be minimized simply by taking the derivative with respect to the capacitance and setting the result equal to zero. The resulting expression for the capacitance that minimizes the specific weight is

$$C_{min(s)} = \frac{P_o}{2\pi f_r V_o^2} \left(\frac{D_c}{r_r D_L}\right)^{1/2}$$

The capacitance that minimizes the specific weight is normally not the same as the one that minimizes the filter energy (also to be considered in this section) so the above capacitance is indicated by Cmin(s).

By substituting Cmin(s) for C in the filter specific weight equation, the minimum specific weight is found to be

$$S_{Lc\ min} = \frac{1}{2\pi f_r} \left(\frac{1}{r_r D_L D_c}\right)^{1/2} \qquad \text{lb/kW}$$

and the specific weight as a function of capacitance can be written in normalized form as

$$\frac{S_{Lc}}{S_{Lc\ min}} = \frac{1}{2}\ \frac{C}{C_{min(s)}} + \frac{1}{2}\ \frac{C_{min(s)}}{C}$$

In some cases, it may be desirable to minimize the energy of the L-C filter rather than the specific weight (because of load fault considerations for example) or it may be desirable to consider a compromise between the minimum energy and the minimum specific weight conditions. The minimum energy condition can be determined by following a procedure identical to that used for the specific weight. When this is done, it is found that the capacitance that minimizes the energy is given by

$$C_{min(E)} = \frac{P_o}{2\pi f_r V_o^2}\left(\frac{1}{r_r}\right)^{1/2}$$

The minimum energy is

$$E_{min} = \frac{P_o}{2\pi f_r}\left(\frac{1}{r_r}\right)^{1/2}$$

and the energy as a function of capacitance written in normalized form is

$$\frac{E}{E_{min}} = \frac{1}{2}\ \frac{C}{C_{min(E)}} + \frac{1}{2}\ \frac{C_{min(E)}}{C}$$

The curves in Figure 5-4 are plots of normalized specific weight and energy as functions of capacitance (normalized with respect to Cmin(s)). The ratio of Cmin(E) to Cmin(S) is

$$\frac{C_{min(E)}}{C_{min(s)}} = \left(\frac{D_L}{D_c}\right)^{1/2}$$

and values of D_L of 25 joules/lb and Dc of 100 joules/lb have been used. Notice that, for this particular example, if the specific weight is minimized, then the energy is 25 per cent above the minimum value. Similarly if the energy is minimized, the specific weight is 25 per cent above its minimum value. If, however, the value of capacitance that causes the two curves to cross is used, then the specific weight and the energy are only about 6 per cent above their minimum values.

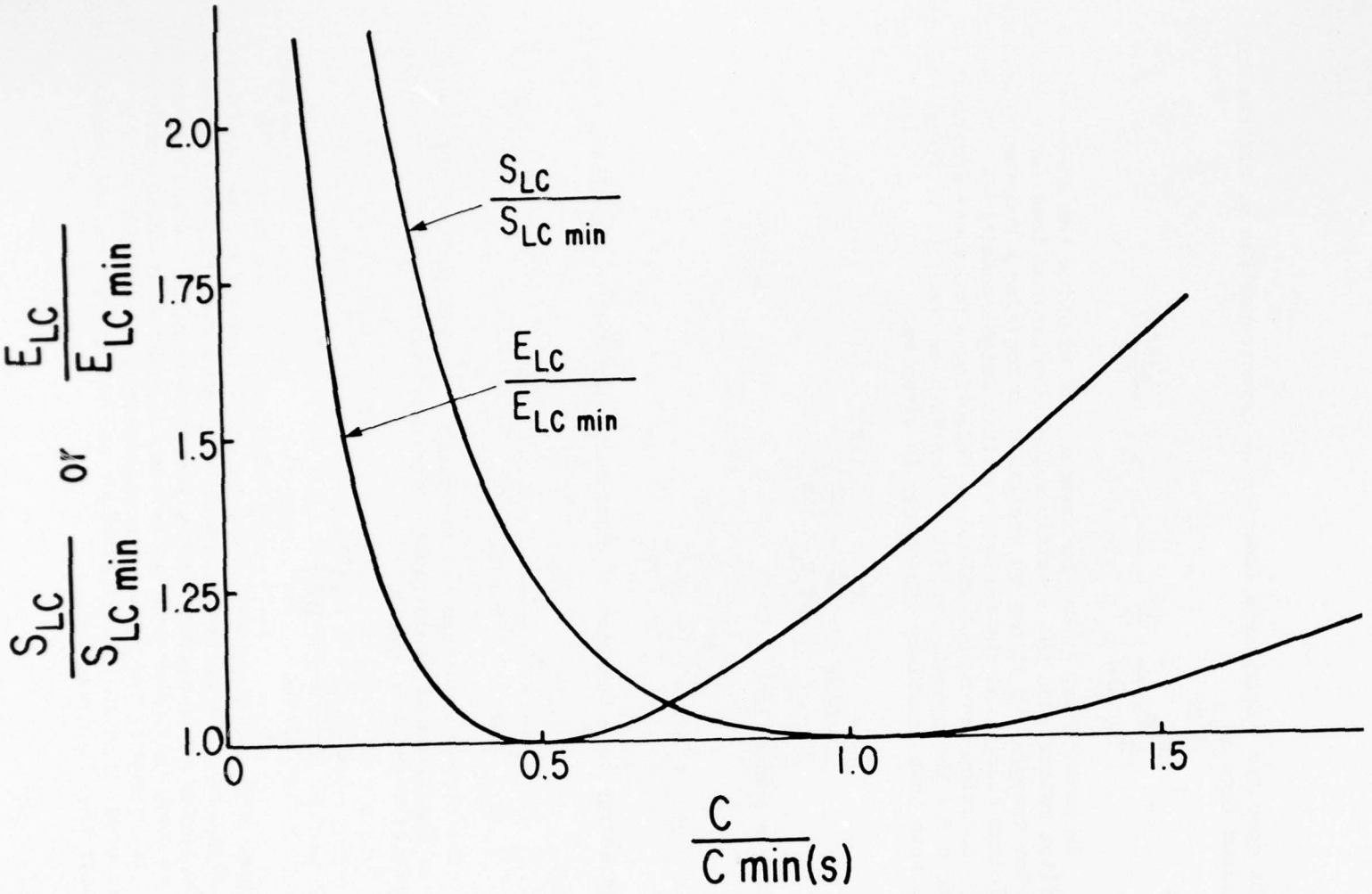


Figure 5-4 Normalized specific weight and energy as functions of capacitance.

As an example of the use of the specific weight and energy equations for an L-C filter, consider a requirement to reduce the ripple of a rectifier by a factor of eight (for example, from eight per cent for a three phase full wave bridge with a 45° conduction overlap to one per cent required by a load). If the alternator frequency is 0.5 kHz, D_L is 25 joules/lb and Dc is 100 joules/lb. Then

$$S_{Lc\ min} = \frac{1}{2\pi \times 3} \left(\frac{1}{0.1 \times 25 \times 100}\right)^{1/2}$$

or

$$S_{Lc\ min} = 3 \times 10^{-3} \quad \text{lb/kW.}$$

For an output power of 25000 kW the minimum energy is

$$E_{min} = \frac{25000}{2\pi \times 3} \left(\frac{1}{0.1}\right)^{1/2}$$

or E_{min} = 3750 joules

For an output voltage of 60,000 volts,

$$C_{min(s)} = 2.08\ \mu f$$

and

$$C_{min(E)} = 1.04\ \mu f.$$

3. Inverter Power Rectification

The output of the series inverter may be full-wave rectified with a bridge rectifier and then filtered as shown in Figure 5-5. The purpose of this section is to describe the waveform of the ripple voltage at the output of the bridge rectifier. Under fully loaded conditions the approximate current waveform in the primary winding of the transformer in Figure 5-5 is as shown in Figure 5-6 (a).[1] The approximate current waveform after rectification is shown in Figure 5-6 (b). During load voltage regulation, the angle α is adjusted to control the average current supplied by the inverter. The angle α may also be modulated to reduce the effects of variations in the voltage supplied to the inverter.

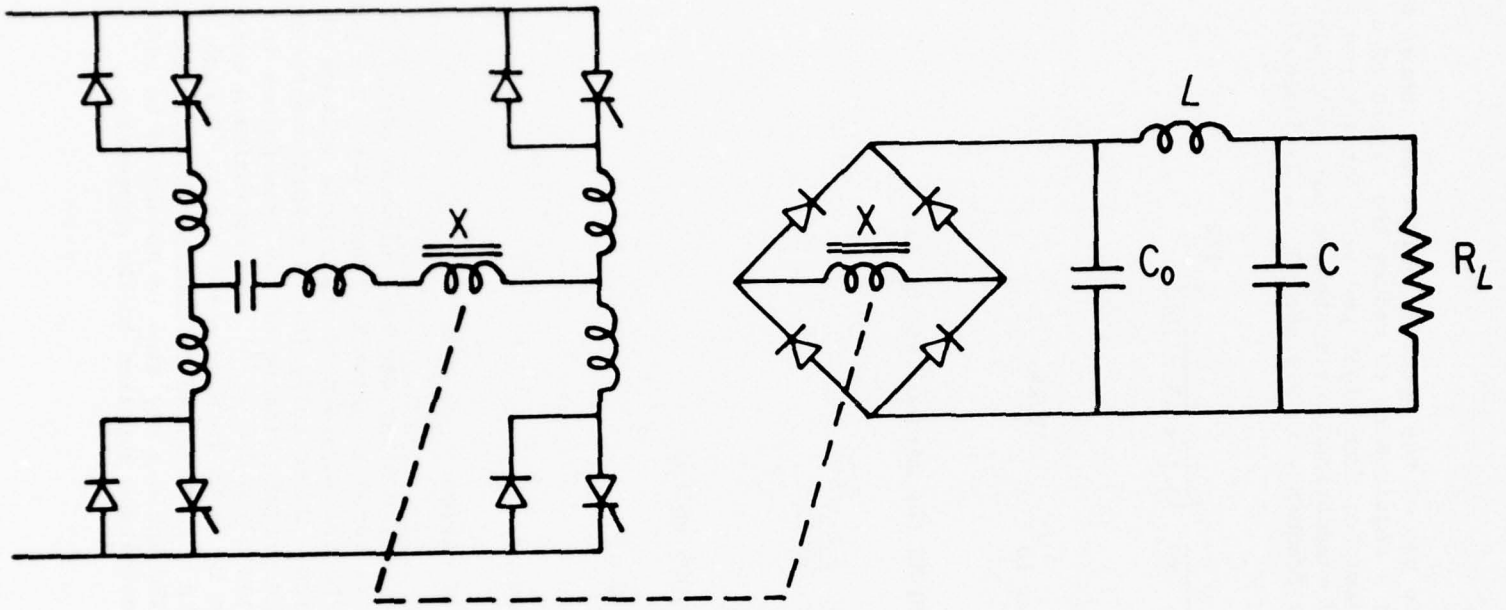


Figure 5-5 Full bridge series inverter with bridge rectifier and π filter.

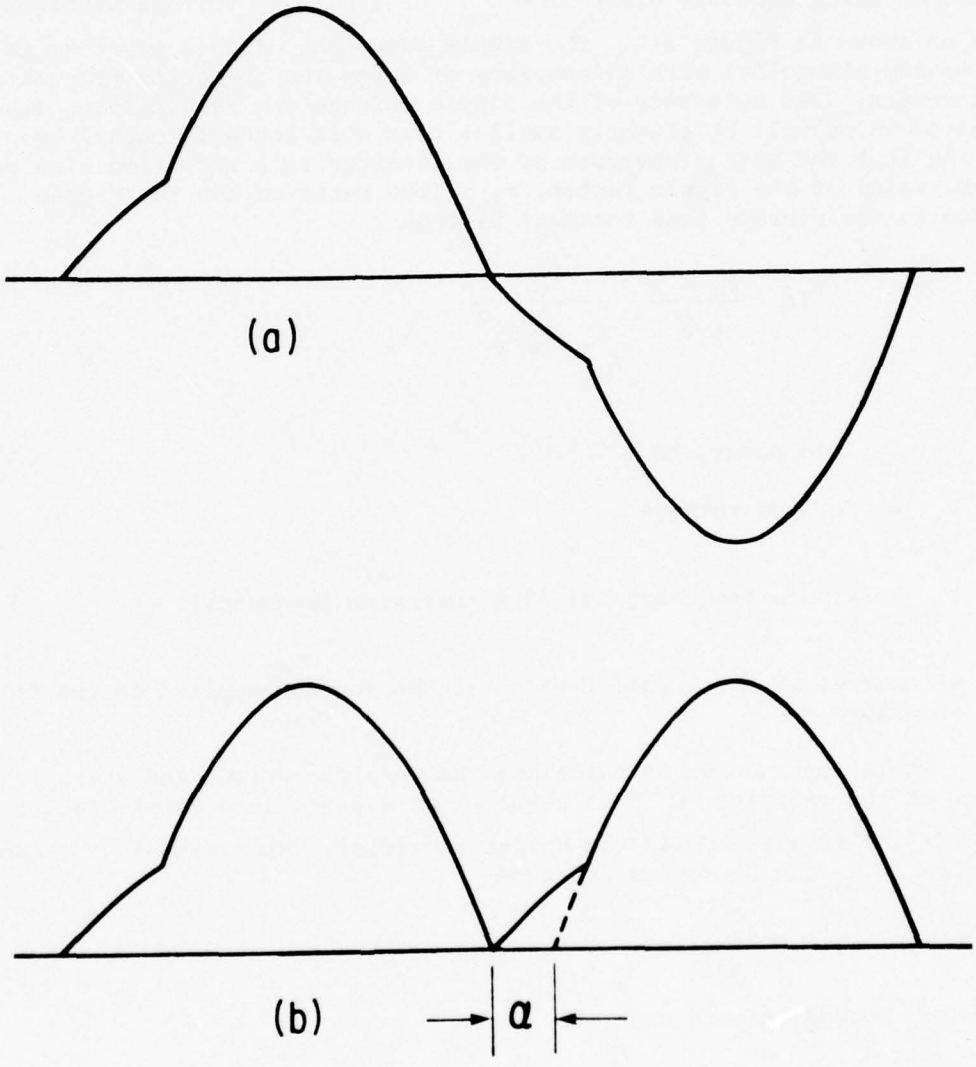


Figure 5-6 (a) Current waveform in primary of inverter transformer.

(b) Current waveform from bridge rectifier.

When the rectifier current is fed into capacitor C_o and load current is simultaneously drawn from C_o, the resulting voltage waveform on C_o is as shown in Figure 5-7. The ripple component of this waveform is very nearly sinusoidal with a frequency of twice the operating frequency of the inverter. The magnitude of the ripple voltage can be estimated (the estimated value will be slightly smaller than will actually occur) by assuming that the output waveform of the inverter is a rectified sine wave. The rms value of the ripple factor, r_{in}, (the ratio of the rms ripple voltage to the average load voltage) is then

$$r_{in} = \frac{\sqrt{2} - 1}{4\sqrt{2}} \quad \frac{P_o}{f_r C_o V_o^2}$$

where

P_o = load power, kW

V_o = dc load voltage

f_r = ripple frequency kHz (2 x inversion frequency).

This, of course, is the ripple factor for the voltage applied to the filter shown in Figure 5-7.

It is instructive to calculate the specific weight and energy content of the capacitor C_o that results for a given load ripple factor if no L-C filter is attached to the bridge rectifier. When this is the case, the value of C_o can be determined from

$$C_o = \frac{\sqrt{2} - 1}{4\sqrt{2}} \quad \frac{P_o}{f_r r_{in} V_o^2}$$

The energy stored in this capacitor is

$$E_{co} = \frac{1}{2} C_o V_o^2 = \frac{\sqrt{2} - 1}{8\sqrt{2}} \quad \frac{P_o}{f_r r_{in}} \quad \text{joules.}$$

If Dc is the energy density of C_o, then the specific weight of C_o is

$$S_{co} = \frac{\sqrt{2} - 1}{8\sqrt{2}} \quad \frac{1}{f_r r_{in} D_c} \quad \text{lb/kW.}$$

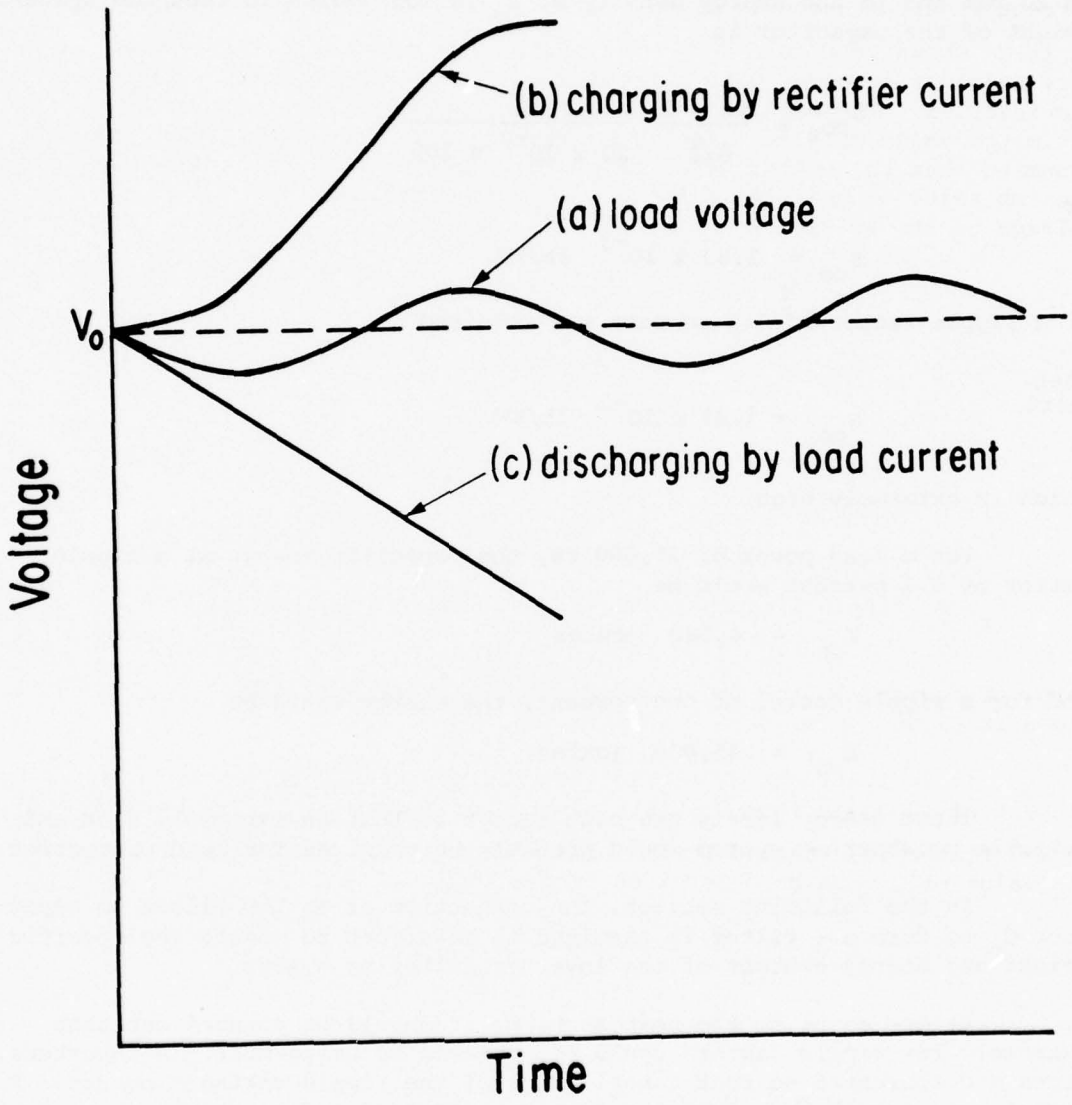


Figure 5-7 Voltage waveform appearing on capacitor Co (curve a) resulting from charging by rectifier current (curve b) and discharging by load current (curve c).

Now, if a ripple factor of one percent is required, if the ripple frequency is 20 kHz and if the energy density of C_o is 100 joules/lb then the specific weight of the capacitor is

$$S_{co} = \frac{\sqrt{2} - 1}{8\sqrt{2}} \quad \frac{1}{20 \times 10^{-2} \times 100}$$

or

$$S_{co} = 1.83 \times 10^{-3} \text{ lb/kW.}$$

If a ripple factor of 0.1 percent was required

Then

$$S_{co} = 1.83 \times 10^{-2} \text{ lb/kW.}$$

which is extermely high.

For a load power of 25,000 kW, the capacitor energy at a ripple factor of 0.1 percent would be

$$E_{co} = 4{,}580 \text{ joules}$$

and for a ripple factor of one percent, the energy would be

$$E_{co} = 45{,}800 \text{ joules.}$$

These energy levels are high enough so that an extremely fast and reliable crowbarring system would probably be required for load protection.

In the following section, the connection of an L-C filter to capacitor C_o to form a π filter is examined in an effort to reduce the specific weight and energy content of the inverter filtering system.

Before going to the next section, it should be pointed out that extremely low ripple factors could be achieved by using multiple inverters, timed and connected so that cancellation of the ripple voltages occurs. For example, in a two phase inverter system the second and sixth harmonic ripple components would add. In a three phase inverter system the second and fourth harmonic ripple components could be eliminated. The sixth harmonic component would add.

4. π Filter Analysis

The specific weight and energy of a π filter, as shown in Figure 5-5 can be determined as follows. The specific weight is

$$S_\pi = S_{co} + S_{LC}$$

where S_{co} and S_{LC} were given in previous sections. Thus

$$S_\pi = \frac{\sqrt{2}-1}{8\sqrt{2}\, f_r\, r_{in}\, D_c} + \frac{m}{2\pi\, f_r} \left(\frac{1}{r_r\, D_L\, D_c}\right)^{1/2}$$

where the factor m is included to take into account the possibility of energy minimization rather than specific weight minimization in the L-C filter. (For specific weight minimization, m = 1.0. For energy minimization, m >1.0).

Now the load ripple factor, r_ℓ, is the product of the input ripple factor, r_{in} and the ripple reduction factor r_r. Thus, the specific weight of the filter can be written in terms of the input and load ripple factors, i.e.

$$S_\pi = \frac{\sqrt{2}-1}{8\sqrt{2}\, f_r\, r_{in}\, D_c} + \frac{m}{2\pi f_r} \left(\frac{r_{in}}{r_\ell\, D_L\, D_c}\right)^{1/2}$$

Now, S_π may be minimized by giving consideration to the amount of filtering accomplished by C_o (which establishes r_{in}) and the amount accomplished by the L-C section. This minimization may be accomplished by taking the derivative of S_π with respect to r_{in} and setting the result equal to zero. When this is done, it is found that

$$r_{in\,(min,s)} = \frac{(\sqrt{2}-1)^{1/3}}{2} \left(\frac{\pi}{m}\right)^{2/3} \left(\frac{r_\ell\, D_L}{D_c}\right)^{1/3}$$

and that the minimum specific weight of the filter is

$$S_{\pi min} = \frac{3(\sqrt{2}-1)}{8\sqrt{2}\, f_r\, D_c\, r_{in\,(min,s)}}$$

or

$$S_{\pi min} = \frac{3(\sqrt{2}-1)^{1/3}}{4\sqrt{2}\, \left(\frac{\pi}{m}\right)^{2/3} f_r^{2/3}\, D_c^{2/3}\, \left(r_\ell\, D_I\right)^{1/3}}$$

The specific weight as a function of input ripple factor can be written in normalized form as

$$\frac{S_\pi}{S_\pi \text{min}} = \frac{1}{3}\,\frac{r_{in}\ (\text{min,s})}{r_{in}} + \frac{2}{3}\left(\frac{r_{in}}{r_{in}\ (\text{min,s})}\right)^{1/2}$$

The minimum energy condition can be determined by following a procedure identical to that used for the specific weight. The energy content of the π filter is given by

$$E_\pi = \frac{(\sqrt{2}-1)}{8\sqrt{2}}\,\frac{P_o}{f_r\, r_{in}} + \frac{n\ P_o}{2\pi\ f_r}\left(\frac{r_{in}}{r_\ell}\right)^{1/2}$$

where the factor n is included to account for a situation in which the energy of the L-C section is not minimized. (For energy minimization, n = 1.) The energy is minimum when

$$r_{in}\ (\text{min E}) = \frac{(\sqrt{2}-1)^{2/3}}{2}\left(\frac{\pi}{n}\right)^{2/3} r_\ell^{\,1/3}$$

and the value of the minimum energy is

$$E_\pi \text{min} = \frac{3(\sqrt{2}-1)^{1/3}\ P_o}{4\sqrt{2}\ \left(\frac{\pi}{n}\right)^{2/3} f_r\, r_\ell^{\,1/3}}$$

The energy as a function of the input ripple factor written in normalized form is

$$\frac{E_\pi}{E_\pi \text{min}} = \frac{1}{3}\,\frac{r_{in}\ (\text{min,E})}{r_{in}} + \frac{2}{3}\left(\frac{r_{in}}{r_{in}\ (\text{min,E})}\right)^{1/2}$$

The curves in Figure 5-8 are plots of normalized specific weight and energy as functions of input ripple factor (normalized with respect to r_{in} (min s). The ratio of r_{in}(min E) to r_{in} (min s) is

$$\frac{r_{in}\ (\text{min,E})}{r_{in}\ (\text{min,s})} = \left(\frac{m}{n}\right)^{2/3}\left(\frac{D_C}{D_L}\right)^{1/3}$$

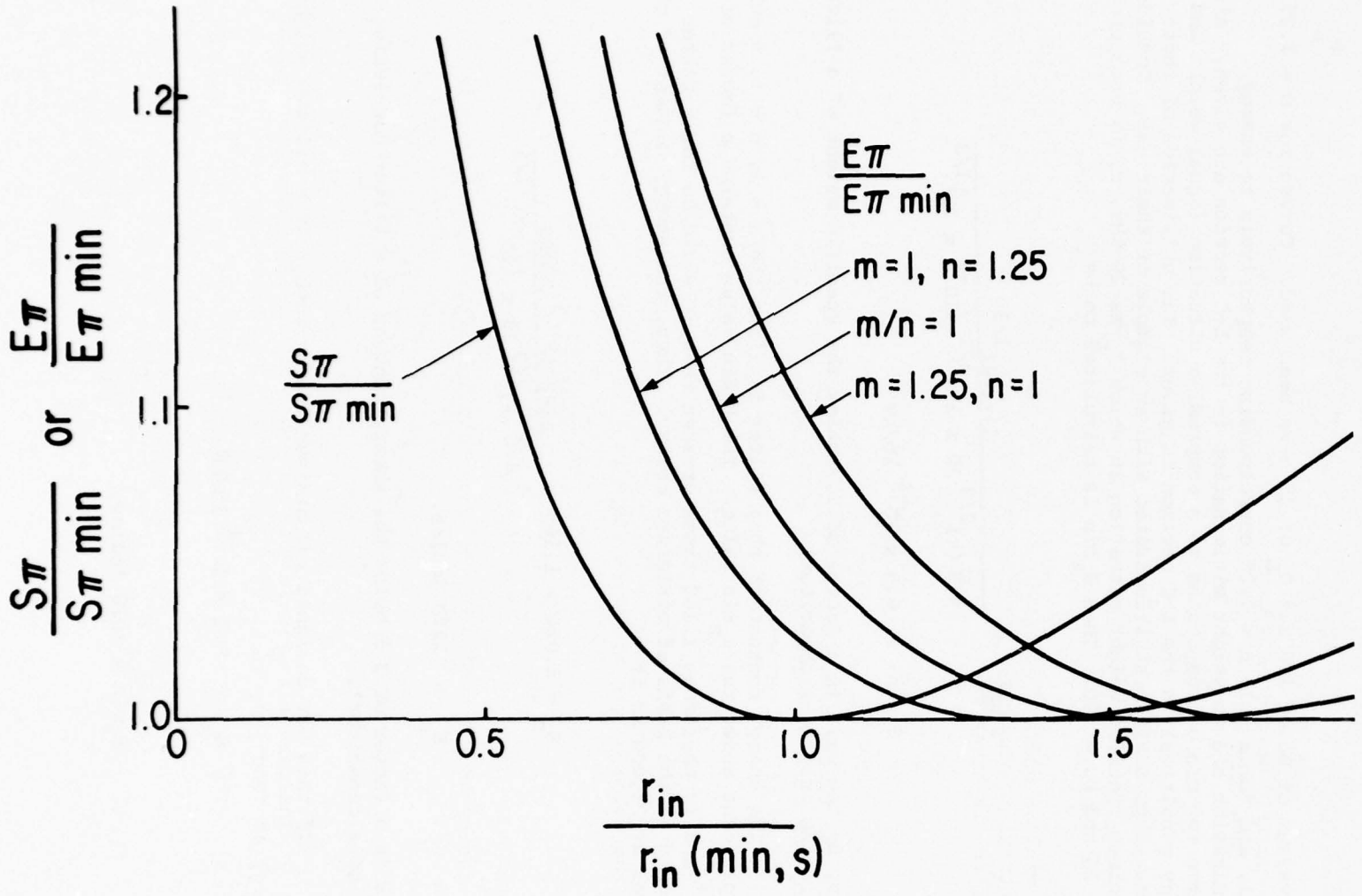


Figure 5-8 Normalized specific weight and energy as functions of input ripple factor.

and values of Dc of 100 and D_L of 25 have been used. Curves for m = 1.25, n = 1, and for m = 1, n = 1.25 corresponding respectively to energy minimization and to weight minimization in the L-C section are given. Also a curve for m/n corresponding to a compromise situation (equal weight and energy penalties) in the L-C section is given. The utilization of these curves is probably best illustrated with an example of their use. Consider a minimum specific weight situation in which f_r is 20 kHz, r_ℓ is one percent, D_L = 25 and Dc = 100. Then $S_\pi min$ is calculated to be

$$S_\pi min = \frac{3\left(\sqrt{2}-1\right)^{1/3}}{4\sqrt{2}\,(\pi)^{2/3}\,20 \times 100^{2/3}\left(10^{-2} \times 25\right)^{1/3}}$$

or

$$S_\pi min = 6.8 \times 10^{-4} \text{ lb/kW}$$

(This, by the way, is a factor of 2.7 below the specific weight of a filter consisting only of a capacitor).

The energy content of this filter is (from the m = 1, n = 1.25 curve) 2.6 per cent above the $E_\pi min$ value. The $E_\pi min$ value contains a factor of $n^{2/3}$ and is therefore 1.160 times greater than it would be for a filter designed on the basis of minimized energy. Thus, the energy content of this filter at 25,000 kW is

$$E_\pi = 1.026 \times 1.160 \times \frac{3\left(\sqrt{2}-1\right)^{1/3}\,25000}{4\sqrt{2}\,(\pi)^{2/3}\,20 \times \left(10^{-2}\right)^{1/3}}$$

or

$$E_\pi = 1270 \text{ joules.}$$

(This is a factor of 3.5 below the energy content of a filter consisting only of a capacitor).

If this was designed for minimum energy rather than minimum weight, then

$$S_\pi = 8.3 \times 10^{-4} \text{ lb/kW}$$

and

$$E_\pi min = 1070 \text{ joules.}$$

In the equation for the specific weight of the π filter, it should be noted that weight varies with the cube root of ripple factor. Thus, if a ripple factor of 0.1 per cent rather than one per cent is desired, the specific weight increases by a factor of $\sqrt[3]{10}$ or 2.15. Thus, for 0.1 per cent ripple

$$S_{\pi}\text{min} = 1.46 \times 10^{-3} \text{ lb/kW}$$

and this is a factor of 12.5 below the specific weight of a filter consisting only of a capacitor. The energy content of this filter would be

$$E_{\pi} = 2740 \text{ joules}$$

which is a factor of 16.7 below the energy content of a filter consisting only of a capacitor.

C. Load Protection

The load protection requirement was not defined at the outset or during the High Power Study. It is likely, considering the nature of the anticipated load, that an extremely fast and reliable load protection circuit will be required. Not only will fast switches be necessary but also, the amount of energy to be diverted by the switches will probably have to be minimized. This means that the energy considerations previously given for filters may become extremely important. In addition, the use of multiple stagger timed inverters may be warranted to further reduce the filter energy content.

VI. ANALYSIS AND COMPARISON OF POWER CONDITIONING TECHNIQUES

Shown in Figures 6-1, 6-2 and 6-3 are the components of the various algorithms, S_1 through S_{13} required to determine the specific weights of the corresponding power conditioning techniques shown in Figures 2-1, 2-2 and 2-3. The quantities $S_{3\phi r}$, S_{LC}, etc. are the algorithms of the various components and subsystems presented earlier in this report. The factors W_1 through W_{13} are used to account for the estimated weight penalty incurred in interconnecting and packaging the components and subsystems. Corresponding factors V_1 through V_{13} (not shown in Figures 6-1, 6-2, and 6-3) may be used to determine the specific volumes of the various power conditioning techniques.

This section contains, first, a listing of the algorithms of the various components, subsystems, and then the various power conditioning techniques. Secondly, the computer program developed for calculating the various algorithms is described. Finally, results are given for certain values of input parameters.

A. Algorithm Compilation

The following is a compilation of the algorithms of the various components and subsystems shown in Figures 6-1, 6-2 and 6-3 and presented previously in this report.

$S_{3\phi r}$

The specific weight of the three phase rectifier is given by

$$S_{3\phi r} = .0073 \left[.945 + .055 \left(\frac{V_o}{100} \right)^{2.2} \right] \left(\frac{\tau}{60} \right)^{0.83} \quad \text{lb/kW}$$

where V_o is the rectifier output voltage and τ is the operating time.

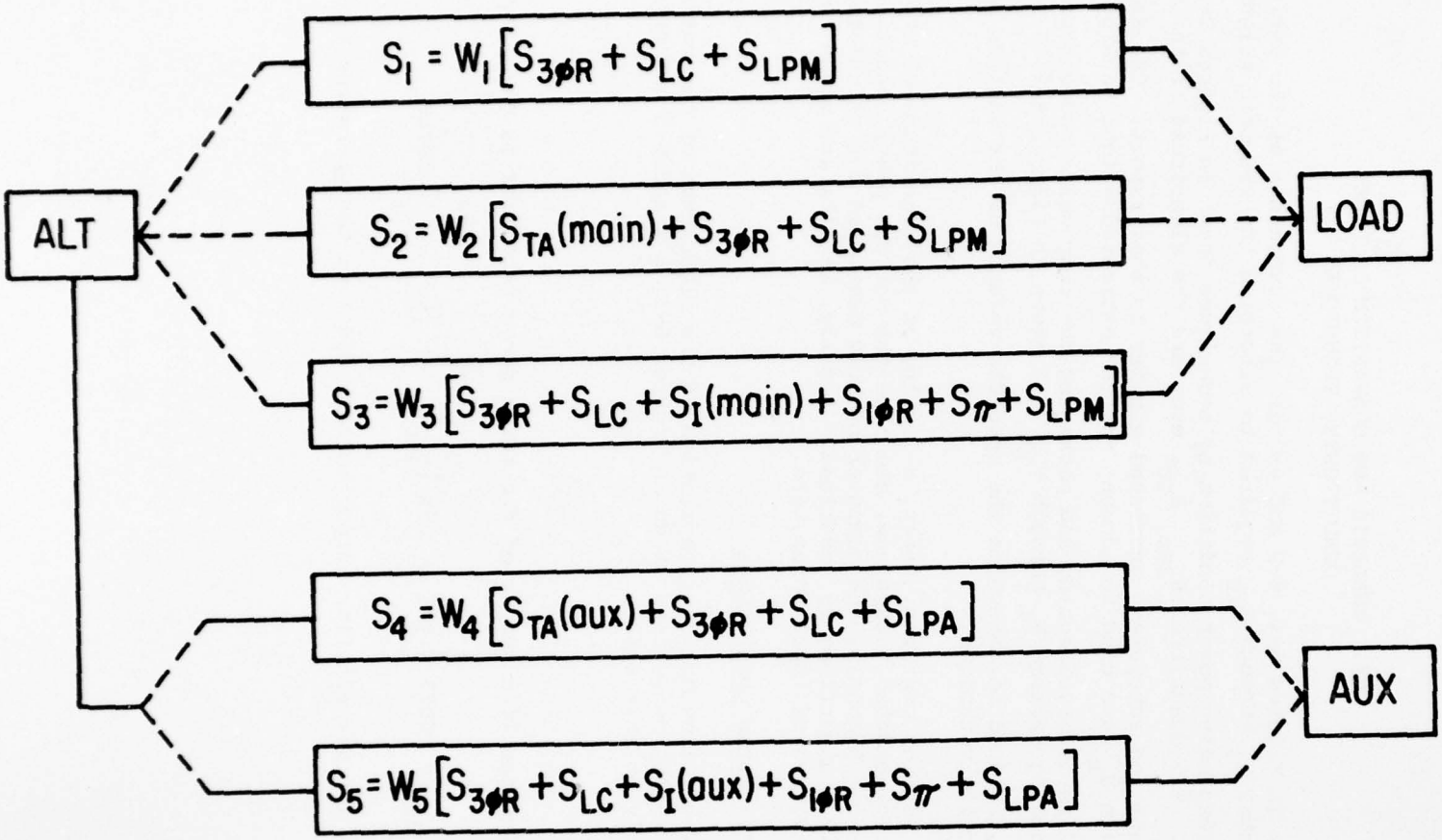


Figure 6-1 Components of algorithms S_1 through S_5

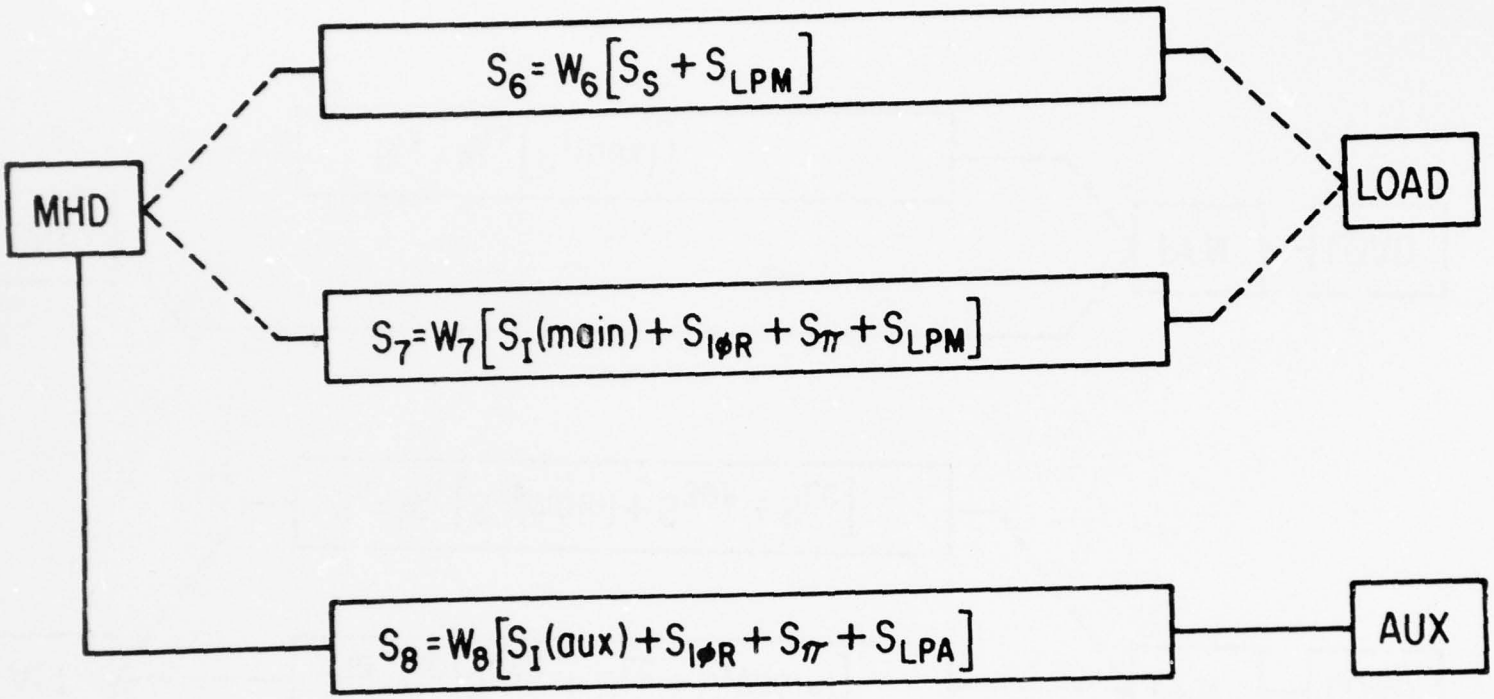


Figure 6-2 Components of algorithms S_6 through S_8

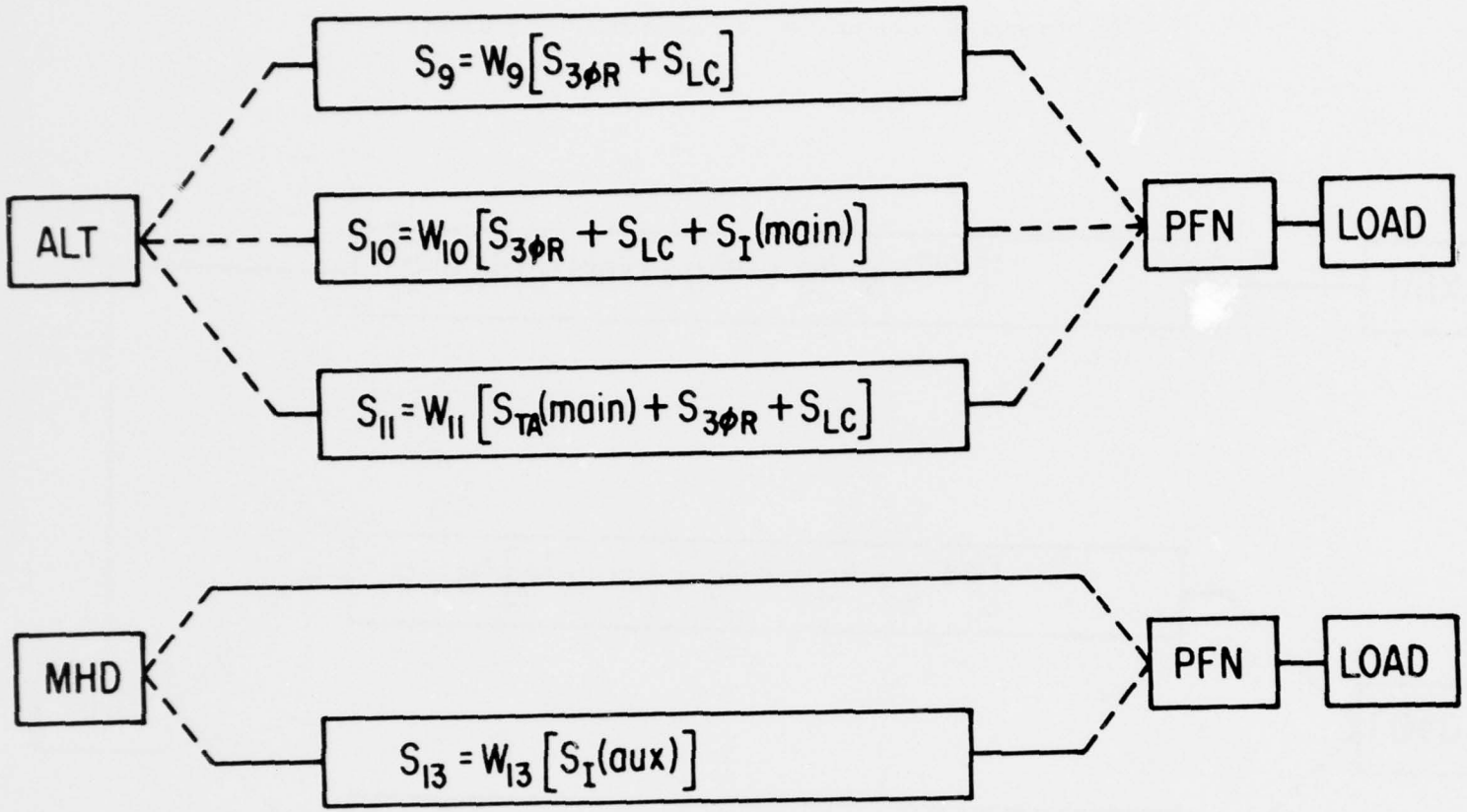


Figure 6-3 Components of algorithms S_9 through S_{13}

S_{LC}

The minimized value of the specific weight of the L-C filter is

$$S_{LC} = \frac{1}{2\pi f_r} \left(\frac{1}{r_r D_L D_c}\right)^{1/2}$$

$$= \frac{1}{2\pi f_r} \left(\frac{r_i}{r_\ell D_L D_c}\right)^{1/2}$$

or

$$S_{LC} \approx \frac{.0090 \left(\frac{r_i}{.08}\right)^{1/2}}{f_r \left(\frac{r_\ell}{.01}\right)^{1/2} \left(\frac{D_L}{25}\right)^{1/2} \left(\frac{D_c}{100}\right)^{1/2}}$$

where

f_r = ripple frequency, kHz (normally 6 x alternator frequency)

r_ℓ = rms load ripple factor

D_c = filter capacitor energy density (100 joules/lb unless otherwise specified)

D_L = filter inductor energy density (25 joules/lb unless otherwise specified)

and r_i is the ripple factor of the voltage applied to the filter.

For $\alpha < \beta$, this factor is given by

$$r_i \approx r_6 = .01 \left\{ .217\beta - .04\alpha + \left[2 + 3.3\left(\frac{\alpha}{30}\right)^2\right] \sin \left[\left(6.32 + \alpha^{.15}\right)(\beta-\alpha)\right] \right.$$
$$\left. + \left[4.1 + 38.8\left(\frac{\alpha}{60}\right)^2 - .217\beta + 1.5 \sin 5\beta + .04\alpha\right] e^{-\left(\frac{\beta-\alpha}{8.5+\sqrt{\alpha}}\right)^{1.5}} \right.$$

and when $\alpha \geq \beta$, then

$$r_i \approx r_6 = .01 \left[4.1 + 38.8 \left(\frac{\alpha}{60}\right)^2 + 1.5 \sin 5\alpha\right]$$

where α is the thyristor firing angle and β is the conduction overlap angle.

S_{TA}(main)

The algorithm for the specific weight of the main alternator transformer is

$$S_{TA}\ (\text{main}) = .0505 \left(\frac{\tau}{120}\right)^{0.337} \left(\frac{V_o}{100}\right)^{-.0413} \times \left[.693 + .307 \left(\frac{P}{25}\right)^{-.79}\right] \times \left[.931 + .069 \left(\frac{V_o}{100}\right)^{1.3}\right] \times \left[.242 + .758 \left(f_a\right)^{-.926}\right] \text{ lb/kW}$$

where

τ = total run time during mission in seconds

P = power level in megawatts

V_o = dc load voltage in kilovolts assuming zero conduction overlap in rectifier

fa = alternator frequency in kHz.

S_I(main)

The algorithm for the specific weight of the main inverter contains several components. That is,

$$S_I(\text{main}) = S_{TI}\ (\text{main}) + S_{scr} + S_c$$

where

$$S_{TI}(\text{main}) = .00940 \left(\frac{\tau}{120}\right)^{0.302} \left(\frac{V_o}{100}\right)^{-.095}$$

$$x\left[.479 + .521 \left(\frac{P}{25}\right)^{-.614}\right]$$

$$x\left[.880 + .120 \left(\frac{V_o}{100}\right)^{1.33}\right]$$

$$x \left[\left(\frac{fi}{10}\right)^{-.754}\right] x \left[\left(\frac{V_{in}}{5}\right)^{-.089}\right] \quad \text{lb/kW.}$$

where

fi = inversion frequency (10 kHz unless otherwise specified)

V_{in} = dc output voltage of L-C filter

$$S_{scr} = .024 \left(\frac{I}{60}\right)^{0.83} \quad \text{lb/kW}$$

and

$$S_c = \frac{1}{124\ fi^{0.72}} \quad \text{lb/kW.}$$

$\underline{S_{1\phi r}}$

The specific weight of the single phase rectifier is given by

$$S_{1\phi r} = .0042 \left[.945 + .055 \left(\frac{V_o}{100}\right)^{2.2}\right] \left(\frac{\tau}{60}\right)^{0.83} \quad \text{lb/kW}$$

$\underline{S_\pi}$

The minimized value of the specific weight of the π filter is

$$S_\pi \text{min} = \frac{3\ (\sqrt{2}-1)^{1/3}}{4\sqrt{2}\ (\pi)^{2/3} f_r\ D_c^{2/3} \left(r_\ell D_L\right)^{1/3}}$$

or

$$S_{\pi}\text{min} = \frac{6.8 \times 10^{-4}}{\left(\frac{f_r}{20}\right)\left(\frac{D_c}{100}\right)^{2/3}\left(\frac{r_\ell}{.01}\right)^{1/3}\left(\frac{D_L}{25}\right)^{1/3}}$$

where

f_r = ripple frequency in kHz (2 x inversion frequency for single inverter)

D_c = filter capacitor energy density (100 joules/lb unless otherwise specified)

D_L = filter inductor energy density (25 joules/lb unless otherwise specified)

$S_{TA}(aux)$

The algorithm for the specific weight of the auxiliary alternator transformer is

$$S_{TA}(aux) = .1275\left(\frac{\tau}{120}\right)^{.281} \times \left[.612 + .388\left(\frac{P}{2.5}\right)^{-.985}\right] \times \left[.608 + .392\left(\frac{V_o}{200}\right)^{.71}\right] \times \left(f_a\right)^{-.767} \quad \text{lb/kW.}$$

$S_I(aux)$

The algorithm for the specific weight of the auxiliary inverter contains several components. That is,

$$S_I(aux) = S_{TI}(aux) + S_{scr} + S_c$$

where

$$S_{TI}(aux) = .0263 \left(\frac{P_a}{2.5}\right)^{-.426} \times \left(\frac{V_o}{200}\right)^{.274}$$

$$\times \left(\frac{T}{120}\right)^{.219} \times \left(\frac{fi}{10}\right)^{-.800} \quad lb/kW.$$

and S_{scr} and S_c were previously given for the main inverter.

S_s

This is the specific weight of an opening switch. It is assumed that a specific weight of .004 lb/kW should be adequate for a vacuum arc switch to fulfill this function.

B. Computer Program

The computer program "POWER" was developed to calculate the specific weights and specific volumes for any selected solution in Figures 6-1 and 6-3. The program output consists of a list of input specifications, subsystems specific weights and volumes, and total specific weights and volumes. The user will specify the solution number, system specifications, and if desired, the W and V factors.

The punched card data input format is as follows:

CARD 1	Description	Default
Column 1-2	Solution Number 1 to 13. This is the subscript attached to each solution in Figures 6.1 to 6.3.	None
CARD 2		
Column 1-10	MHD dc input in kV	None
11-20	Alternator L-L rms input in kV	None
21-30	Dc output in kV	None
31-40	Mission duration in seconds	None
41-50	Inverter frequency in kHz	10.0
51-60	Capacitive energy density in Joules/LB	100.0
61-70	Inductive energy density in Joules/LB	25.0

CARD 3		Description	Default
Column	1-10	RMS load ripple factor	.01
	11-20	Energy minimization factor	1.0
	21-30	Alternator frequency in kHz	.5
	31-40	Auxiliary power in kW	None
	41-50	Main power in kW	None
	51-60	Phase control angle in degrees	45.0
	61-70	Conduction angle in degrees	45.0
CARD 4			
Column	1-10	W1	1.2
	11-20	W2	1.1
	21-30	W3	1.15
	31-40	W4	1.1
	41-50	W5	1.15
	51-60	W6	1.15
	61-70	W7	1.15
CARD 5			
Column	1-10	W8	1.15
	11-20	W9	1.2
	21-30	W10	1.15
	31-40	W11	1.1
	41-50		
	51-60	W13	1.15
	61-70		

CARD 6		Description	Default
Column	1-10	V1	.012
	11-20	V2	.006
	21-30	V3	.009
	31-40	V4	.006
	41-50	V5	.009
	51-60	V6	.009
	61-70	V7	.009
CARD 7			
Column	1-10	V8	.009
	11-20	V9	.012
	21-30	V10	.009
	31-40	V11	.006
	41-50		
	51-60	V13	.009
	61-70		

If a field is left blank, that variable will take on the default value. For example, if none of the W or V factors are to be changed, Card 4 through Card 7 must be blank (but not omitted!). This will cause the W and V factors to take on their default values. If a field is left blank for a variable with no default, the job will be aborted. The above sequence of cards 1 through 7 may be repeated for as many solutions as desired.

The program "POWER" is contained in the following pages.

```
      PROGRAM POWER      73/74   OPT=1                              FTN 4.5+410

 1                PROGRAM POWER (INPUT,OUTPUT,TAPE5=INPUT,TAPE6=OUTPUT)
                  DIMENSION DATIN(3,14),CONFIG(10,14),WORK(7)
                  DATA(DATIN(2,N),N=1,14)/0.,0.,0.,0.,10.,100.,25.,.01,1.,.5,
                 10.,0.,45.,45./
 5                DATA(DATIN(3,N),N=1,14)/6HMHD IN,10HL-L RMS KV,9HOUTPUT KV,
                 110HMISS. TIME,10HINV. FREQ.,9HCAP DENS.,9HIND DENS.,
                 16HRIPPLE,9HENERGY MIN,10HALTRN FREQ,7HAUX PWR,8HMAIN PWR,
                 14HBETA,5HALPHA/
                  DATA(CONFIG(N,1),N=1,10)/1.2,.012,7.,9.,3.,0.,0.,0.,0.,0./
10                DATA(CONFIG(N,2),N=1,10)/1.1,.006,7.,5.,9.,3.,0.,0.,0.,0./
                  DATA(CONFIG(N,3),N=1,10)/1.15,.009,7.,9.,3.,1.,8.,4.,0.,0./
                  DATA(CONFIG(N,4),N=1,10)/1.1,.006,7.,6.,9.,3.,0.,0.,0.,0./
                  DATA(CONFIG(N,5),N=1,10)/1.15,.009,7.,9.,3.,2.,8.,4.,0.,0./
                  DATA(CONFIG(N,6),N=1,10)/1.15,.009,11.,0.,0.,0.,0.,0.,0.,0./
15                DATA(CONFIG(N,7),N=1,10)/1.15,.009,1.,8.,4.,0.,0.,0.,0.,0./
                  DATA(CONFIG(N,8),N=1,10)/1.15,.009,2.,8.,4.,0.,0.,0.,0.,0./
                  DATA(CONFIG(N,9),N=1,10)/1.2,.012,7.,9.,3.,0.,0.,0.,0.,0./
                  DATA(CONFIG(N,10),N=1,10)/1.15,.009,7.,9.,3.,1.,0.,0.,0.,0./
                  DATA(CONFIG(N,11),N=1,10)/1.1,.006,7.,5.,9.,3.,0.,0.,0.,0./
20                DATA(CONFIG(N,12),N=1,10)/0.,0.,0.,0.,0.,0.,0.,0.,0.,0./
                  DATA(CONFIG(N,13),N=1,10)/1.15,.009,2.,0.,0.,0.,0.,0.,0.,0./
                  DATA(CONFIG(N,14),N=1,10)/0.,0.,0.,0.,0.,0.,0.,0.,0.,0./
               * INPUT SCHEMATIC CODE
               260   READ(5,1000) NSEQ
25                 IF(EOF(5))270,280
               1000  FORMAT(I2)
               * INPUT DATA
               280   READ(5,1001)(DATIN(1,N),N=1,14)
               1001  FORMAT(7F10.0/7F10.0)
30             * REPLACE DATA WITH DEFAULT
                     DO 10 I=1,14
                     IF (DATIN(1,I).NE.0.)GO TO 20
                     IF(DATIN(2,I).EQ.0.) GO TO 30
                     DATIN(1,I)=DATIN(2,I)
```

```
      GO TO 20
   30 WRITE(6,1002)DATIN(3,I)
 1002 FORMAT(1H1,*THE*,A10,*SPECIFICATION IS MISSING.*/
     1* JOB ABORTED.*)
      STOP
   20 CONTINUE
   10 CONTINUE
* REPLACE W AND V FACTORS IF REQUESTED
      DO 50 I=1,8,7
      READ(5,1003)(WORK(N),N=1,7)
      IF(EOF(5))60,70
 1003 FORMAT(7F10.0)
   70 DO 50 N=1,7
      J=I+N-1
      IF(WORK(N).EQ.0.) GO TO 40
      CONFIG(1,J)=WORK(N)
   40 CONTINUE
   50 CONTINUE
      DO 80 I=1,8,7
      READ(5,1003)(WORK(N),N=1,7)
      IF(EOF(5))60,100
  100 DO 80 N=1,7
      J=I+N-1
      IF (WORK(N).EQ.0.)GO TO 90
      CONFIG(2,J)=WORK(N)
   90 CONTINUE
   80 CONTINUE
   60 CONTINUE
* PRINT INPUT DATA
      WRITE(6,1008)NSEQ
 1008 FORMAT(1H1,30X,*S Y S T E M  S P E C I F C A T I O N S*,//,
     1* SOLUTION NUMBER *,I2//)
      WRITE(6,1004)(DATIN(1,N),N=1,14)
 1004 FORMAT(* MHD DC INPUT*,18X,F10.3,* KV*,12X,
     1*ALTERNATOR L-L RMS*,12X,F10.3,* KV*/
     1* DC OUTPUT*,21X,F10.3,* KW*,12X,*MISSION DURATION*,14X,
     1F10.3,* SECONDS*/* INVERSION FREQUENCY*,11X,F10.3,
     1* KHZ*,11X,*CAPACITIVE ENERGY DENSITY*,5X,F10.3,*JOULES/LB*/
     1* INDUCTIVE ENERGY DENSITY*,6X,F10.3,*JOULES/LB*,6X,
     1*RMS LOAD RIPPLE FACTOR*,8X,F10.3/
```

```
      1* ENERGY MINIMIZATION FACTOR*,4X,F10.3,15X,
     1*ALTERNATOR FREQUENCY*,10X,F10.3,* KHZ*/
     1* AUXILIARY POWER*,15X,F10.3,* MW*,12X,
     1**AIN POWER*,20X,F10.3,* MW*/
     1* PHASE CONTROL ANGLE*,11X,F10.3,* DEGREES*,7X,
     1*CONDUCTION ANGLE*,14X,F10.3,* DEGREES*)
      WRITE(6,2000)
2000  FORMAT(////, 6X,*SUBSYSTEM*,20X,*SPECIFIC WEIGHT*,5X,
     1*SPECIFIC VOLUME*/38X,*LB/KW*,15X,*CU.FT./KW*)
* DO CALCULATION SEQUENCE
      VAVG=DATIN(1,1)
      SPEC=0.
      DO 110 I=3,10
      X=CONFIG(I,NSEQ)
      IF(X.EQ.0.)GO TO 125
      IF(X.EQ.1.)GO TO 130
      IF(X.EQ.2.) GO TO 140
      IF(X.EQ.3.)GO TO 150
      IF(X.EQ.4.) GO TO 160
      IF(X.EQ.5.) GO TO 170
      IF(X.EQ.6.) GO TO 180
      IF(X.EQ.7.)GO TO 190
      IF(X.EQ.8.)GO TO 200
      IF(X.EQ.9.)GO TO 210
      IF(X.EQ.10.)GO TO 220
      IF(X.EQ.11.)GO TO 230
      STOP
130   CALL TIMAIN(DATIN(1,4),DATIN(1,12),DATIN(1,3),DATIN(1,5),
     1VAVG,SI)
      CALL SCAP(DATIN(1,5),SC)
      CALL ROTSCR(DATIN(1,3),DATIN(1,4),SR)
      WSI=SI*CONFIG(1,NSEQ)
      VSI=SI*CONFIG(2,NSEQ)
      WSC=SC*CONFIG(1,NSEQ)
      VSC=SC*CONFIG(2,NSEQ)
      WSR=SR*CONFIG(1,NSEQ)
      VSR=SR*CONFIG(2,NSEQ)
      WS=WSI+WSC+WSR
      VS=VSI+VSC+VSR
      WRITE(6,2001)WS,VS
```

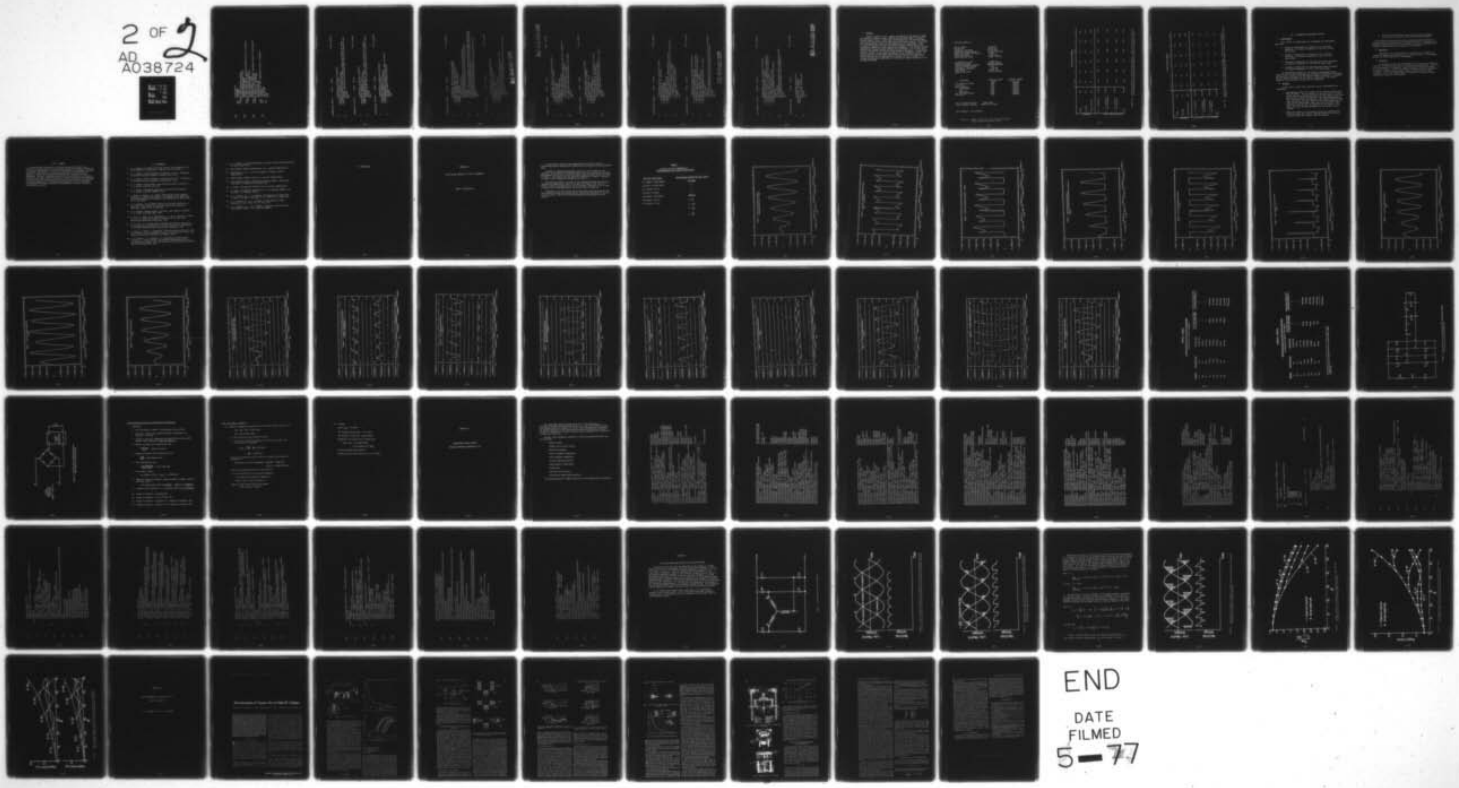
```
      2001  FORMAT(* MAIN INVERTER*,17X,F10.3,15X,F10.6)
            WRITE(6,2011)WSI,VSI
      2011  FORMAT(5X,*TRANSFORMER*,15X,F10.3,15X,F10.6)
            WRITE(6,2012)  WSR,VSR
      2012  FORMAT(5X,*SCR*,23X,F10.3,15X,F10.6)
            WRITE(6,2013)WSC,VSC
      2013  FORMAT(5X,*CAPACITOR*,17X,F10.3,15X,F10.6)
            S=SI+SC+SR
            GO TO 120
      140   CALL TIAUX(DATIN(1,4),DATIN(1,11),DATIN(1,3),DATIN(1,5),SI)
            CALL SCAP(DATIN(1,5),SC)
            CALL RCTSCR(DATIN(1,3),DATIN(1,4),SR)
            WSI=SI*CONFIG(1,NSEQ)
            VSI=SI*CONFIG(2,NSEQ)
            WSC=SC*CONFIG(1,NSEQ)
            VSC=SC*CONFIG(2,NSEQ)
            WSR=SR*CONFIG(1,NSEQ)
            VSR=SR*CONFIG(2,NSEQ)
            WS=WSI+WSC+WSR
            VS=VSI+VSC+VSR
            WRITE(6,2002)WS,VS
      2002  FORMAT(* AUXILIARY INVERTER*,12X,F10.3,15X,F10.6)
            WRITE(6,2011)WSI,VSI
            WRITE(6,2012)  WSR,VSR
            WRITE(6,2013)WSC,VSC
            S=SI+SC+SR
            GO TO 120
      150   CALL FILTLC(DATIN(1,6),DATIN(1,7),DATIN(1,8),DATIN(1,10),
           1DATIN(1,1),S)
            WS=S*CONFIG(1,NSEQ)
            VS=S*CONFIG(2,NSEQ)
            WRITE(6,2003)WS,VS
      2003  FORMAT(* LC FILTER*,21X,F10.3,15X,F10.6)
            GO TO 120
      160   CALL FILTPI(DATIN(1,5),DATIN(1,6),DATIN(1,7),DATIN(1,8),
           1DATIN(1,9),S)
            WS=S*CONFIG(1,NSEQ)
            VS=S*CONFIG(2,NSEQ)
            WRITE(6,2004)WS,VS
      2004  FORMAT(* PI FILTER*,21X,F10.3,15X,F10.6)
```

```
      GO TO 120
  170 CALL TAMAIN(DATIN(1,4),DATIN(1,12),DATIN(1,3),DATIN(1,10),S)
      WS=S*CONFIG(1,NSEQ)
      VS=S*CONFIG(2,NSEQ)
      WRITE(6,2005)WS,VS
 2005 FORMAT(* TA MAIN*,23X,F10.3,15X,F10.6)
      GO TO 120
  180 CALL TAAUX(DATIN(1,4),DATIN(1,11),DATIN(1,3),DATIN(1,10),S)
      WS=S*CONFIG(1,NSEQ)
      VS=S*CONFIG(2,NSEQ)
      WRITE(6,2006)WS,VS
 2006 FORMAT(* TA AUXILIARY*,18X,F10.3,15X,F10.6)
      GO TO 120
  190 CALL RIPPLE(DATIN(1,14),DATIN(1,13),DATIN(1,2),RA,VAVG)
      S=0
      GO TO 120
  200 CALL RCTSP(DATIN(1,3),DATIN(1,4),S)
      WS=S*CONFIG(1,NSEQ)
      VS=S*CONFIG(2,NSEQ)
      WRITE(6,2007)WS,VS
 2007 FORMAT(* 1-P RECTIFIER STACK*,11X,F10.3,15X,F10.6)
      GO TO 120
  210 CALL RCTTP(DATIN(1,3),DATIN(1,4),S)
      WS=S*CONFIG(1,NSEQ)
      VS=S*CONFIG(2,NSEQ)
      WRITE(6,2008)WS,VS
 2008 FORMAT(* 3-P RECTIFIER STACK*,11X,F10.3,15X,F10.6)
      GO TO 120
  220 CALL RCTSCR(DATIN(1,3),DATIN(1,4),S)
      WS=S*CONFIG(1,NSEQ)
      VS=S*CONFIG(2,NSEQ)
      WRITE(6,2009)WS,VS
 2009 FORMAT(* SCR STACK*,21X,F10.3,15X,F10.6)
      GO TO 120
  230 S=.002
      VS=S*CONFIG(2,NSEQ)
      WS=S*CONFIG(1,NSEQ)
      WRITE(6,2010)WS,VS
 2010 FORMAT(* SWITCH*,24X,F10.3,15X,F10.6)
  120 CONTINUE
```

AD-A038 724 STATE UNIV OF NEW YORK AT BUFFALO DEPT OF ELECTRICAL --ETC F/G 10/2
HIGH POWER STUDY - POWER CONDITIONING.(U)
JAN 76 A S GILMOUR F30602-75-C-0122

UNCLASSIFIED AFAPL-TR-76-101 NL

2 OF 2
AD A038724



END

DATE FILMED
5-77

```
195               SPEC=SPEC+S
              125 CONTINUE
              110 CONTINUE
              *  PRINT TOTAL SPECIFIC WEIGHT
                  WSPEC=CONFIG(1,NSEQ)*SPEC
200               WRITE(6,1006)WSPEC
              1006 FORMAT(////* TOTAL SPECIFIC WEIGHT=*,F10.3,* LB/KW*)
              *  PRINT TOTAL SPECIFIC VOLUME
                  VSPEC=CONFIG(2,NSEQ)*SPEC
                  WRITE(6,1007) VSPEC
205           1007 FORMAT(* TOTAL SPECIFIC VOLUME=*,F10.6,* CU.FT./KW*)
              *  PRINT RIPPLES IF AVAILABLE
                  IF(RA.EQ.0.) GO TO 240
                  WRITE(6,1005)RA
              1005 FORMAT(///* 6TH HARMONIC=*,F6.3,* PERCENT*)
210           240 CONTINUE
                  GO TO 260
              270 STOP
                  END
```

```
 SUBROUTINE RCTSP      73/74    OPT=1                                    FTN 4.5+410

1               SUBROUTINE RCTSP(VO,T,SRCTSP)
               *VO=OUTPUT VOLTAGE IN KV
               *T=MISSION DURATION IN SECONDS
               *SRCTSP=SPECIFIC WEIGHT OF SINGLE PHASE RECTIFIER IN LB/KW
5              SRCTSP=.0042*(.945+.055*((VO/100.)**2.2))*((T/60.)**.83)
               RETURN
               END

 SUBROUTINE RCTTP      73/74    OPT=1                                    FTN 4.5+410

1               SUBROUTINE RCTTP(VO,T,SRCTTP)
               *VO=OUTPUT VOLTAGE IN KV
               *T=MISSION DURATION IN SECONDS
               *SRCTTP=SPECIFIC WEIGHT OF THREE PHASE RECTIFIER IN LB/KW
5              SRCTTP=.0073*(.945+.055*((VO/100.)**2.2))*((T/60.)**.83)
               RETURN
               END

 SUBROUTINE RCTSCR     73/74    OPT=1                                    FTN 4.5+410

1               SUBROUTINE RCTSCR(VO,T,SRCTSCR)
               *VO=OUTPUT VOLTAGE IN KV
               *T=MISSION DURATION IN SECONDS
               *SRCTSCR=SPECIFIC WEIGHT OF SCR STACK IN LB/KW
5              SRCTSCR=.024*((T/60.)**(.83))
               RETURN
               END
```

```
SUBROUTINE RIPPLE      /3/74   OPT=1                                  FTN 4.5+410

      1               SUBROUTINE RIPPLE(B,A,VLL,PA,VAVG)
                    * B=CONDUCTION OVERLAP ANGLE IN DEGREES
                    * A=PHASE CONTROL ANGLE IN DEGREES
                    * PA=6TH HARMONIC PERCENTAGE
      5             * VAVG=DC VOLTAGE
                      IF(A.LT.B) GO TO 10
                      PA=.01*(4.1+38.8*((A/60.)**2.)+1.5*SIN(5.*A))
                      VAVG=VLL*1.35*COS(.66*A+2.E-5*(A**3))*COS(.693*A)
                      RETURN
     10               PA=.01*(.217*B-.04*A*((2.+3.3*((A/30.)**2))*SIN((6.32+A**.15)
                     1*(B-A)))+((4.1+38.8*((A/60.)**2)-.217*B+1.5*SIN(5.*B)+.04*A)
                     1*EXP((A-B)/(8.5+((A**.5)/1.5)))))
                      VAVG=VLL*1.35*COS(.66*A+2E-5*(A**3))*COS(.692*B+.07*A)
                      RETURN
     15               END
```



```
SUBROUTINE TIAUX       /3/74   OPT=1                                  FTN 4.5+410

      1               SUBROUTINE TIAUX (T,PA,VO,FI,STIA)
                    * T=MISSION DURATION IN SECONDS
                    * PA=AUXILIARY POWER LEVEL
                    * VO=OUTPUT VOLTAGE
      5             * FI=INVERSION FREQUENCY
                    * STIA=SPECIFIC WEIGHT OF TRANSFORMER IN LB/KW
                      STIA=(.263*((PA/2.5)**(-.426)))
                     1 *((VO/200.)**.274)*((T/120.)**.219)*((FI/10.)**(-.8))
                      RETURN
     10               END
```

BEST AVAILABLE COPY

BEST AVAILABLE COPY

```
  SUBROUTINE TIMAIN      73/74    OPT=1                          FTN 4.5+410

 1                SUBROUTINE TIMAIN (T,P,VO,FI,VIN,STIM)
                * T=MISSION DURATION IN SECONDS
                * P=MAIN POWER LEVEL
                * VO=OUTPUT VOLTAGE
 5              * FI=INVERSION FREQUENCY
                * VIN=INVERTER INPUT VOLTAGE
                     STIM=(.0094*((T/120.)**(.302*((VO/100.)**(-.095)))))
                    1 *(.479+.521*((P/25.)**(-.614)))
                    1 *(.89+.12*((VO/100.)**1.33))
10                  1 *((FI/10.)**(-.754))*((VIN/5.)**(-.089))
                     RETURN
                     END
```



```
  SUBROUTINE TAAUX       73/74    OPT=1                          FTN 4.5+410

 1                SUBROUTINE TAAUX (T,PA,VO,FA,STAA)
                * T=MISSION DURATION IN SECONDS
                * PA=AUXILIARY POWER LEVEL
                * VO=OUTPUT VOLTAGE
 5              *FA=ALTERNATOR FREQUENCY
                * STAA=SPECIFIC WEIGHT OF TRANSFORMER IN LB/KW
                     STAA=(.1275*((T/120.)**.281))
                    1 *(.612+.388*((PA/2.5)**(-.985)))
                    1 *(.608+.392*((VO/200.)**.718))*(FA**(-.767))
10                   RETURN
                     END
```

```
  SUBROUTINE TAMAIN     73/74   OPT=1                          FTN 4.5+410

 1                SUBROUTINE TAMAIN (T,P,VO,FA,STAM)
                * T=MISSION DURATION IN SECONDS
                * P=MAIN POWER LEVEL
                * VO=OUTPUT VOLTAGE
 5              * FA=ALTERNATOR FREQUENCY
                * STAM=SPECIFIC WEIGHT OF TRANSFORMER IN LB/KW
                     STAM=(.0505*((T/120.)**(.337*((VO/100.)**(-.0413)))))
                    1 *(.693+.307*((P/25.)**(-.79)))
                    1 *(.931+.069*((VO/100.)**1.31))
 10                 1 *(.242+.758*(FA**(-.926)))
                     RETURN
                     END


  SUBROUTINE FILTPI     73/74   OPT=1                          FTN 4.5+410

 1                SUBROUTINE FILTPI (FI,DC,DL,RL,EM,SPI)
                * FI=INVERSION FREQUENCY IN KHZ
                * DC=ENERGY DENSITY OF CAPACITOR IN JOULES/LB
                * DL=ENERGY DENSITY OF INDUCTOR IN JOULES/LB
 5              * RL=RMS LOAD RIPPLE FACTOR
                * EM=ENERGY MINIMIZATION FACTOR
                * SPI=MINIMUM SPECIFIC WEIGHT OF PI FILTER
                     RPI=3.14159
                     FR=2.*FI
 10                  SPI=(3.*((SQRT(2.)-1.)**(1./3.)))/(4.*SQRT(2.)*((RPI/EM)
                    1 **(2./3.))*FR*(DC**(2./3.))*((RL*DL)**(1./3.)))
                     RETURN
                     END
```


BEST AVAILABLE COPY

```
SUBROUTINE FILTLC      73/74   OPT=1                          FTN 4.5+410

1                SUBROUTINE FILTLC (DC,DL,RL,FA,B,SLC)
               * FI=INVERSION FREQUENCY IN KHZ
               * DC=ENERGY DENSITY OF CAPACITOR IN JOULES/LB
               * DL=ENERGY DENSITY OF INDUCTOR IN JOULES/LB
5              * RL=RMS LOAD RIPPLE FACTOR
               * FA=ALTERNATOR FREQUENCY IN KHZ
               * B=CONDUCTION OVERLAP ANGLE IN DEGREES
                     FR=6.*FA
                     RPI=3.14159
10                   RIN=.00217*B+.02*SIN(6.32*B)+.041*EXP(-B/8.5)
                     SLC=(RIN/(RL*DL*DC))**.5)/(2.*RPI*FR)
                     RETURN
                     END
```



```
SUBROUTINE SCAP        73/74   OPT=1                          FTN 4.5+410

1                SUBROUTINE SCAP(FI,SC)
               *FI=INVERSION FREQUENCY
               *SC=SW OF CAP IN LB/KW
                     SC=1./(124.*(FI**.72))
5                    RETURN
                     END
```

BEST AVAILABLE COPY

C. Results

Shown in Figure 6-4 is a sample calculation of the specific weight and specific volume for power conditioning technique number 3 and point designs number 1 and 2. (Note that the program lists the input voltage as an input from an MHD source and from an alternator source. The program uses the appropriate input for the calculation to be performed. Also, it should be pointed out that the specific weights calculated for the components include the weight penalty for packaging.) The specific weights and specific volumes of power conditioning techniques 1, 2, 3, and 7 are given in Figures 6-5 and 6-6 for point designs 1 through 8. Of particular interest are the results shown in Figure 6-5 for techniques 2 and 3. A weight reduction in the power conditioning system of from 17 percent to over 40 percent can be realized if an inverter is used in place of an alternator-frequency transformer for boosting the output voltage of a low voltage alternator.

SOLUTION NUMBER 3

MHD DC INPUT	5.000 KV
DC OUTPUT	60.000 KV
INVERSION FREQUENCY	10.000 KHZ
INDUCTIVE ENERGY DENSITY	25.000JOULES/LB
ENERGY MINIMIZATION FACTOR	1.000
AUXILIARY POWER	1.000 MW
PHASE CONTROL ANGLE	45.000 DEGREES

ALTERNATOR L-L RMS	5.000 KV
MISSION DURATION	63.000 SECONDS
CAPACITIVE ENERGY DENSITY	100.000JOULES/LB
RMS LOAD RIPPLE FACTOR	.010
ALTERNATOR FREQUENCY	.500 KHZ
MAIN POWER	10.000 MW
CONDUCTION ANGLE	45.000 DEGREES

SUBSYSTEM	SPECIFIC WEIGHT LB/KW	SPECIFIC VOLUME CU.FT./KW
3-P RECTIFIER STACK	.008	.000066
LC FILTER	.002	.000018
MAIN INVERTER	.041	.000319
TRANSFORMER	.011	.000081
SCR	.029	.000225
CAPACITOR	.002	.000014
1-P RECTIFIER STACK	.005	.000038
PI FILTER	.001	.000006

TOTAL SPECIFIC WEIGHT= .058 LB/KW
TOTAL SPECIFIC VOLUME= .000448 CU.FT./KW

6TH HARMONIC= .245 PERCENT

Figure 6-4. Sample calculation of power conditioning system specific weight and specific volume

			POINT DESIGN NUMBER					
			1 & 2	3	4	5 & 6	7	8
PARAMETER	Power	MW	10	25	25	25	50	50
	Voltage	kV	60	60	60	60	200	200
	Total Run Time	Sec	63	64	120	63	75	120
SPECIFIC WEIGHT lb/kW	H. V. Alternator	S_1(wt)	.011	.011	.017	.011	.014	.020
	L. V. Alternator and Transformer	S_2(wt)	.106	.083	.106	.082	.090	.108
	L. V. Alternator and Inverter	S_3(wt)	.058	.057	.089	.056	.065	.091
	MHD	S_7(wt)	.050	.047	.073	.046	.054	.075

Figure 6-5. Specific weights for various point designs. (Add ~.010 lb.kW to account for inverter system supplying additional 10% power to auxiliary load.)

			POINT DESIGN NUMBER					
			1 & 2	3	4	5 & 6	7	8
PARAMETER	Power	MW	10	25	25	25	50	50
	Voltage	kV	60	60	60	60	200	200
	Total Run Time	Sec	63	64	120	63	75	120
SPECIFIC VOL. $ft^3/kW \times 10^{-4}$	H. V. Alternator	S_1(vol)	1.1	1.1	1.7	1.1	1.4	2.0
	L. V. Alternator and Transformer	S_2(vol)	5.8	4.5	5.8	4.5	4.9	5.9
	L. V. Alternator and Inverter	S_3(vol)	4.5	4.5	7.0	4.4	5.1	7.1
	MHD	S_7(vol)	3.9	3.7	5.7	3.6	4.2	5.9

Fig. 6-6. Specific volumes for various point designs. (Add $\sim 0.8 \times 10^{-4}$ ft^3/kW to account for inverter system supplying additional 10% power to auxiliary load.)

VII. RECOMMENDED DEVELOPMENT PROGRAM

A. Transformers

Four classes of transformers are recommended for development. These are:

1. Adiabatic transformers for operation with sinusoidal waveforms at alternator frequencies in the 10 to 50 MW power range.

2. Adiabatic transformers for operation with sinusoidal waveforms at alternator frequencies in the 1 to 5 MW power range.

3. Adiabatic transformers for operation with square waveforms at inverter frequencies in the 10-50 MW power range.

4. Adiabatic transformers for operation with square waveforms at inverter frequencies in the 1-5 MW power range.

The development program for the inverter transformers should contain a task in which techniques are developed for accurately specifying and carefully controlling the transformer leakage inductance. By specifying the leakage reactances of the inverter transformers, the series inductors in the inverter circuits can be eliminated.

B. Switches

In the area of solid state switching, several developments are recommended.

1. Approximately half of the weight of the inverters results from the SCR stacks. The two reasons for the high weight of these stacks are that a substantial amount of loss occurs in the SCR's and the SCR's cannot be operated at very high temperatures so that large heat sinks are required. By decreasing the recovery time, increasing the peak inverse voltage (PIV) capability and reducing the forward drop, fewer SCR's, each having a lower power loss could be used to fabricate the SCR stacks. As a result the heat sinking requirement and the weight would be reduced.

2. While the weights of the rectifier stacks are expected to be relatively low, they could be reduced further if rectifiers having increased PIV ratings could be developed.

3. The load fault protection circuitry may require extremely fast solid state switches which may require development.

In the area of vacuum arc switching, substantial weight savings are projected if SCR's are replaced by vacuum-arc switches. Continuation of existing university work in this area along with the establishment of an industrial switch manufacturing program is recommended.

C. Capacitors

High power, high energy density ac capacitors for operation at inverter frequencies are nonexistent at the present time. A development program for these capacitors is recommended.

D. Inverters

At the present time, the development of a 200 kW series capacitor inverter is being carried out by the Aeropropulsion Laboratory. This work must be extended to the megawatt range for power conditioning systems utilizing inverters. The use of multiple inverters should be examined in an effort to reduce the development effort required for very large inverters. Also, the stagger timing of inverters to reduce filtering requirements should be investigated.

VIII. SUMMARY

A study has been carried out to estimate the specific weights and volumes of various high power conditioning systems that might be considered for airborne applications. The critical components (transformers, switches, capacitors, and inductors) for these systems have been identified and analyzed in detail and algorithms describing their weights have been developed. The major subsystems envisioned for possible use in the power conditioning systems have been analyzed. Finally an analysis and comparison of the various power conditioning techniques for the point design operating conditions supplied by the Aeropropulsion Laboratory has been performed. A recommended development program for transformers, switches, capacitors, and inverters is given.

IX. REFERENCES

1. F. C. Schwarz, "A method of resonant current pulse modulation for power converters", IEEE Trans. IECI-17, No. 3, May 1970.

2. F. C. Schwarz, "Switch modulation techniques, Part I", Proceedings of the Power Sources Conference, Atlantic City, 1962.

3. F. C. Schwarz, "Switch modulation techniques, Part II", Proceedings of the Power Sources Conference, Atlantic City, 1963.

4. F. C. Schwarz, "Controllable, load insensitive power converters", U. S. Patent 3,663,940, May 1972.

5. F. C. Schwarz, "Frequency modulated self stabilizing inverter", U. S. Patent 3,303,405, February 1967.

6. J. Biess, L. Inouye, J. H. Shank, "High voltage series resonant inverter ion engine screen supply", Proceedings of the IEEE Power Electronics Specialists Conference, Bell Laboratories, Murray Hill, N. J., June 1974.

7. F. C. Schwarz, "A time domain analysis of the power factor for a rectifier filter system with over and subcritical inductance", IEEE Trans. IECI-20, No. 2, May 1973.

8. F. C. Schwarz, "Analog signal to discrete time interval converter", U. S. Patent 3,659,184, April 1972.

9. Y. Yu, J. J. Biess, A. D. Schoenfeld, V. R. Lalli, "Circuits to three d.c. to d.c. power converters", Proceedings of the IEEE Power Electronics Specialists Conference, 1973.

10. R. P. Iwens, Y. Yu, "Time domain modeling and stability analysis of an integral pulse modulated dc to dc power converters", Proceedings of the IEEE Power Electronics Specialists Conference, 1975.

11. J. Biess, L. Inouye, A. Schoenfeld, "Thyristor power processor for the 30 cm mercury electric propulsion engine", AIAA Paper No. 75-433, 11th Electric Propulsion Conference, New Orleans, 1975.

12. F. C. Schwarz, J. B. Klaassens, "A controllable secondary multi-kilowatt d.c. current source with constant maximum power factor in its three phase supply line", Proceedings of the IEEE Power Electronics Specialists Conference, 1975.

13. F. C. Schwarz, "An improved method of resonant current pulse modulation for power converters."

14. Paul Hoffman, Maxwell Laboratories, Inc., private communication.

15. Louis Baldwin, E. I., du Pont de Nemours & Company, private communication.

16. Robert Parker, Hughes Aircraft Co., private communication.

17. "Fast Recovery Diodes - Calculating Recovery Losses," application note AN-B-6, International Rectifier Corp.

18. M. Chase, International Rectifier Corp., private communication.

19. F. Grover, "Inductance Calculations," D. Can Nostrand Company, Inc. New York, N.Y. 1946 pp. 91-105.

20. A. S. Gilmour, Jr., D. L. Lockwood, "Interruption of Vacuum Arcs at High DC Voltages," IEEE Trans., Vol. ED-22, No. 4, April 1975.

21. A. S. Gilmour, Jr., D. L. Lockwood, "Pulsed Metallic Plasma Generators," Proc. IEEE, vol. 60, Aug. 1972.

22. A. S. Gilmour, Jr., D. L. Lockwood, "Vacuum Arc Inverter Switch Development Program," Proc. IEEE 1975 NAECON.

X. APPENDICES

APPENDIX A

POINT DESIGN ANALYSIS OF A DC-DC CONVERTER

Maxwell Laboratories

A Point Design Study has been completed for the DC-DC Converter. Design equations for weights and volumes have been obtained and are presented here.

A number of different performance points of a DC-DC Converter were analyzed. This analysis has been done using a per unit system; the relationship between the per unit of percent values used and actual values are shown in Table I. The results for two cases are presented in Figures 1 through 9 for Case I and in Figures 10 through 18 for Case II.

The results of Case I in terms of the operating voltages and currents obtained are summarized in Table 2 for Case I and Table 3 for Case II. Figure 19 shows the diagram of the DC-DC Converter connected to an AC load. To obtain DC out requires adding a rectifier shown in Figure 20.

Combining all of the results for the two cases forms the basis for the DC-DC Converter weight and volume design calculations presented at the end of this section. All of the resulting equations are presented in that section.

TABLE I

VALUE OF CIRCUIT PARAMETERS OF
TRANSFORMERLESS HIGH VOLTAGE POWER SUPPLY

Per Unit Values Used	Relationship Between Per Unit Value
	Selected
1 pu Ampere = 1000 Amperes	E
1 pu Volt = 10,000 Volts	I
1 pu Second = 16 μs	t
1 pu Ohm = 10 ohms	Derived
1 pu Joule = 160 Joules	$R = \frac{E}{I}$
1 pu Henry = 166 μh	$W = EIt$
1 pu Farad = 1.6 μf	$L = \frac{Et}{I}$
	$C = \frac{tI}{E}$

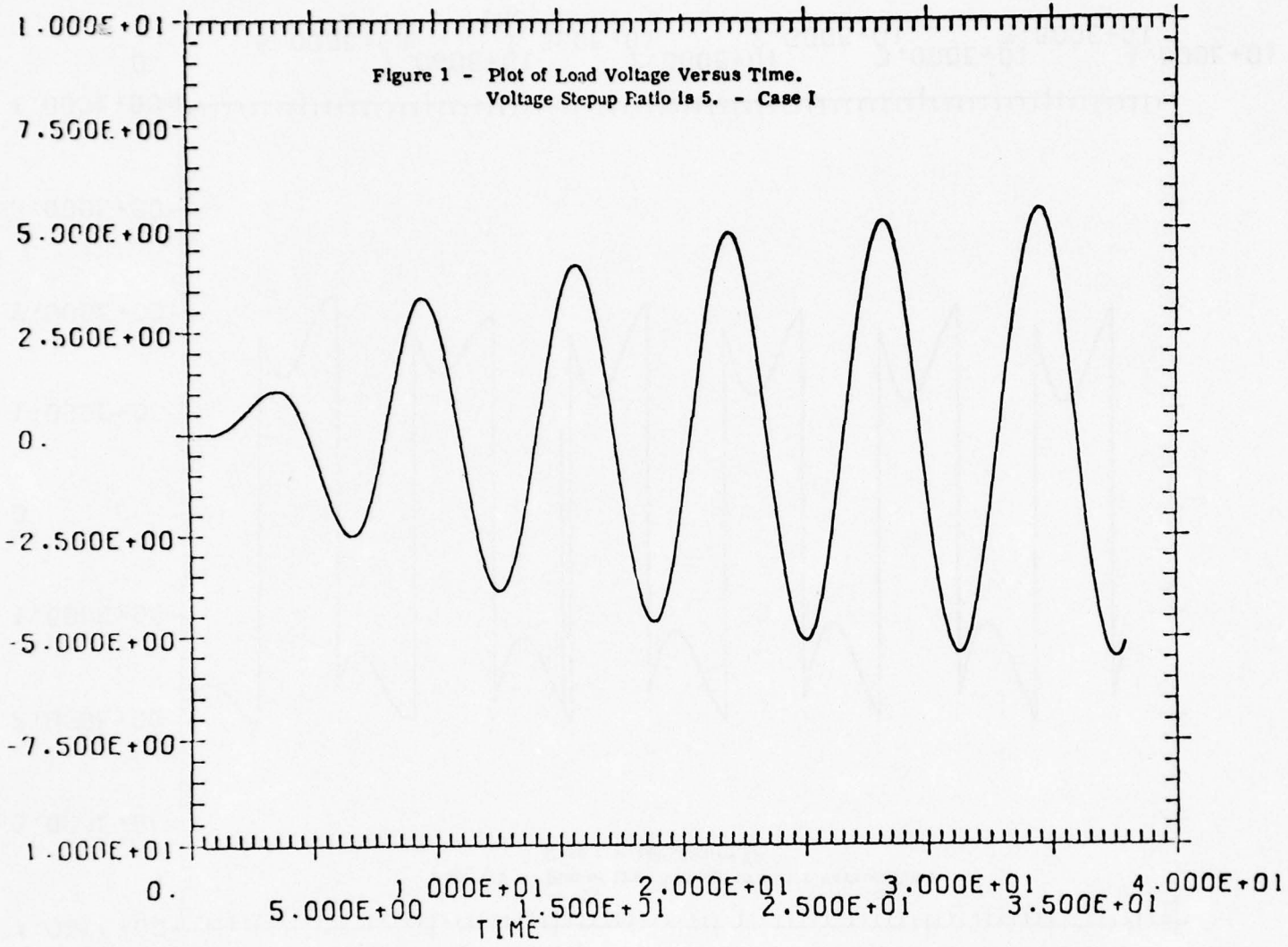


Figure 1 - Plot of Load Voltage Versus Time.
Voltage Stepup Ratio is 5. - Case I

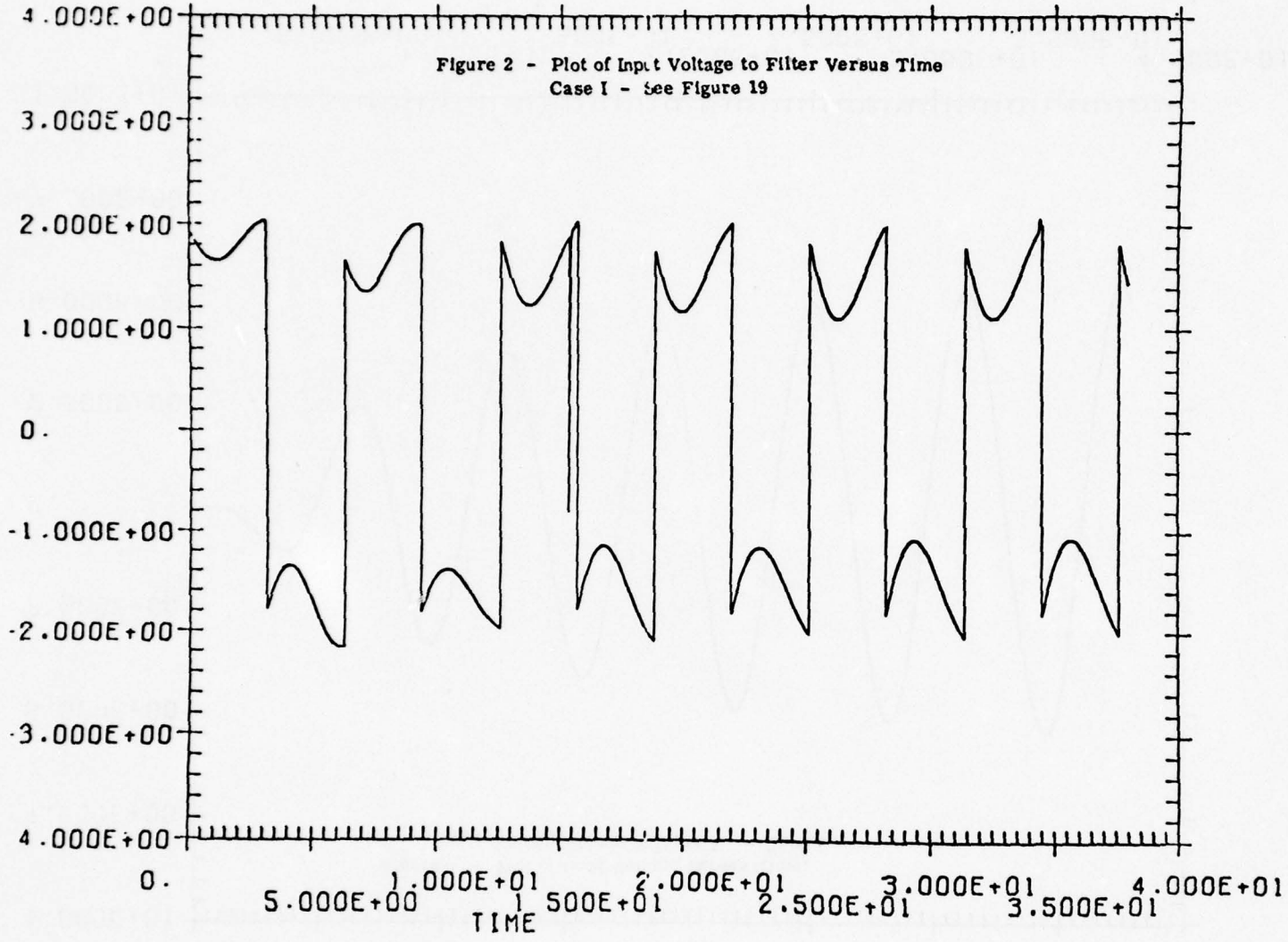


Figure 2 - Plot of Input Voltage to Filter Versus Time
Case I - See Figure 19

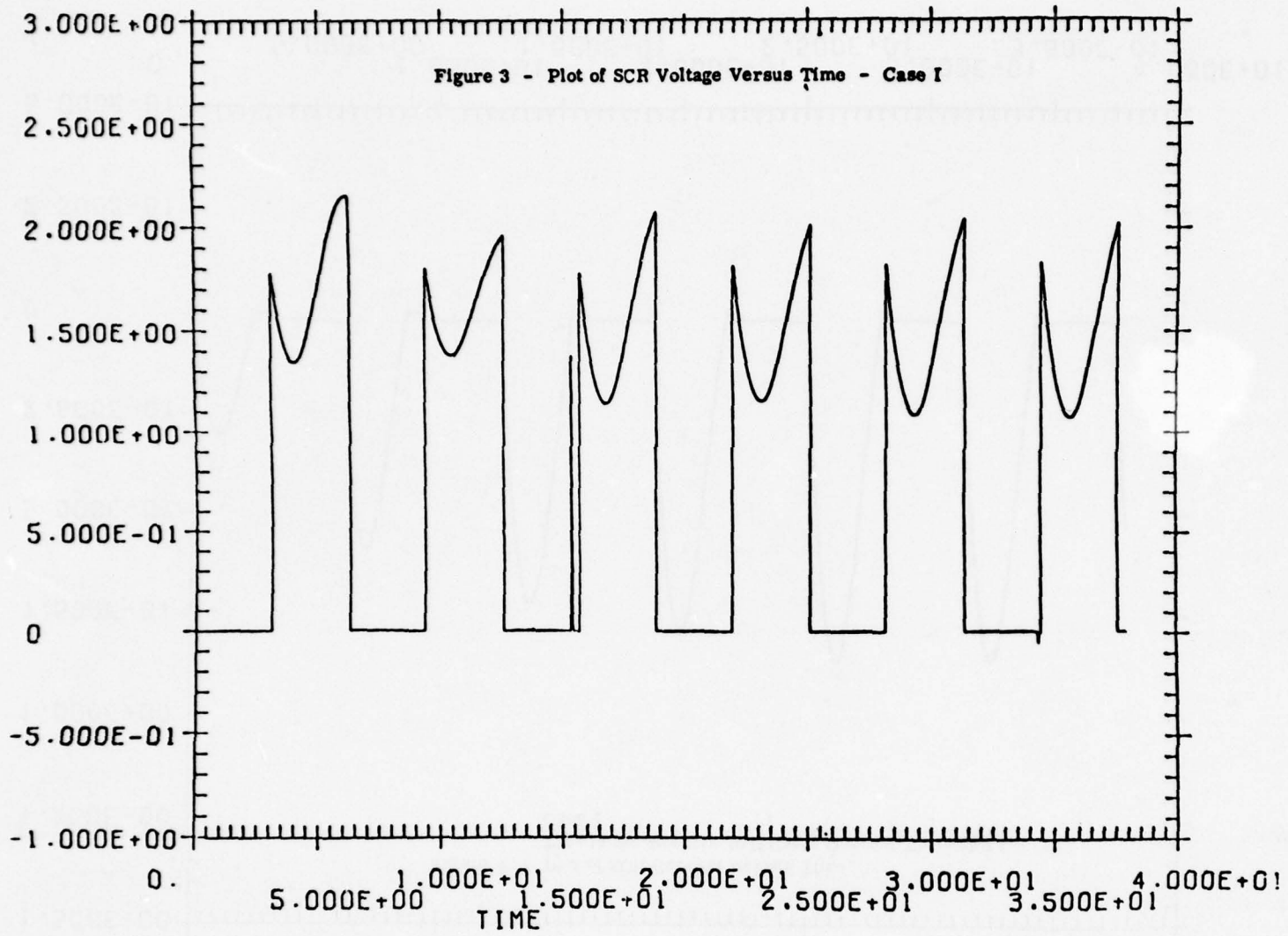


Figure 3 - Plot of SCR Voltage Versus Time - Case I

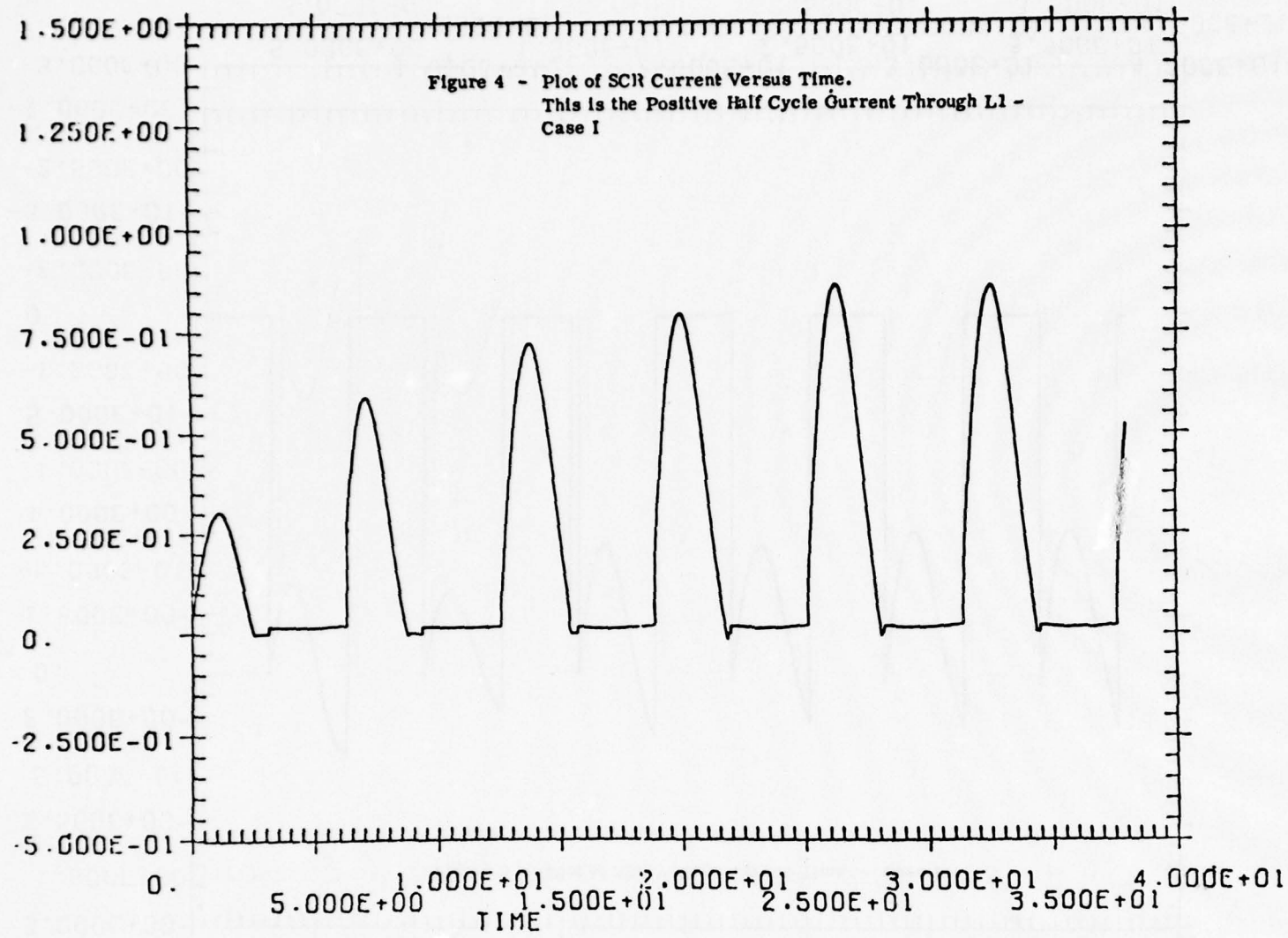


**Figure 4 - Plot of SCR Current Versus Time.
This is the Positive Half Cycle Current Through L1 -
Case I**

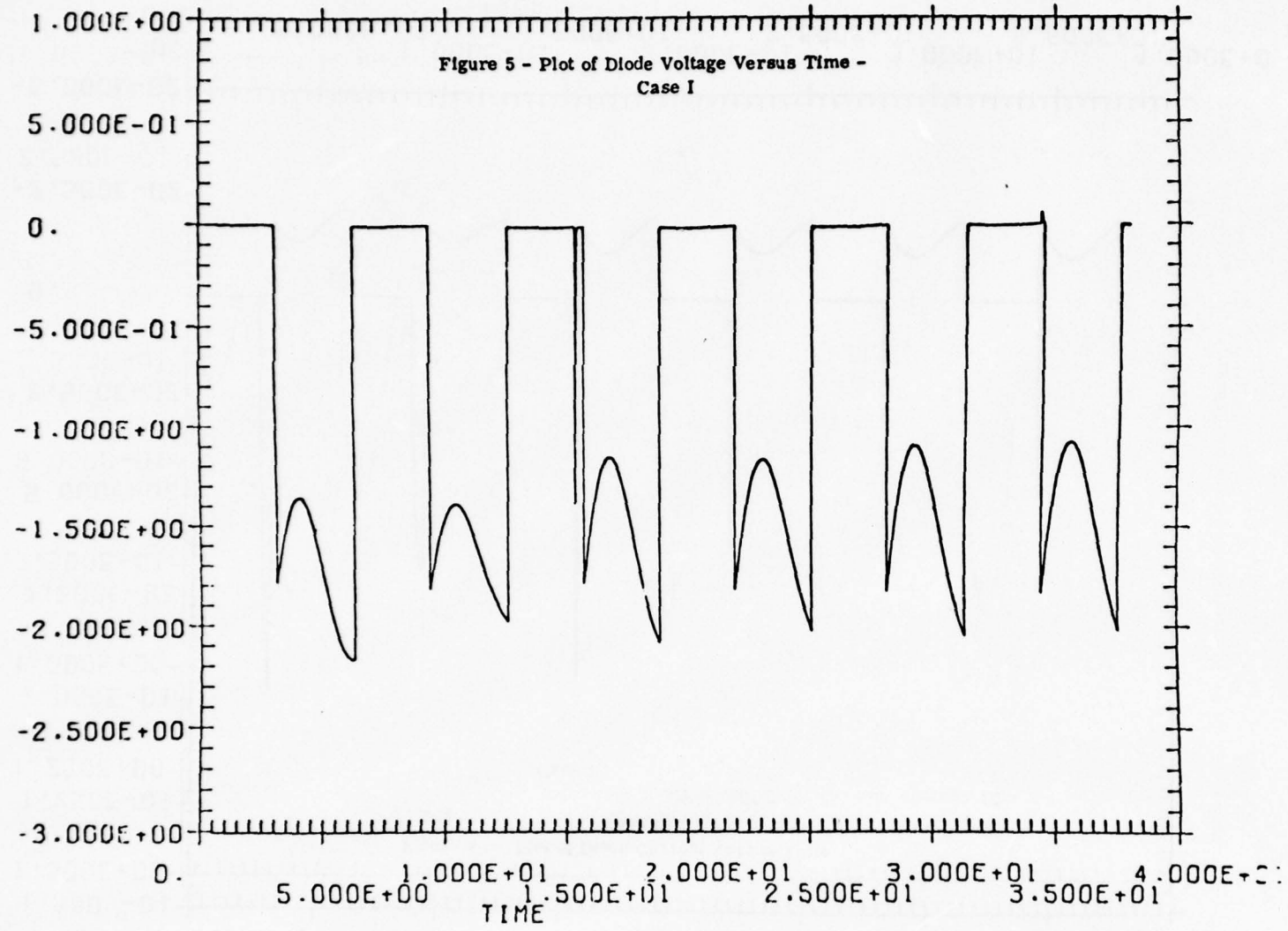


Figure 5 - Plot of Diode Voltage Versus Time - Case I

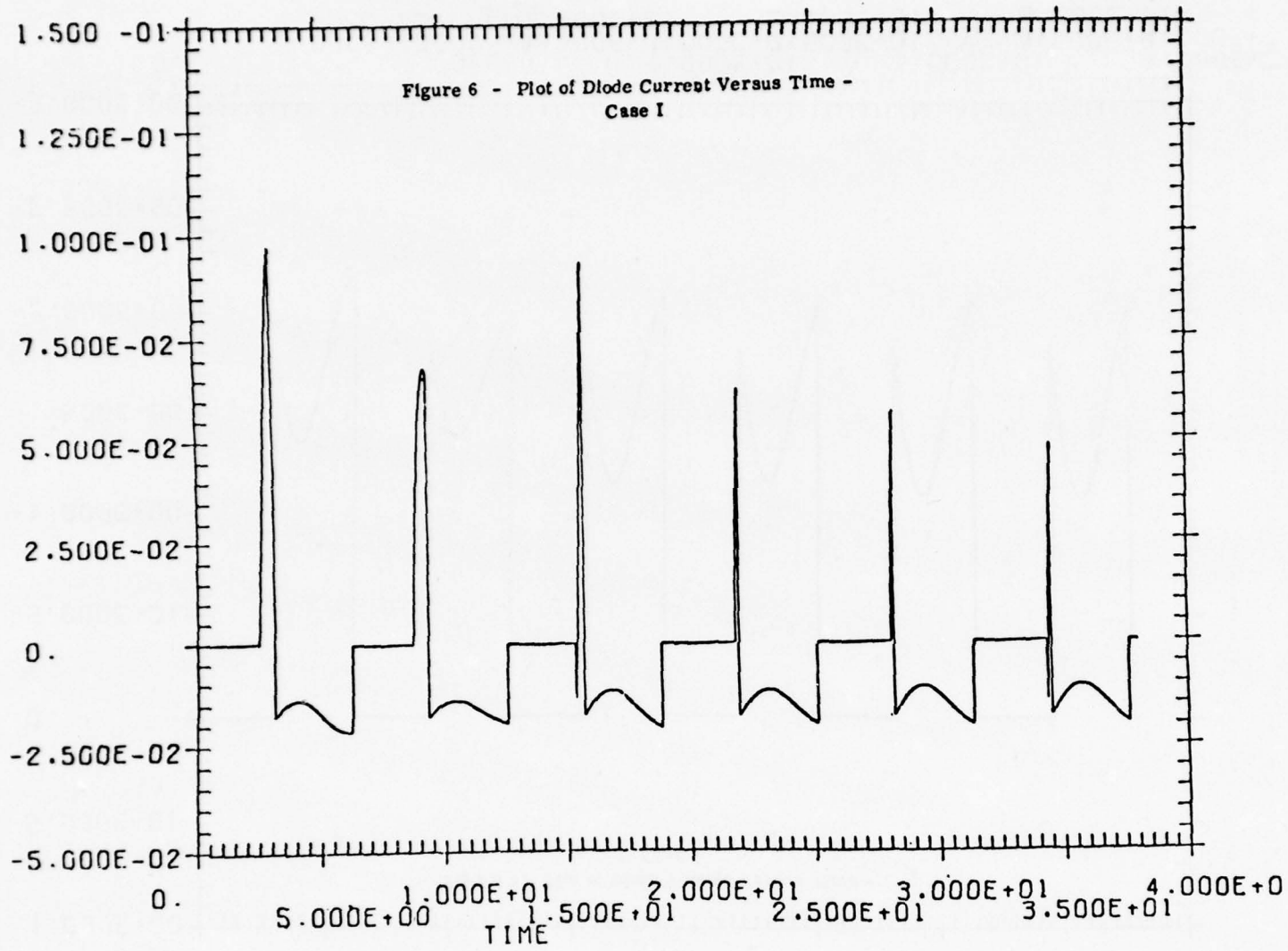


Figure 6 - Plot of Diode Current Versus Time - Case I

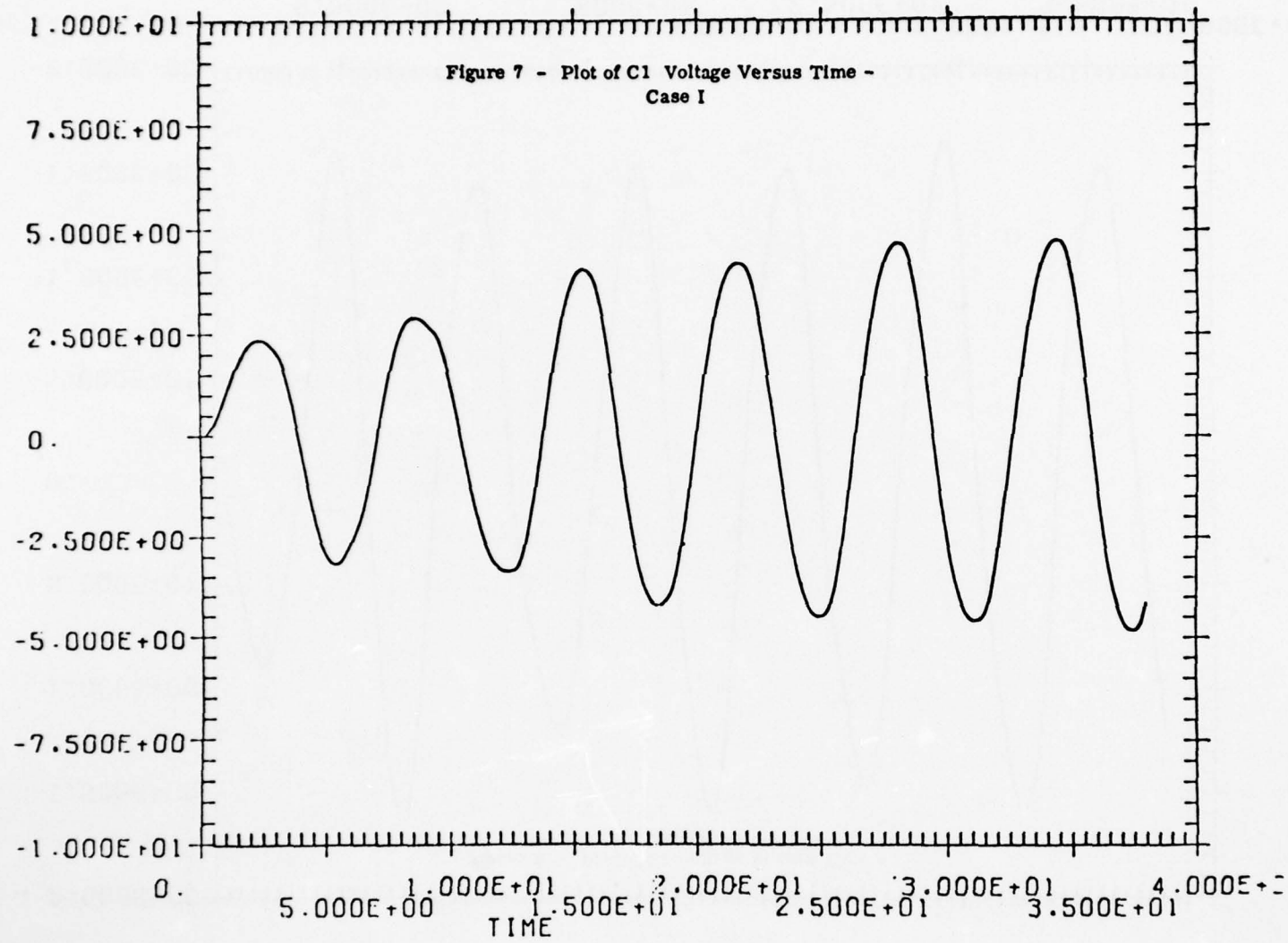


Figure 7 - Plot of C1 Voltage Versus Time - Case I

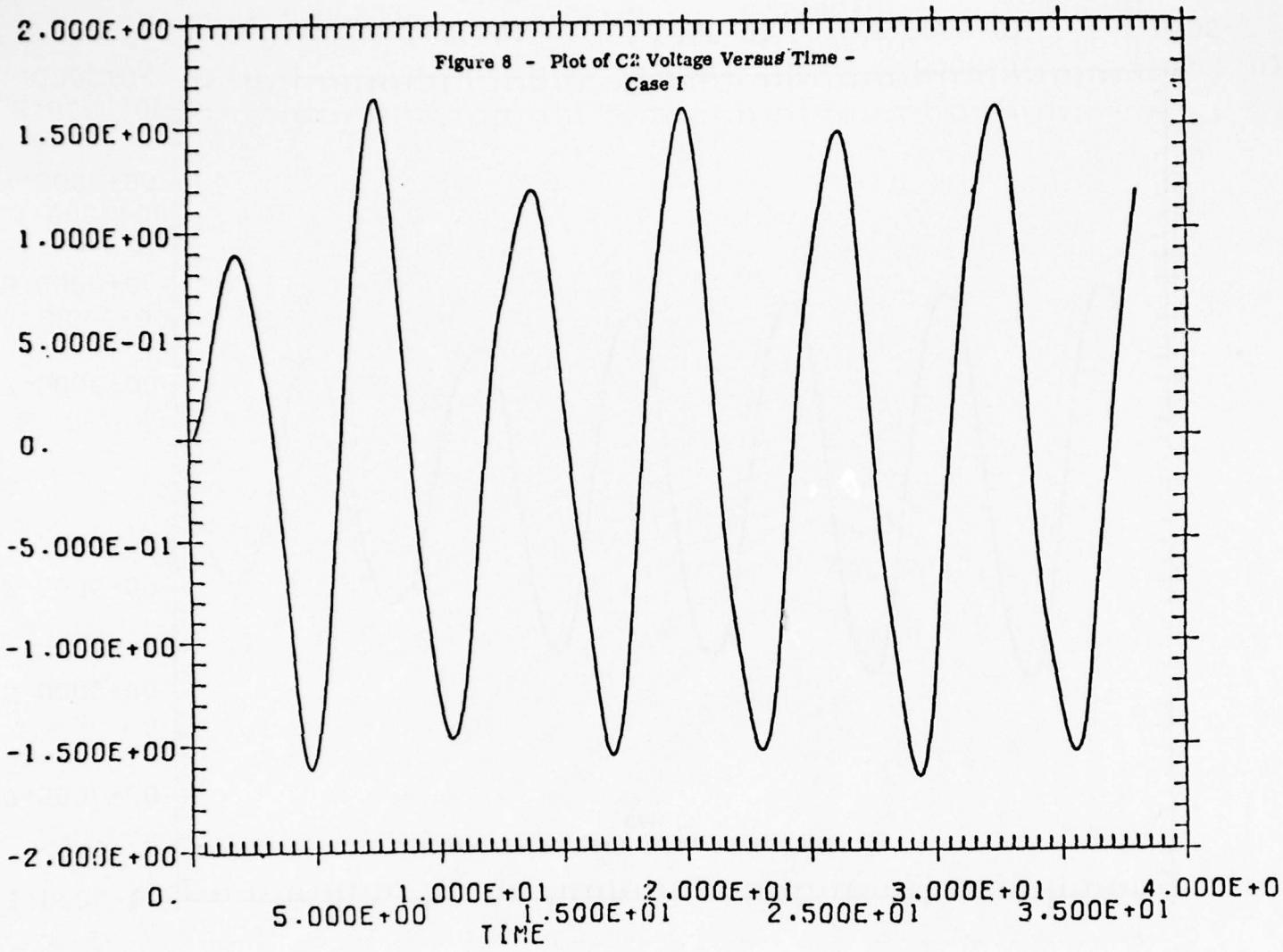


Figure 8 - Plot of C2 Voltage Versus Time - Case I

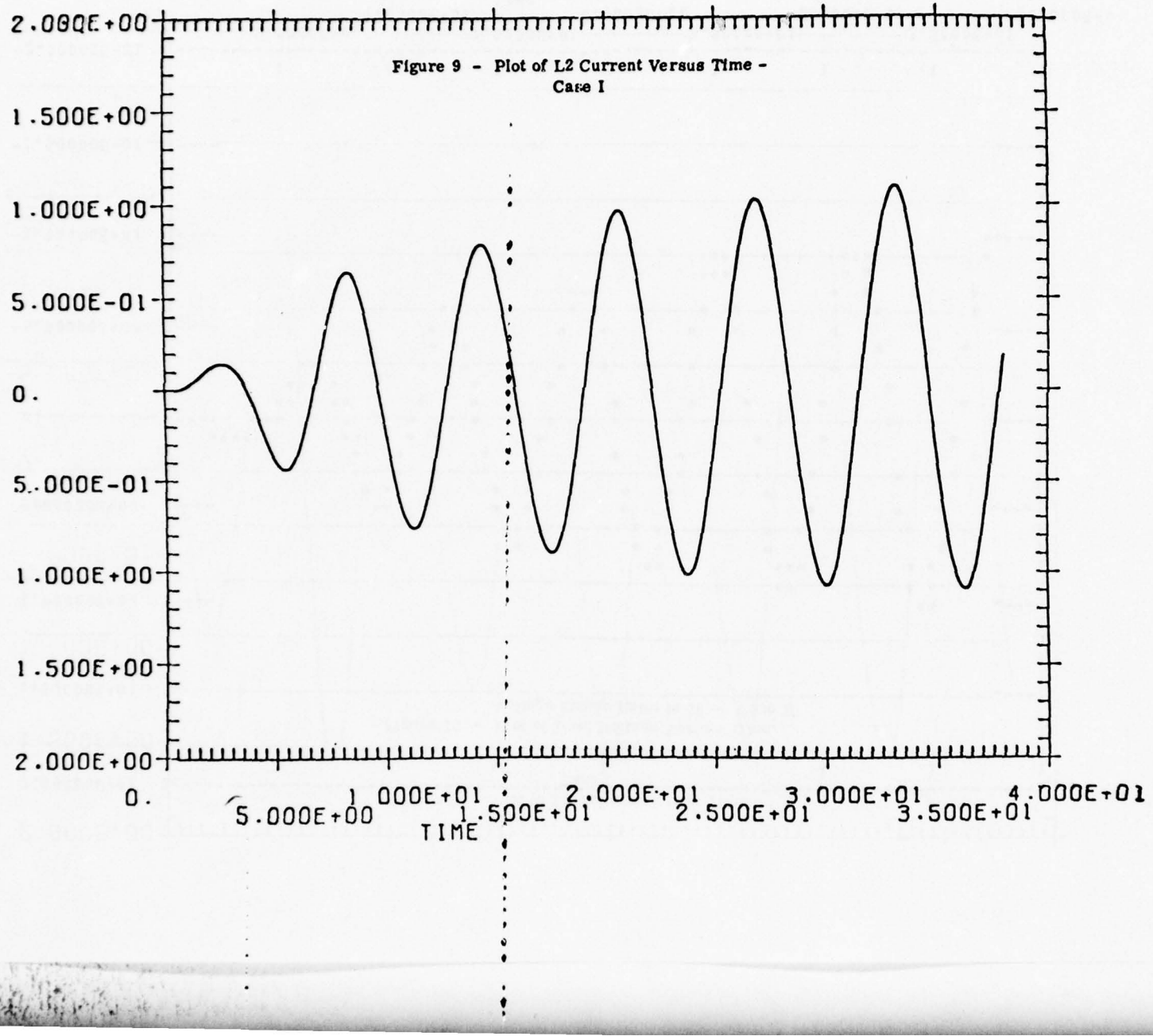


Figure 9 - Plot of L2 Current Versus Time - Case I

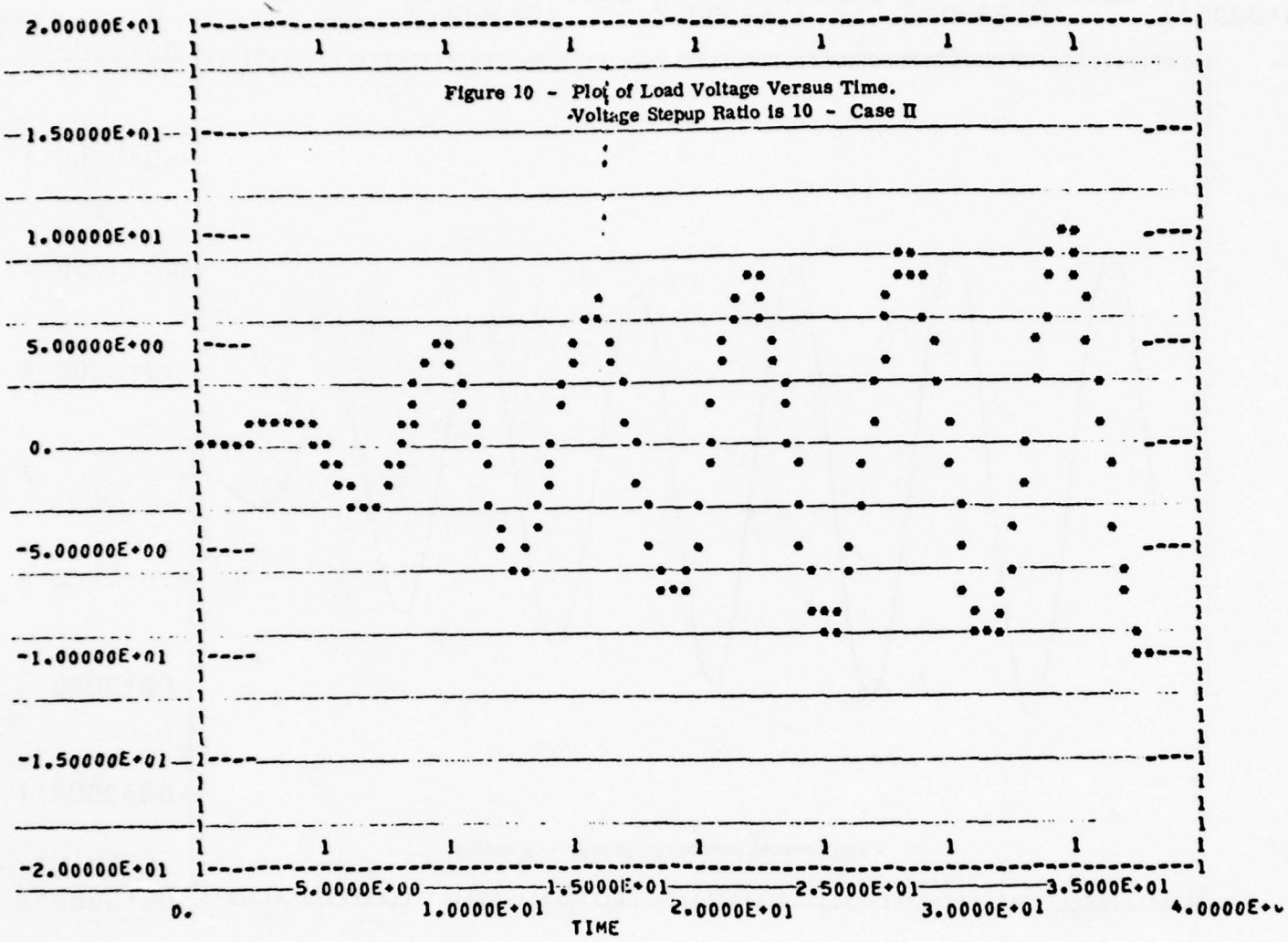


Figure 10 - Plot of Load Voltage Versus Time.
Voltage Stepup Ratio is 10 - Case II

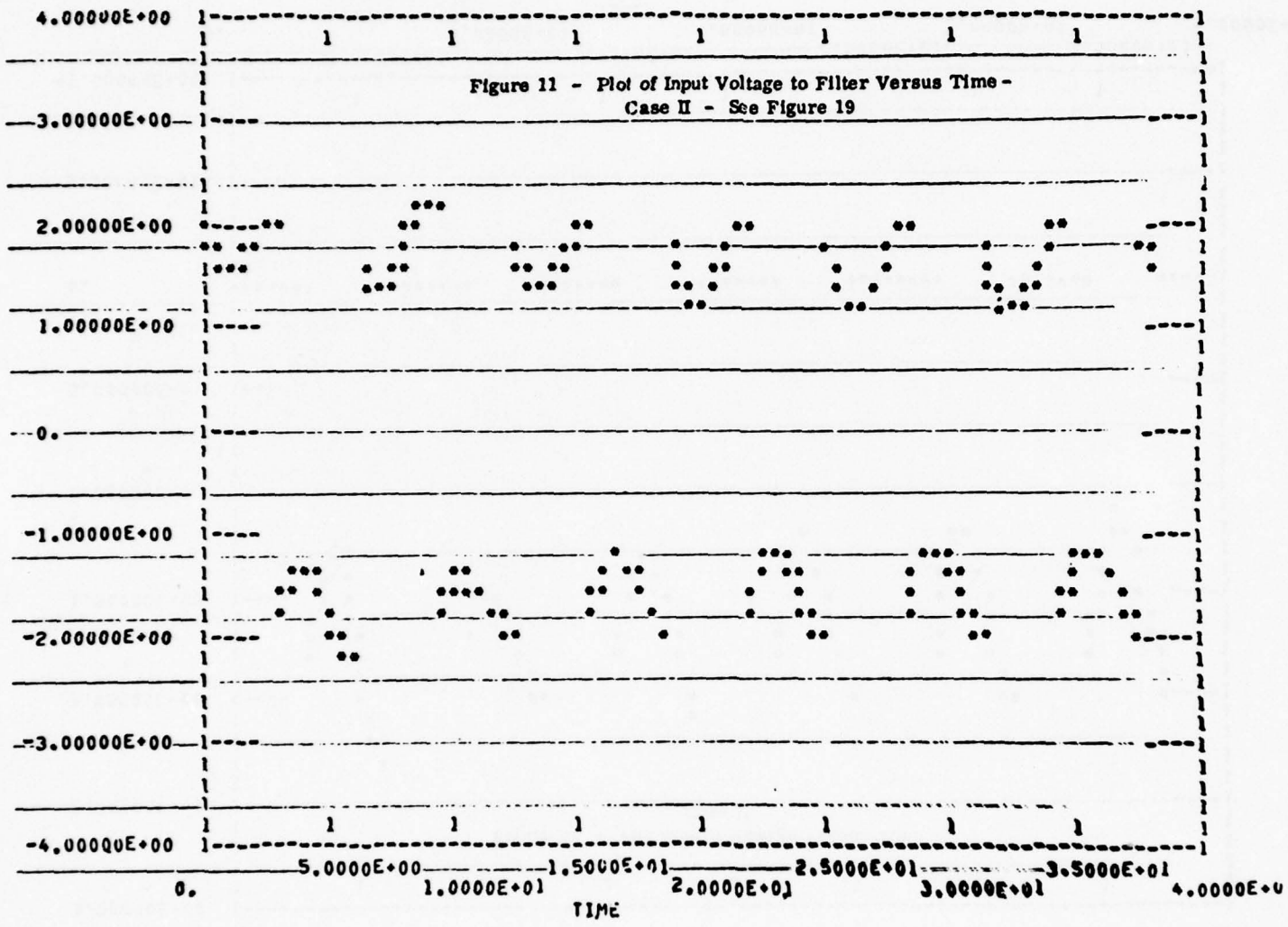


Figure 11 - Plot of Input Voltage to Filter Versus Time - Case II - See Figure 19

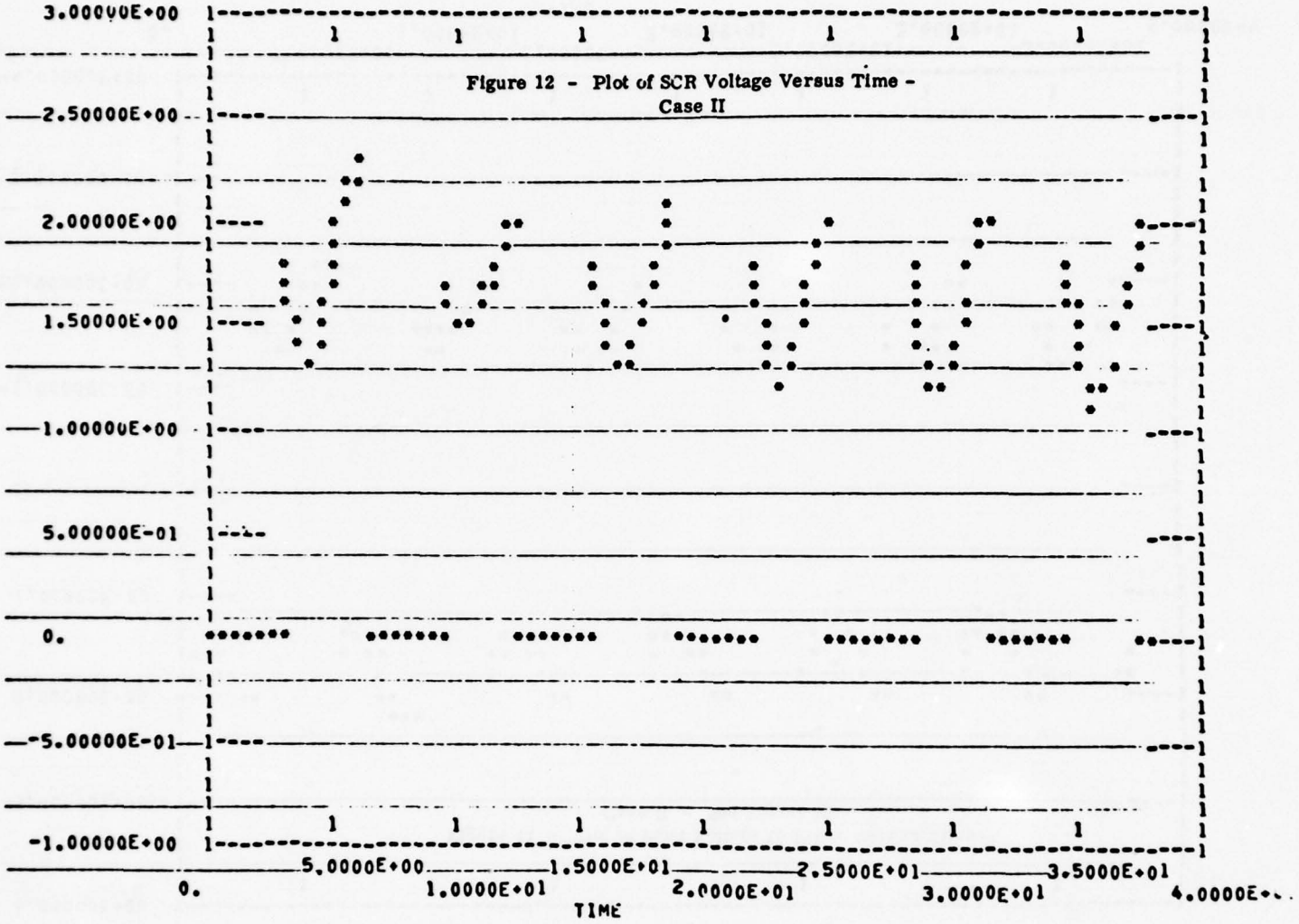


Figure 12 - Plot of SCR Voltage Versus Time - Case II

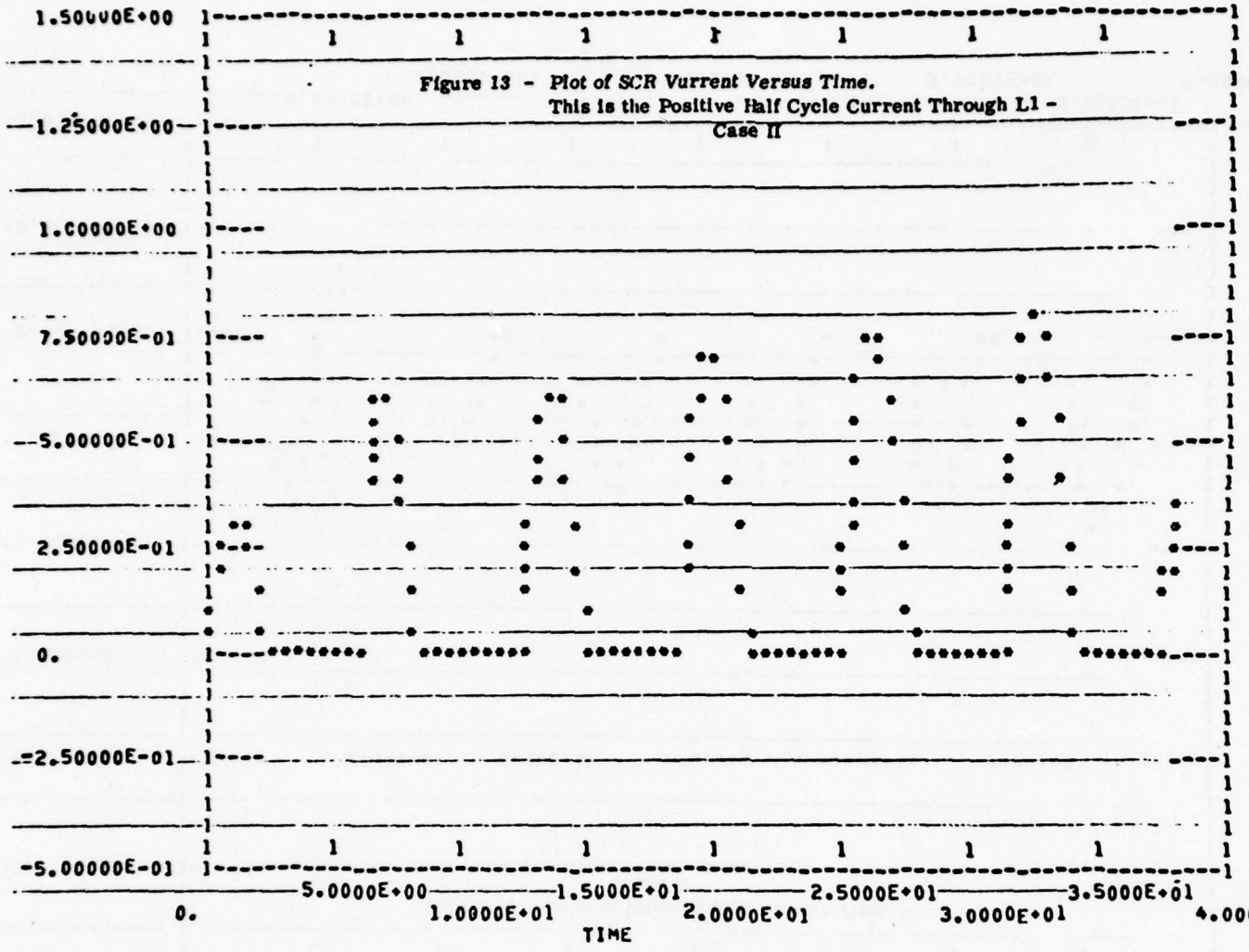


Figure 13 - *Plot of SCR Vurrent Versus Time.*
This is the Positive Half Cycle Current Through L1 -
Case II

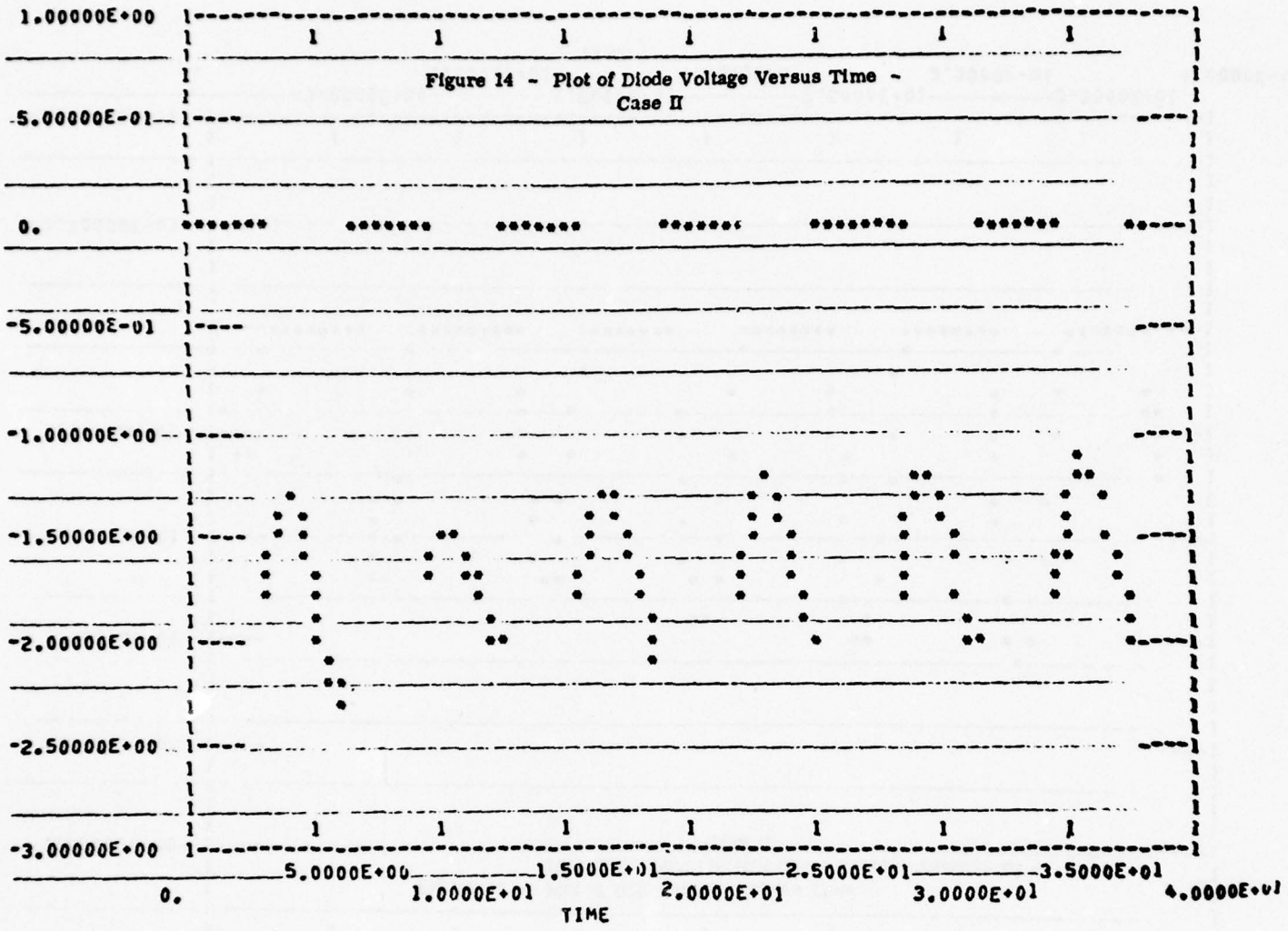


Figure 14 - Plot of Diode Voltage Versus Time - Case II

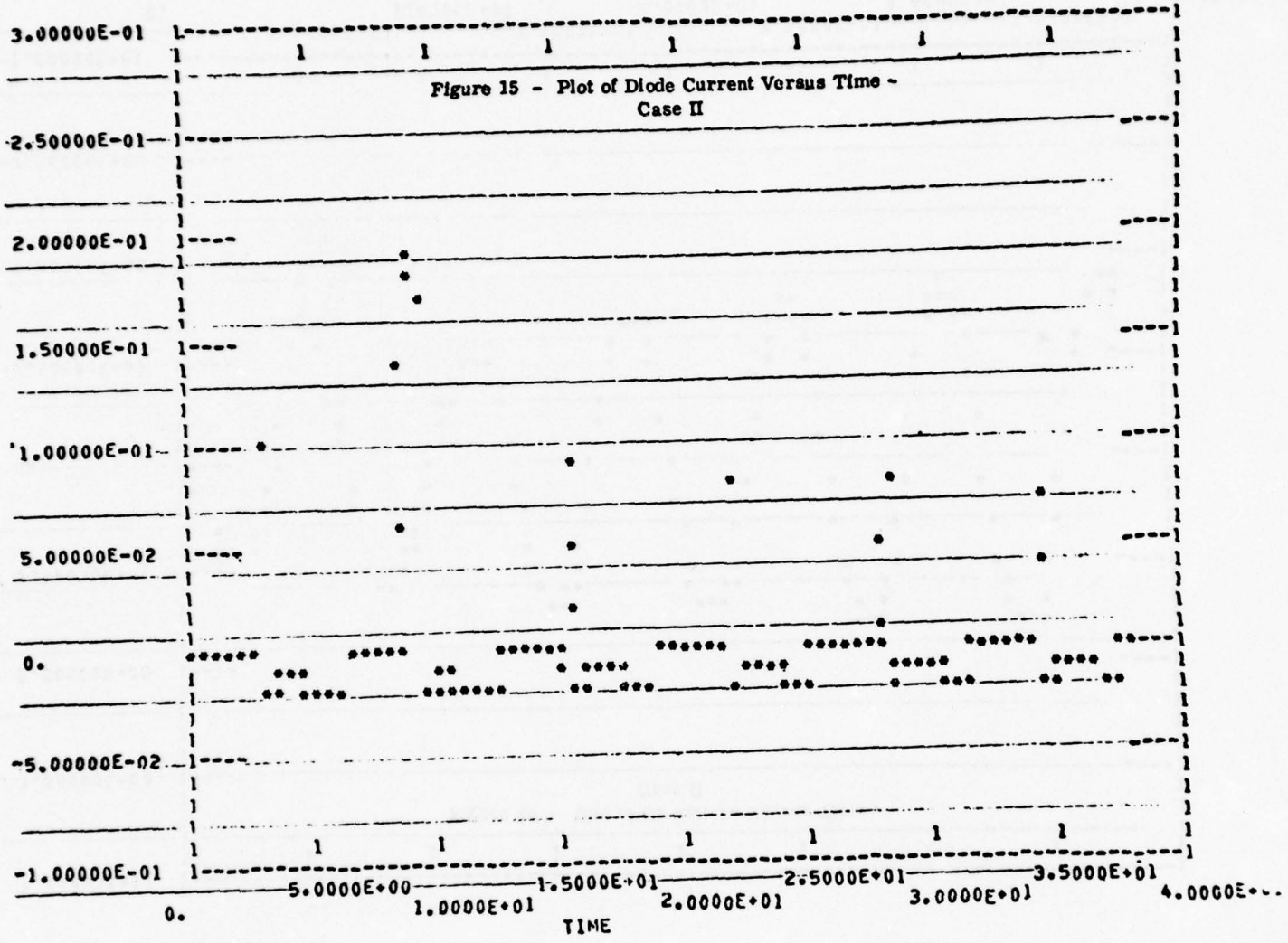


Figure 15 - Plot of Diode Current Versus Time - Case II

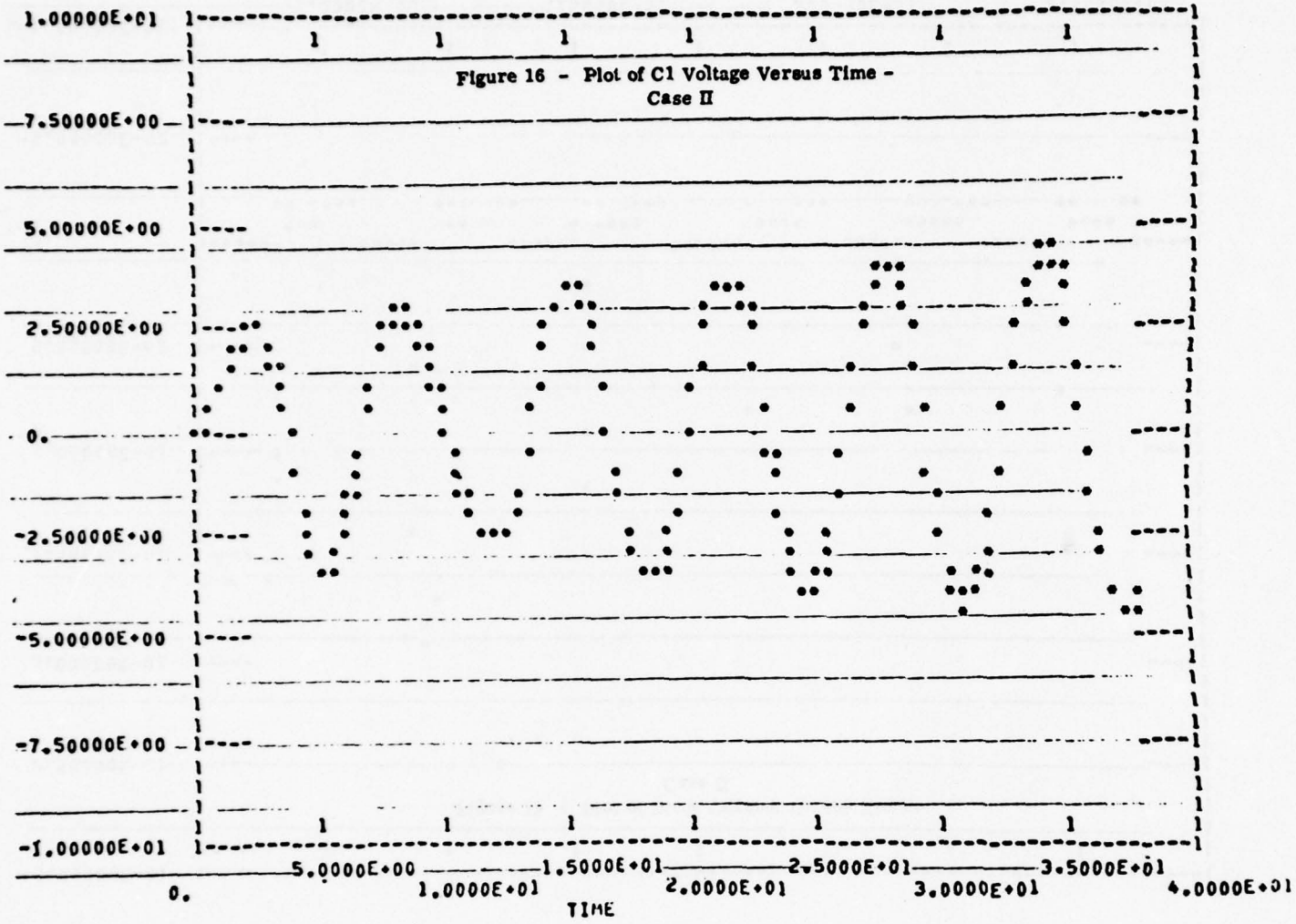


Figure 16 - Plot of C1 Voltage Versus Time - Case II

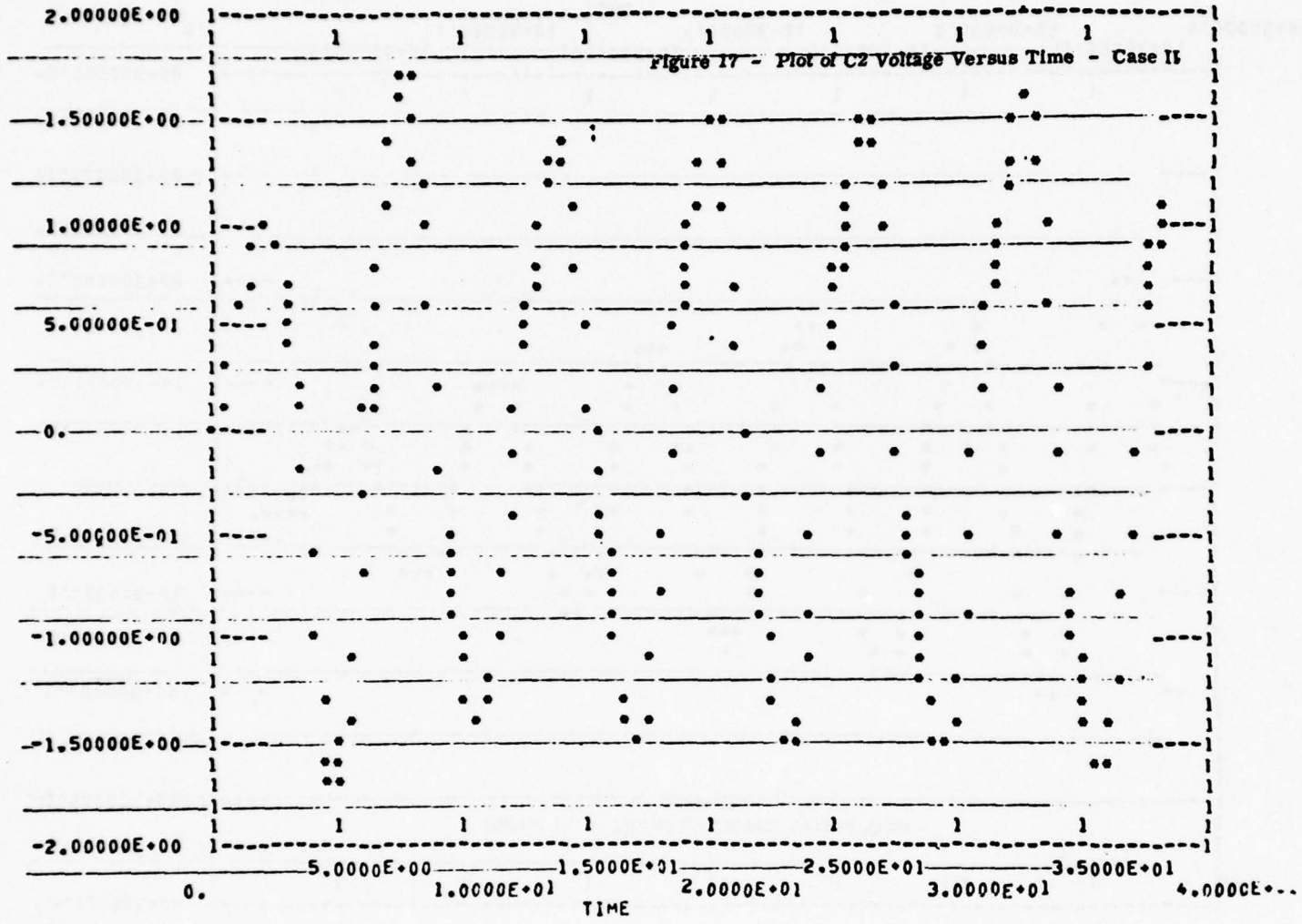


Figure 17 - Plot of C2 Voltage Versus Time - Case II

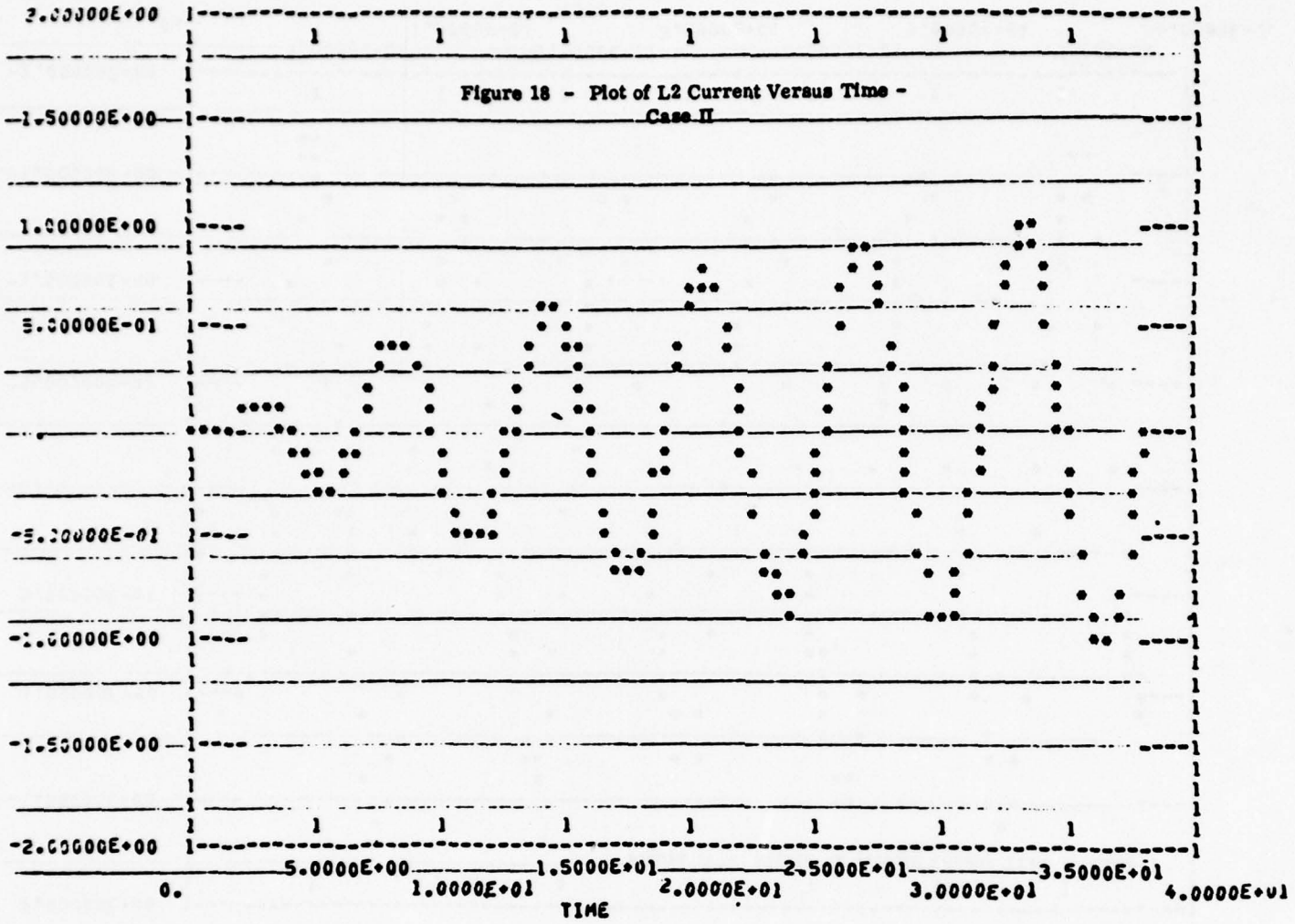


Figure 18 - Plot of L2 Current Versus Time - Case II

TABLE 2 - CASE I

RESULTS OBTAINED ON THE BASIS OF ANALYSIS

As Presented in Figures 1 Through 9

Quantity	Per Unit Values	Actual Values	Peak Operating Voltage or Current (Calculated)	Peak Stored Energy Under Operating Conditions
E	2.0	20,000 volts	--	--
R3	1.0	10 ohms	--	--
R	25.0	250 ohms	--	--
C1	0.167	0.2672 μf	50 KV	334 joules
C2	0.333	0.5328 μf	15 KV	60 joules
C3	0.196	0.3136 μf	50 KV	392 joules
L1	4.5	747 μh	1 KA	374 joules
L2	5.9	979.4 μh	1.25 KA	765 joules
				1925 joules

TABLE 3 - CASE II

RESULTS OBTAINED ON THE BASIS OF ANALYSIS

As Presented in Figures 10 Through 18

Quantity	Per Unit Values	Actual Values	Peak Operating Voltage or Current (Calculated)	Peak Stored Energy Under Operating Conditions
E	2.0	20,000 volts	--	--
R3	1.0	10 ohms	--	--
R	100	1000 ohms	--	--
C1	0.167	0.2672 μf	50 KV	334 joules
C2	0.333	0.5328 μf	15 KV	60 joules
C3*	0.10204	0.163264	100 KV	816 joules
L1	4.5	747 μh	1 KA	374 joules
L2*	10.8	1793 μh	1 KA	897 joules
				2481 joules

*L2 and C3 for Case II changed from Case I to obtain higher voltage set up ratio.

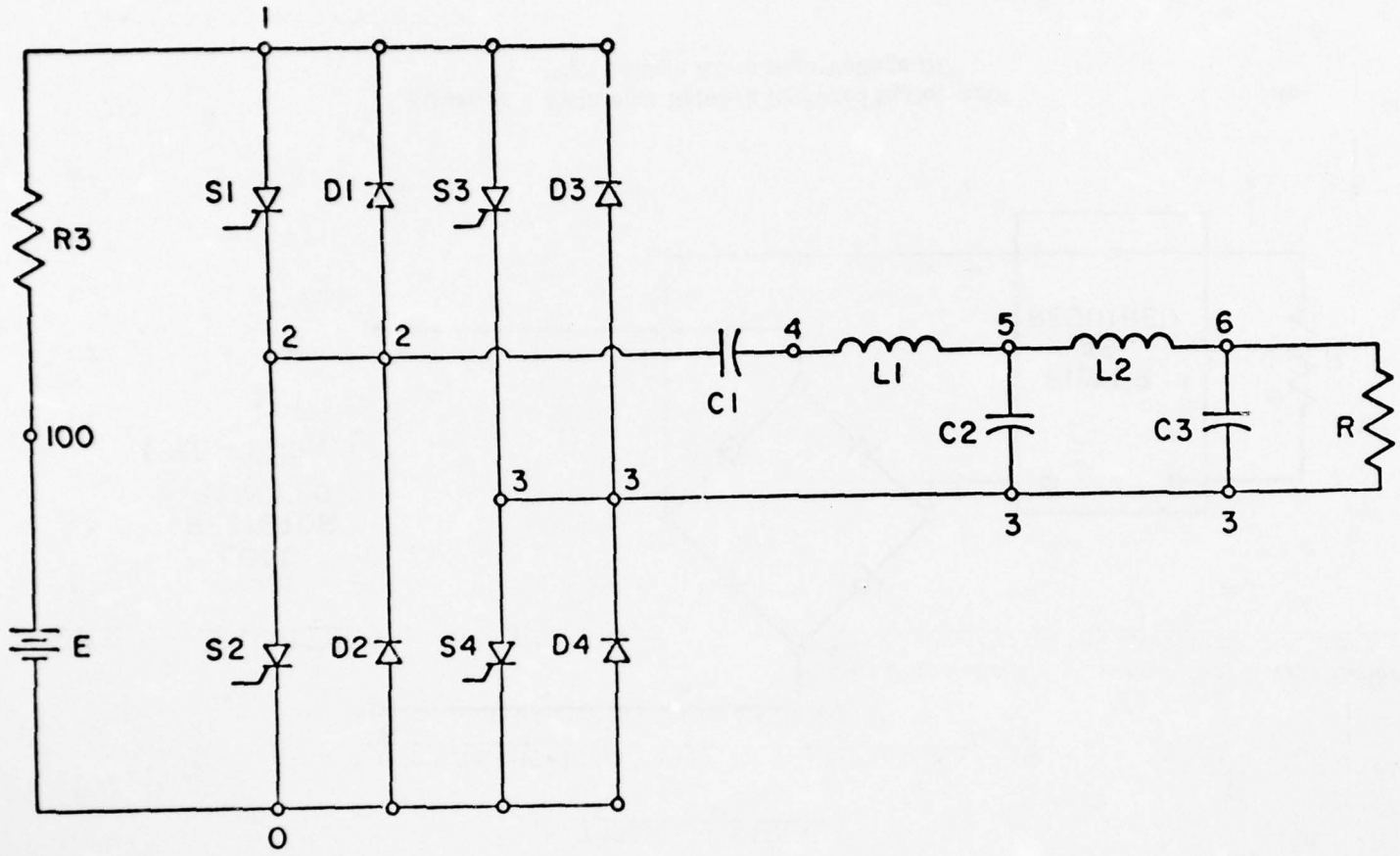


Figure 19 Circuit Diagram of Transformerless High Voltage Power Supply For Conversion of DC to High Voltage AC

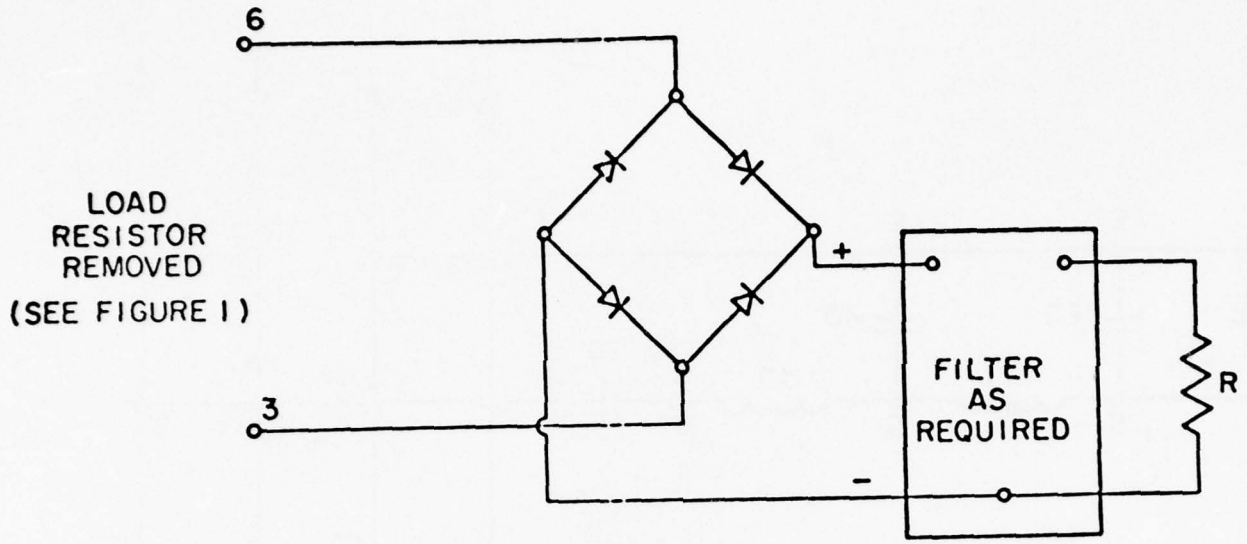


Figure 20 Additional Network Required to Convert High Voltage AC to High Voltage DC

DC-DC Converter Weight and Volume Design Calculations

Conditions:

1. The SCR current is equal to the generator current IGEN.

2. The actual inverse and forwarded voltage requirements are VGEN/0.8 = 1.25 VGEN

3. Use SCR's (IR or W) conservatively rated at 800 volts and 2400 amperes (180° conduction) Note: See Figure 1.

4. Number of series units required per leg.

$$\frac{1.25\ VGEN}{800} \quad \text{(1600 volt SCR's)}$$

5. Number of pressure units required per leg

$$\frac{IGEN}{2400} \quad \text{(2400 ampere SCR's)}$$

6. Total required per leg.

$$\frac{1.25\ VGEN\ IGEN}{800\ X\ 2400} \approx 0.651\ PGEN\ (MW)$$

7. For 4 arms or legs -

the number of SCR's = N_{SCR} = 2.6 PGEN (MW)

8. Weight of SCR with structure, surge protection, clamps, controls, structure, water -

Use conservative value of 4.0#/SCR. Complete of 1.8Kg/SCR.

9. Volume of SCR including a 2 to 1 packing factor $\cong$ $3 \times 10^{-3} M^3$/SCR

10. Weight of inverter = 4.68 POUT (Kg)

11. Volume of inverter = 7.8×10^{-3} POUT (M^3)

12. Weight of inverter + rectifier = 2 X (weight of inverter) (Kg)

13. Volume of inverter + rectifier = 2 X (volume of inverter) (M^3)

Note: See Case I - Table 2

14. Reactive components requirement for 10 MW and voltage step up of 5

$WC1 + WC2 + WL1 \cong 800$ joule.

$WC3 + WL2 \cong 1200$ joules

1) The energy will vary directly with MW

2) The resonant circuit consisting of C3 and L2 will vary with the step up (N), therefore

$$\text{Energy} = \frac{POUT}{10} \left[800 + \frac{N}{5} 1200\right]$$

$$= \left[80 + 24.N\right] POUT$$

Taking a conservative value of 25J/# or 55J/Kg for the reactive components -

$$\text{The weight of reactive components} = \frac{1}{55} \left[80 + 24.N\right] POUT$$

$$= \left[1.45 + 0.436N\right] POUT \text{ (kg)}$$

Taking a conservative value of 10 joules/in^3 or

6.1×10^4 joules/M^3 for the reactive components

The volume of the reactive components =

$VOLRS \cong \left[13 + 4.N\right] 10^{-4} POUT\ M^3$.

Adding a packing factor of $\frac{1}{3}$ this becomes

$\left[39 + 12N\right] 10^{-4} POUT\ M^3$.

15. Cooling

Since N_{SCR} = 2.6 PGEN

The voltage drop per SCR $\sim$ 1.5 volts.

The current in each SCR = 1200 average.

Therefore, the loss per SCR $\cong$ 1800 watts

Total loss = 2.6 PGEN (1800)

= 4.68 PGEN X 10^{-3} (MW)

For the inverter and rectifier

multiply by two of the total loss $\cong$ 10^{-2} PGEN.

APPENDIX B

TRANSFORMER DESIGN PROGRAM

THERMAL TECHNOLOGY LABORATORY, INC.

The transformer design program contained in this Appendix was developed by Thermal Technology Laboratory, Inc. and is an improved version of a program previously supplied to the Air Force Aeropropulsion Laboratory. The primary advantage of the program given here over the previous program is that it automatically designs a minimum weight transformer for a given set of operating conditions.

The main input parameters required in using the program given here are the following.

Output voltage

Primary line-to-line voltage

Operating Frequency

Initial conductor temperature

Final conductor temperature

On time (operating period)

Single phase or three phase

Output power

Litz wire or solid wire

Sine wave or square wave operation.

The program produces a complete design for the minimum weight transformer.

```
 1=EMFDCOUT   :AVG.DC.OUTPUT EMF,3-PHASE BRIDGE RECTIF (VOLTS,AVG.
 2=EMFPRILL   :PRIMARY LINE-LINE EMF                   (VOLTS,RMS
 3=RYPRI      :PRIMARY CONDUCTOR RESISTIVITY           (OHM-INCHES
 4=RYSEC      :SECONDARY WINDING CONDUCTOR RESISTIVITY (OHM-INCHES
 5=BMAXMUTUAL:PEAK MAGNETIC INDUCTION DENSITY          (LINES/SQ.IN.
 6=FREQMIN    :MINIMUM OPERATEING FREQUENCY            (HERTZ
 7=DENCONPRI  :PRIMARY WINDING CONDUCTOR DENSITY       (POUNDS/CUBIC INCH
 8=DENCONSEC  :SECONDARY WINDING CONDUCTOR DENSITY     (POUNDS/CUBIC-INCH
 9=DENCORE    :CORE DENSITY                            (POUNDS/CUBIC-INCH
10=DENCOOLANT:COOLANT DENSITY                         (POUNDS/CUBIC-INCH
11=CLRTPRI    :PRIMARY WINDING CONDUCTOR COOLING RATE  (WATTS/SQUARE-INCH
12=CLRTSEC    :SECONDARY WINDING CONDUCTOR COOLING RATE(WATTS/SQUARE-INCH
13=RTDISCORE :CORE DISSIPATION RATE                   (WATTS/POUND
14=WDCORELEG :CORE LEG WIDTH                          (INCHES
15=DPCORELEG :CORE LEG DEPTH                          (INCHES
16=TPLPRI    :NUMBER OF PRIMARY TURNS PER LAYER       (TURNS/LAYER
17=FACSTKCORE:CORE STACKING FACTOR                    (UNITS/UNITS
18=SPRIWNTURF:PRIMARY SPACING BTWN TURNS              (INCHES
19=FREQMAX   :MAXIMUM OPERATEING FREQUENCY            (HERTZ
20=DENCOREINS:CORE INSULATION DENSITY (=.095)         (POUNDS/CUBIC INCH
21=SPTURNSEC :SPACING BETWEEN TURNS IN SECONDARY LAYER(INCHES
22=TCI       :INITIAL CONDUCTOR TEMPERATURE           (DEG.F.
23=TCF       :FINAL CONDUCTOR TEMPERATURE             (DEF.F.
24=ERRORCONVG:EFFICIENCY CONVERGENCE CRITERION        (
25=TON       :ON TIME                                 (SECONDS
26=FACCONPRI :PRIMARY CONNECTION FACTOR ( 3 = DELAA ) (
27=FACCONSEC :SECONDARY CONNECTION FACTOF ( 1 = WYE ) (
28=FREQDROOP/:PER UNIT FREQUENCY DROOP                (
29=FACTCROUT :OUTPUT WAVEFORM FACTOR                  (
30=INTERLEAVI:NUMBER OF INEERLEAVINGS                 (INTERLEAVINGS
```

```
31=FACTSPCOOL:COOLING SPACING FACTOR                    (IN/(IN-WATT/SQ.IN)
32=STRDIELBRK:DIELECTRIC BREAKDOWN STRENGTH             (KILOVOLTS/INCH,RMS
33=EFFM IN    :MINIMUM EFFICIENCY                       (
35=POWER,OUT  :OUTPUT POWER                             (WATTS , DC
36=WTCOREIRON:CORE IRON WEIGHT                          (POUNDS
37=COEFCRLOSS:CORE LOSS COEFFICIENT                     (
38=EXBMCRLOSS:CORE LOSS BM EXPONENT                     (
39=EXFRCRLOSS:CORE LOSS FREQUENCY EXPLNENT              (
40=DIAWIRPRI  :PRIMARY WIRE DIAMETER                    (INCHES
41=DIAWIRSEC  :SECONDARY WIRE DIAMETER                  (INCHES
42=WDWINDOW   :WINDOW WIDTH                             (INCHES
43=HIWINDOW   :WINDOW HEIGHT                            (INCHES
44=TRN/COIPRI:NUMBER OF PRIMARY TURNS PER COIL          (TURNS
45=TRN/COISEC:NUMBER OF SECONDARY TURNS PER COIL        (TURNS
46=LAY/COIPRI:NUMBER OF PRIMARY LAYERS PER COIL         (LAYERS
47=TRN/LAYSEC:NUMBER OF SECONDARY TURNS PER LAYER       (TURNS/LAYER
48=LAY/COISEC:NUMBER OF SECONDARY LAYERS PER COIL       (LAYERS/COIL
49=EFFICIENCY:COMPUTED EFFICIENCY                       (/UNIT
50=WEIGHT-TOT:TOTAL WEIGHT                              (POUNDS
51=REGULATION:REGULATION                                (/UNIT
52=CURLININ   :INPUT LINE CURRENT                       (AMPERES,RMD
53=CURRENTOUT:RECTIFIED OUTPUT CURRENT                  (AMPERES,DC
54=POWERINTOT:TOTAL INPUT POWER                         (WATTS
55=CURWINDPRI:PRIMARY WINDING CURRENT                   (AMPERES,RMS
56=DENCURPRI  :PRIMARY CURRENT DENSITY                  (AMPERES/SQ.IN.
57=DENCURSEC  :SECONDARY CURRENT DENSITY                (AMPERES/SQ.IN
58=AREACROSPR:PRIMARY WIRE CROSSECTIONAL AREA           (SQUARE-INCHES
59=AREACRSSE:SECONDARY WIRE CROSS-SECTIONAL AREA        (SQUARE-INCHES
60=INDMAGCORE:MAGNETIC INDUCTION IN CORE                (LINES
61=RESISTANC/:PER UNIT RESISTANCE                       (
62=SPPR-SETOT:TOTAL PRIMATY-TO-SECONDARY SPACING        (INCHES
63=DPWINDING  :WINDING DEPTH                            (INCHES
64=LEN/COIPRI:PRIMARY LENGTH PER COIL                   (INCHES
65=LEN/COISEC:SECONDARY LENGTH PER COIL                 (INCHES
```

```
66=RESISPRI  :PRIMARY RESISTANCE PER COIL                    (OHMS/COIL
67=RESISSEC  :SECONDARY RESISTANCE PER COIL                  (OHMS/COIL
68=DIS/COIL  :DISSIPATION PER COIL                           (WATTS
69=VOLUMEWIRE:TOTAL WIRE VOLUME                              (CUBIC-INCHES
70=WEIGHTWIRE:TOTAL WIRE WEIGHT                              (POUNDS
71=VOLUMECORE:CORE VOLUME , PHYSICAL                         (CUBIC-INCHES
72=WEIGHTCORE:CORE WEIGHT , TOTAL                            (POUNDS
73=DISCORE   :CORE DISSIPATION                               (WATTS
74=DISTOTAL  :TOTAL DISSIPATION                              (WATTS
75=VOLCONPRI :PRIMARY CONDUCTOR VOLUME                       (CUBIC-INCHES
76=VOLCONSEC :SECONDARY WIRE VOLUME                          (CUBIC-INCHES
77=VOLTANKINT:TANK INTERNAL VOLUME                           (CUBIC-INCHES
78=VOLCOOLANT:COOLANT VOLUME                                 (CUBIC-INCHES
79=WTCOOLANT :COOLANT WEIGHT                                 (POUNDS
80=EMF/TRNPRI:PRIMARY EMF PER TURN                           (VOLTS/TURN
81=EMF/TRNSEC:SECONDARY EMF PER TURN                         (VOLTS/TURN
84=INDLELEAK:LEAKAGE INDUCTANCE REFERRED TO SECONDARY        (HENRIES
85=REALEAKSEC:LEAKAGE REACTANCE REFERED TO SECONDARY         (OHMS
86=EFFICINIT :ASSUMED INITIAL TRANSFORMER DESIGN EFFIC       (/UNIT
87=SPACMINABS:ABSOLUTE MINIMUM SPACING                       (INCHES
88=REACTANCE/:PER UNIT REACTANCE                             (
89=IMPEDANCE/:PER UNIT IMPEDANCE                             (
90=MERFIT-OF :EFFICIENCY PER POUND PER KILLOWATT OUT         (1/LBS*KILLOWATTS
91=AGCORELEG :CORE LEG CROSS-SECTIONAL AREA                  (SQUARE-INCHES
92=RATASPCRLG:CORE LEG ASPECT RATIO (DEPTH/WIDTH)            (
93=HEIGHTCASE:CASE INTERNAL HEIGHT                           (INCHES
94=DEPTHCASE :CASE DEPTH                                     (INCHES
95=WIDTHCASE :CASE WIDTH                                     (INCHES
96=CURLINSEC :SECONDARY LINE CURRENT                         (AMPERES,RMS
97=CURWINDSEC:SECONDARY WINDING CURRENT                      (AMPERES,RMS
98=EMFLLSEC  :SECONDARY LINE-TO-LINE EMF                     (VOLTS,RMS
99=FACWAVDRI :DRIVING WAVEFORM FACTOR (4E-8=SQ,4.44=SIN
100=EMFLLSECNL:NO LOAD SECONDARY LINE-TO-LINE EMF            (VOLTS,RMS
```

```
101=RYPRIZERO :ZERO DEGREE PRIMARY CONDUCTOR RESISTIVIT(OHM-INCHES
102=RYSECZERO :ZERO DEGREE SECONDARY CONDUCTOR RESISTIV(OHM-INCHES
103=TEMPCONPRI:PRIMARY CONDUCTOR TEMPERATURE          (DEGREES
104=TEMPCONSEC:SECONDARY CONDUCTOR TEMPERATURE        (DEGREES
105=RYCOEFTMPR:PRIMARY CONDUCTOR TEMPERATURE COEFFICIEN(UNITS/DEGREE
106=RYCOEFTMSE:SEC.CON.TEMPERATURE COEFF.OF RESISTIVITY(UNITS/DEBREE
107=RATREA/DPR:PRIMARY AC-TO-DC RESISTANCE RATIO      (
108=RATREA/DSE:SECONDARY AC-TO-DC RESISTANCE RATIO    (
109=GAGEWIREPR:PRIMARY WIRE GAUGE / NO. LITZ WIRE     (STRANDS
110=GAGEWIRESE:SECONDARY WIRE AAUGE/NO.LITZ WIRE      (STRANDS
111=RECDEV/STA:NUMBER OF RECTIFIER DEVICES PER STACK  (RECTIFIERS/STACK
112=FACBRKDWNR:RECTIFIER BREAKDOWN FACTOR             (
113=EMFRECREVP:RECTIVIER PEAK REVERSE EMF             (VOLTS
114=EMF/WINDSE:SECONDARY EMF PER WINDING              (VOLTS/WINDING ,RMS
115=EMFRECFOR :FORMARD VMF DROP PER RECTIVIER ELEMENT (VOLTS/ELEMENT
116=VASEC     :SECONDARY VA                           (VOLTS-AMPERES
117=HEIGHTPRI :PRIMARY HEIGHT                         (INCHES
118=HEIGHTSEC :SECONDARY HEIGHT                       (INCHES
119=RTCOOLCORE:CORE COOLING RATE                      (WATTS/SQ.IN.
120=FACSERIER :SERIES FACTOR , INSULATION             (
121=SPMINREL  :MINIMUM RELATIVE SPACING FACTOR        (/UNIR
122=RTHEATEN  :ENCLOSURE HEATING RATE                 (WATTS/SQ.IN.
123=EMF/LAYSEC:SECONDARY EMF PER LAYER                (VOLTS/LAYER
125=DPCR/2    :CORE DEPTH / 2                         (INCHES
126=SPRATSEC  :SEC-SEC SPAC /(SEC-SEC SPAC + DS)      (
127=DENRATCOL :RATIO COOLANT VAPOR/LIQUID DENSITY     (
128=DISRIPR-SE:PRIMARY COOLING RATE REFRENCED TO SECOND(WATTS/SQ.IN.
129=EMFSLL+PLL:EMF SEC.L-L + EMF PRI.L-L              (VOLTS
130=SPHIL-C   :SPACING,HOR.INSIDE LAYER-TO-CORE INSIDE (INCHES
131=SPHCI-C   :SPACING,HOR.INNER LAYER-TO-CORE OUTSIDE (INCHES
132=SPHOL-EN  :SPACING,HOR.OUTER LAYER-TO-ENCLOSURE   (INCHES
133=SPSECTOSEC:SPACING,HORIZONTAL,SECONDARY-TO-SEC.LAYE(INCHES
134=SPHOUT-OUT:SPACING,HOR.OUTER-TO-OUTER LAYER       (INCHES
135=SPVSTCT   :SPACING,VERTICAL,TOP SECONDARY-TO-CORE (INCHES
```

```
136=SPVSTCB    :SPACING,VERT.BOTTOM SECONDARY-TO-CORE    (
137=SPHSTP     :SPACING,HORIZONTAL,SECONDARY-TO-PRIMARY  (INCHES
138=SPVPTCT    :SPACING,VERTICAL,TOP PRIMARY-TO-CORE     (INCHES
139=SPVPTCB    :SPACING,VER.BOTTOM PRIMARY-TO-CORE       (INCHES
140=EMFWINDPRI :PRIMARY WINDING EMD                      (VOLTS,RMS
141=SPHPTP     :SPACING,HORIZONTAL,PRIMARY-TO-PRIMARY LA (INCHES
142=DIAMOSOP   :MAXIMUM OF DS OR DP                      (INCHES
143=SPRATPTS   :PR-SE SPC / (PR-SE SP + MAX(DS,DP))      (
144=IMPSEC     :SECONDARY IMPEDANCE                      (OHMS
145=HIWNPR     :NECESSARY WINDAW HEIGHT FOR PRIMARY      (INCHES
146=HIWDSE     :NECESSARY WINDOW HEIGHT FOR SECONDARY    (INCHES
147=GROUPSEC   :NUMBER OF SECONDARY GROUPS               (GROUPS
148=LAYMIN/SEC :MINIMUM NUMBER OF LAYERS IN A SECONDARY  (LAYERS/GROUP
149=LAY/GRPXSE :MAXIMUM NO.OF LAYERS PER SECONDARY GROUP (LAYERS/GROUP
151=GRPSMAXSEC :NUMBER OF SEC.GROUPS WITH MAX.NO.LAYERS  (GROUPS
150=GRPSMINSEC :NUMBER OF SEC.GROUPS WITH MIN.NO.LAYERS  (GROUPS
152=PERCOIMEAN :MEAN COIL PERIMETER                      (INCHES
153=ASCOREGL   :EFFECTIVE CORE COOLING SURFACE AREA      (SQUARE-INCHES
154=SPCOHEAD   :CORE-TO-CASE HEAD SPACE, TOTAL           (INCHES
155=SPHSPST    :SPACING,HORIZONTAL FOR SUPPORT STRUCTURE (INCHES
156=EMFFACOVB  :EMF WINDING BREAKDOWN FACTOR             (
157=GRPS PRI   :NUMBER OF PRIMARY GROUPS                 (GROUPS
158=LAYPGMNPR  :MINIMUM NUMBER OF LAYERS PER PRIMARY GRO (LAYERS/GROUP
159=LAYPGMXPR  :MAXIMUM NUMBER OF LAYERS PER PRI.GROUP   (LAYERS/GROUP
160=GRPSMNPR   :NUMBER OF MINIMUM LAYER PRIMARY GROUPS   (GROUPS
161=GRPSMXLYPR :NUMBER OF MAXIMUM LAYER PRIMARY GROUPS   (GROUPS
165=DUTY FACTO :DUTY FACTOR                              (/UNIT
166=WEIGHTENC  :ENCLOSURE WEIGHT                         (POUNDS
167=WDAIRPATH  :AIR FLOW PATH WIDTH                      (INCHES
168=DPAIRPATH  :AIR FLOW PATH DEPTH                      (INCHES
169=DIA.TUBE   :TUBE DIAMETER                            (INCHES
170=SPAC.TUBE  :TUBESPACING                              (INCHES
171=ROWS DEEP  :NUMBER OF ROWS DEEP                      (ROWS
172=ROWS WIDE  :NUMBER OF ROWS WIDE                      (ROWS
```

```
173=XT.FLOWAIR:AIR MASS FLOW RATE                              (LBS/HR-SQ.FT
174=TEMPAIRAMB:AMBIANT AIR TEMPERATURE                         (DEG.FARENHEIGHT
175=TEMPCOLAVG:AVERAGE COOLANT TEMPERATURE                     (DEGREES FARENHEIGHT
176=COEF.H.T.A:AIR HEAT TRANSFER COEFFICIENT                   (BTU/HR/SQ.FT./DEG.F
177=AS.H.E.AIR:HEAT EXCHANGER SURFACE AREA TO AIR              (SQUARE FEET
178=DIA.FAN   :FAN DIAMETER                                    (INCHES
179=HI.TRANE  :HEIGHT TRANSFORMER + HEAT EXCHANGER             (INCHES
180=VOL.SYSTEM:VOLUME TRANSFORMER + HEAT EXCHANGER             (CUBIC INCHES
181=VOL.H.E.  :VOLUME HEAT EXCHANGER LESS FAN                  (CUBIC INCHES
182=SHCP      :PRIMARY CONDUCTOR SPECIFIC HEAT                 (BTU/HR./DEG.F.
183=SHCS      :SECONDARY CONDUCTOR SPECIFIC HEAT               (BTU/HR./DEG.F.
184=RYCPI     :INITIAL PRI.COND.RESISTIVITY                    (OHM-INCHES
185=RYCSI     :INITIAL SEC.COND.RESISTIVITY                    (OHM-INCHES
186=CTRYCPI   :INITIAL PRI.COND.RY.TEMP.COEFFICIENT            (
187=CTRYCSI   :INITIAL SEC.COND.RESISTIVITY TEMP.COEFF.        (
188=AS.H.E.CON:HEAT EXCHANGER SURFACE AREA TO INSIDE CO        (SQUARE FEET
189=COEF.CONDE:HEAT EXCHANGER VAPOR CONDENSATION COEFFI        (BTU/HR/SQ.FT./DEG.F
190=H.P.BLOWER:BLOWER HORSE POWER                              (WATTS
191=TEMP.TUBES:TUBE TEMPERATURE                                (DEGREES FERENHEIGHT
192=HEIGHTH.E.:HEAT EXCHANGER HEIGHT                           (FEET
193=PRESSURE D:PRESSURE DROP                                   (
194=VEL.AIR   :AIR VELOCITY                                    (
195=CFM       :CFM                                             (CUBIC-FEET/MINUTE
196=WEIGHTBLOW:BLOWER WEITHT                                   (POUNDS
197=WT.TUBES  :FIN TUBE WEIGHT                                 (POUNDS
198=WT.H.E.   :HEAT EXCHANGER WEIGHT                           (POUNDS
199=WT.TRANS.S:TRANSFORMER SYSTEM WEIGHT                       (POUNDS
200=O.F.SYS.  :SYSTEM OBJECTIVE FUNCTION                       (EFF/HZ/LB/WATT
```

```
NO.    CONSTANT INDEPENDENT PARAMETER VALUE

 87      .50000E-01

NO.    FIXED INDEPENDENT PARAMETER VALUES

  1      .20000E+05
  2      5000.0
  3      100000
  7      .32400
  8      .32400
  9      .27600
 10      0.
 17      .90000
```



```
FUNCTION FNOB        73/74   OPT=2                    FTN 4.4+R401      7

1                FUNCTION FNOB(DUMMY)
                 REAL M,KG
                 REAL K(200)
                 COMMON / FVC / K
5                DATA PI / 3.1415962 /
                 SQR(X) = SQRT(X)
                     FNA(D)=0.9908+0.1768*((D-2.11)+SQR((D-2.11)**2+0.283))
                 FNOB = -1
                 SQR3 = SQRT(3.)
10               K(6) = K(29) * K(28)
                 K(13) = K(37) * K(5)**K(38) * K(19)**K(39)
                 K(14)=SQR(K(91)/K(92))
                 K(15)=SQR(K(91)*K(92))
                 K(163) = 0.3259596727 * EXP(-0.16042 * K(162))
```

```
      K(164) = 0.32246 * EXP(-0.11310 * K(162))
      K(83) = PI * K(164) * K(164) / 4.
      K(82) = PI * K(163) * K(163) / 4.
      K(103) = K(104) = (K(22) + K(23)) / 2.
      K(184) = K(101) * (1. + K(105) * K(22))
      K(185) = K(102) * (1. + K(106) * K(22))
      K(186) = (1. - K(101) / K(184)) / K(22)
      K(187) = (1. - K(102) / K(185)) / K(22)
      K(56)=SQRT(K(7)*K(182)/K(106)*ALOG( 1.0    +K(186)*(K(23)-K(22)))
     +    /K(184) /K(25))
      K(57) = SQRT(K(8) * K(183) / K(187) * ALOG ( 1.0    + K(187) * (K(
     +23) - K(22)))         / K(185)  / K(25))       *
      K(5)=K(101)*(1+K(105)*K(103))
      K(4)=K(102)*(1+K(106)*K(104))
      K(66)=K(67)=K(85)=K(119)=0
      DO 3010 I=1,10
      K(129+I) = K(87)
 3010 CONTINUE
      K(53)=K(35)/K(1)
      IF(K(26) .GT. 0.) K(96) = K(53) * 0.816 * K(29)
      IF(K(26) .EQ. 0.) K(97) = K(96) = K(53) * K(29) * 1.
      IF(K(26) .GT. 0.) K(97) = K(96) / SQRT(K(27))
      IF(K(26) .GT. 0.) K(98) = 0.74 * K(1)
      IF(K(26) .EQ. 0.) K(114) = K(98) = K(1) * 1.11
      IF(K(26) .GT. 0.) K(114) = K(98) * SQRT(K(27)/3.)
      K(110) = K(96) * K(98)
      IF(K(26) .GT. 0.) K(116) =  K(110) * SQRT(3.)
C     K(41)=0.005*2**(6-K(120)/6)
      K(120) = AINT(K(97) / K(57) / K(82) + 1.)
      K(41) = 1.27 * K(164) * SQRT(K(110))
      K(12) = 2.*K(97)**2*K(4)/PI/K(41)**3
C     B=2.238E-04*K(41)*SQR(K(19)/K(4))
C     K(108) = FNA(B)
      K(59)=K(41)**2*PI/4
      K(108) = K(59) / K(82) / K(110)
```

```
50                K(60)=K(91)*K(5)*K(17)
                  K(140) = K(2)
                  IF(K(26) .GT. 0.) K(140) = K(140) * SQRT(K(26) / 3.)
                  K(86)=1
               3100 CONTINUE
55                K(54) = K(116) / K(86)
                  K(55) = K(52) = K(54) / K(2)
                  IF(K(26) .GT. 0.) K(52) = K(52) / SQR3
                  IF(K(26) .GT. 0.) K(55) = K(52) / SQRT(K(26))
               C  K(40)=0.000*2**(6-K(109)/6)
60                K(109) = AINT(K(55) / K(56) / K(82) + 1.)
                  K(140) = 1.17 * K(164) * SQRT(K(109))
                  K(11)=2*K(55)**2*K(3)/PI/K(40)**3
               C  C=2.638E-04*K(40)*SQR(K(19)/K(3))
               C  K(107) = FNA(C)
65                K(58)=K(40)**2*PI/4
                  K(167) = K(58) / K(82) / K(109)
                  K(44)=(K(140)-K(55)*K(66))/K(6)/K(60)/K(99)
                  IF(K(44) .LE.0.) GOTO 3770
                  K(45)=(SQR((K(114)+K(67)*K(97))**2+(K(97)*K(85))**2))/K(6)/K(60)/K
70               +(99)
                  K(80)=K(140)/K(44)
                  K(81)=K(114)/K(45)
                  K(16)=K(44)/K(46)
                  K(117)=K(16)*(K(40)+K(18))
75                K(47)=K(45)/K(48)
                  K(118)=K(47)*(K(41)+K(21))
                  K(145)=K(117)+K(138)+K(139)
                  K(146)=K(118)+K(135)+K(136)
                  K(43) = AMAX1(K(145),K(146))
80                K(123)=K(114)/K(48)*K(80)/K(81)
                  K(100)=K(98)*K(80)/K(81)
                  K(125) = K(15) / 2.
                  K(126)=K(135)/(K(133)+K(41))
               C  K(128)=K(11)*K(117)/K(118)
```

```
      K(129)=K(100)+K(2)
      K(142) = AMAX1(K(40),K(41))
      K(145)=K(137)/(K(137)+K(142))
C       SPACING COMPUTATIONS
C       K(133) : SECONDARY-SECONDARY HORIZONTAL SPACING
C     K(133) = AMAX1(K(31)*K(118)*K(12),K(156)*K(123)*2./K(32)/1000.,K(1
      K(130) = AMAX1(                    K(156)*K(123)*2./K(32)/1000.,K(1
     +21)*K(42),K(87))
C       K(135) : SPACING, VERTICAL, TOP SECONDARY - CORE
C     K(135) = AMAX1(K(125)*K(126),K(156)*K(100)*K(120)/K(32)/1000.,
      K(135) = AMAX1(                K(156)*K(100)*K(120)/K(32)/1000.,
     +K(121)*K(41),K(87))
C       K(136) : SPACING, VERTICAL, BOTTOM SECONDARY - CORE
C     K(136) = AMAX1(K(127)*K(135),K(156)*K(100)*K(120)/K(32)/1000.,
      K(136) = AMAX1(                K(156)*K(100)*K(120)/K(32)/1000.,
     +K(121)*K(41),K(87))
C       K(137) : SPACING, HORIZONTAL PRIMARY - SECONDARY
C     K(137) = AMAX1(K(31)*K(118)*(K(12)+K(128))/2. ,
      K(137) = AMAX1(
     +K(156)*K(129)*K(120)/K(32)/1000. , K(121)*K(142) , K(87) )
C       K(138) : SPACING, VERTICAL, TOP PRIMARY - CORE
C     K(138) = AMAX1(K(125)*K(145), K(156)*K(2)/K(32)/1000. ,
      K(138) = AMAX1(                K(156)*K(2)/K(32)/1000. ,
     +K(121)*K(42) , K(87) )
C       K(139) : SPACING, VERTICAL, BOTTOM PRIMARY - CORE
C     K(139) = AMAX1(K(127)*K(138) , K(156)*K(2) /K(32)/1000. ,
      K(139) = AMAX1(                 K(156)*K(2) /K(32)/1000. ,
     +K(121)*K(40) , K(87) )
      K(147) = K(157) = K(46)
C       DETERMIN INNER / OUTER LAYER SPACINGS
```

```
      IF(K(46) .LE. K(48)) GOTO 3510
      K(157) = K(157) + 1
C       PRIMARY INNER LAYER
C       K(130) : SPACING, HORIZONTAL, INNER LAYER - CORE LEG FACE INSIDE
C     K(130) = AMAX1(K(31)*K(117)*K(11)/2. , K(156)*K(2)/K(32)/1000. ,
      K(130) = AMAX1(                        K(156)*K(2)/K(32)/1000. ,
     +K(121)*K(40) , K(87) )
C       K(131) : SPACING, HORIZONTAL, INNER LAYER - OUTER CORE LEG FACE
C     K(131) = AMAX1(K(31)*K(117)*(K(11)+K(119))/2. ,
      K(131) = AMAX1(
     +K(156)*K(2)/K(31)/1000. , K(121)*K(40) , K(87) )
      GOTO 3520
 3510 CONTINUE
C       SECONDARY INNER LAYER
C     K(130) = AMAX1(K(31)*K(118)*K(12)/2. ,
      K(130) = AMAX1(
     +K(156)*K(100)*K(120)/K(32)/1000. , K(121)*K(41) , K(87) )
C     K(131) = AMAX1(K(31)*K(118)*(K(12)+K(119))/2. ,
      K(131) = AMAX1(
     +K(156)*K(100)*K(120)/K(32)/1000. , K(121)*K(41) , K(87) )
      IF(K(46) .GE. K(48)) GOTO 3520
      K(147) = K(147) + 1.
C       SECONDARY OUTER LAYER
C       K(132) : SPACING, HORIZONTAL, OUTER LAYER - ENCLOSURE
C     K(132) = AMAX1(K(31)*K(118)*(K(12)+K(122))/2. ,
      K(132) = AMAX1(
     +K(156)*K(100)*K(120)/K(32)/1000. , K(121)*K(41) , K(87) )
C       K(134) : SPACING, HORIZONTAL, OUTER - OUTER LAYER
C     K(134) =AMAX1(K(31)*K(118)*K(12) ,
      K(134) =AMAX1(
```

```
145               +K(156)*K(100)/K(32)/1000.  , K(121)*K(41), K(87) )
                   GOTO 3530
                 3520 CONTINUE
                C       PRIMARY OUTER LAYER
                C      K(132) = AMAX1(K(31)*K(117)*(K(11)+K(122))/2. ,
150                    K(132) = AMAX1(
                      +K(156)*K(2)/K(32)/1000. , K(121)*K(40) , K(87) )
                C      K(134) = AMAX1(K(31)*K(117)*K(11) ,
                C     +K(156)*K(2)/K(32)/1000. , K(121)*K(40) , K(87) )
                       K(134)=AMAX1(K(156)*K(2)/K(32)/1000.,K(121)*K(40),K(87))
155              3530 CONTINUE
                C      K(141) = AMAX1(K(31)*K(117)*K(11) ,
                       K(141) = AMAX1(
                      +K(156)*K(2)*2./K(46)/K(32)/1000. , K(121) * K(40) , K(87) )
                C       END OF SPACING COMPUTATIONS
160                    K(158) = INT(K(46) / K(157))
                       K(159) = K(158) + 1
                       K(160) = K(157) * K(159) - K(46)
                       K(161) = K(46) - K(157) * K(158)
                       K(146)=INT(K(48)/K(147))
165                    K(149)=K(148)+1
                       K(150)=K(147)*K(149)-K(48)
                       K(151)=K(46)-K(147)*K(148)
                       K(30) = 2. * AMIN1(K(147),K(157))
                       IF(K(147) .EQ. K(157)) K(30) = K(30) - 1.
170                    K(62)=K(30)*K(137)
                       K(63) = K(48)*K(41) + K(46)*K(40) + K(62) +
```

```
     +K(130)*((K(148)-1)*K(150)  + K(148)*K(151)) +
     +K(142)*((K(158)-1)*K(160)  + K(158)*K(161))
      IF(K(26).GT.0.)K(42)=2*K(63)+K(134)+2*K(130)
175   IF(K(26).EQ.0.)K(42)=K(63)+K(130)+K(132)
      K(152)=2*K(14)+2*K(15)+2*(K(131)-K(130))+2*PI*(K(63)/2+K(130))
      K(64)=K(152)*K(44)
      K(65)=K(152)*K(45)
      K(66)=K(3)*K(64)/K(58)*K(107)
180   K(67)=K(4)*K(65)/K(59)*K(108)
      K(84)=3.19E-08*K(152)*K(45)**2/K(30)**2/K(43)*(K(62)+(K(63)-K(62))
     +/3)
      K(85)=2*PI*K(19)*K(84)
      K(88)=K(66)*K(55)**2+K(67)*K(97)**2
185   IF(K(26).GT.0.)
     +K(71)=K(15)*(((K(14)*3+2*K(42))*(2*K(14)+K(43)))-2*K(42)*K(43))
      IF(K(26).EQ.0.)K(71)=2*K(15)*K(14)*(K(14)+K(42)+K(43))
      K(36)=K(71)*K(9)*K(17)
      K(72)=K(36)+K(71)*K(23)*(1-K(17))
190   K(73)=K(36)*K(13)
      IF(K(26).GT.0.)
     +K(153)=2*((3*K(14)+2*K(42))*(K(43)+2*K(14))-2*K(42)*K(43))*K(17)
      IF(K(26).EQ.0.)K(153)=2*((2*K(14)+2*K(42))*(K(43)+K(14))-2*K(42)
     +*K(43))*K(17)
195   K(119)=K(73)/K(153)
      K(74)=K(73)+  K(68)
      IF(K(26).GT.0.) K(74) = K(74) + 2.*K(68)
      K(49)=K(116)/(K(74)+K(116))
      IF(ABS(K(49)-K(86))-K(24) .LT. 0) GOTO 3620
200   K(86)=SQR(K(86)*K(49))
      IF ( K(86) .GT. K(33) ) GOTO 3100
      FNUB = 1
      GOTO 3770
3620  CONTINUE
```

```
      K(51) = K(80) / K(81) - 1.
      K(112) = 1.0D+K(112)*K(1)*K(80)/K(81)/K(113)
      K(75)=K(64)*PI/4*(K(42)       )**2  /K(107)
      K(76)=K(65)*PI/4*(K(41)       )**2 /K(108)
      K(69)=   (K(75)+K(76))
      IF(K(26).GT.0.)K(69)=K(69)*3
      K(70)=   (K(7)*K(75)+K(8)*K(76))
      IF(K(26).GT.0.)K(70)=3*K(70)
      K(93)=K(43)+  K(14)+K(154)
      IF(K(26).GT.0.)K(93)=K(93)+K(14)
      K(94)=K(15)+2*(K(63)+K(152)+K(131))
      IF(K(26).GT.0.)
     *K(93)=K(14)+2*(K(63)+K(14)+K(42)+K(152)+K(130)+K(155))
      IF(K(26).EQ.0.)K(95)=2*(K(14)+K(42))+K(155)
      K(77)=K(93)*K(94)*K(95)
      K(78)=K(77)-K(69)-K(70)-K(154)*K(94)*K(95)
      K(79)=K(76)*K(10)
      K(80)=K(79)+K(70)+K(72)
      K(81)=K(97)/K(114)*(K(66)+(K(45)/K(44))**2+K(67))
      K(88)=K(97)/K(114)*K(85)
      K(89) = SQRT(K(81)*K(81) + K(88)*K(88))
      K(144) = SQRT(K(67) * K(67)  +  K(85)*K(85))
C     K(90) = K(49) * K(116) / K(50) / K(19)
      K(90) = K(49) * K(116) / K(50) / K(19) /K(77)
```

APPENDIX C

FULL-WAVE THREE-PHASE RECTIFIER VOLTAGE WAVEFORMS

A circuit for the full wave rectification of the output of a three-phase alternator (or three-phase alternator/transformer package) is shown in Figure 1. The line to neutral voltages appearing at terminals A, B, and C are shown in Figure 2. When the reactance of the alternator or the alternator/transformer package is low, rectifier conduction occurs during the periods indicated in Figure 2 and the rectified waveform is as shown. When appreciable reactances exist in the alternator or the alternator/transformer package, inductive voltages are generated which extend the conduction periods of the rectifiers. As a result, periods exist in which two rectifiers are conducting simultaneously. The voltage is approximately the average of the two phase voltages during the conduction overlap period. This conduction overlap situation is shown in Figure 3 along with the rectified waveform.

It is evident from Figures 2 and 3 that there is an appreciable increase in the ripple content of the rectified voltage when conduction overlap occurs. In addition, there is a decrease in the average value of the rectified voltage.

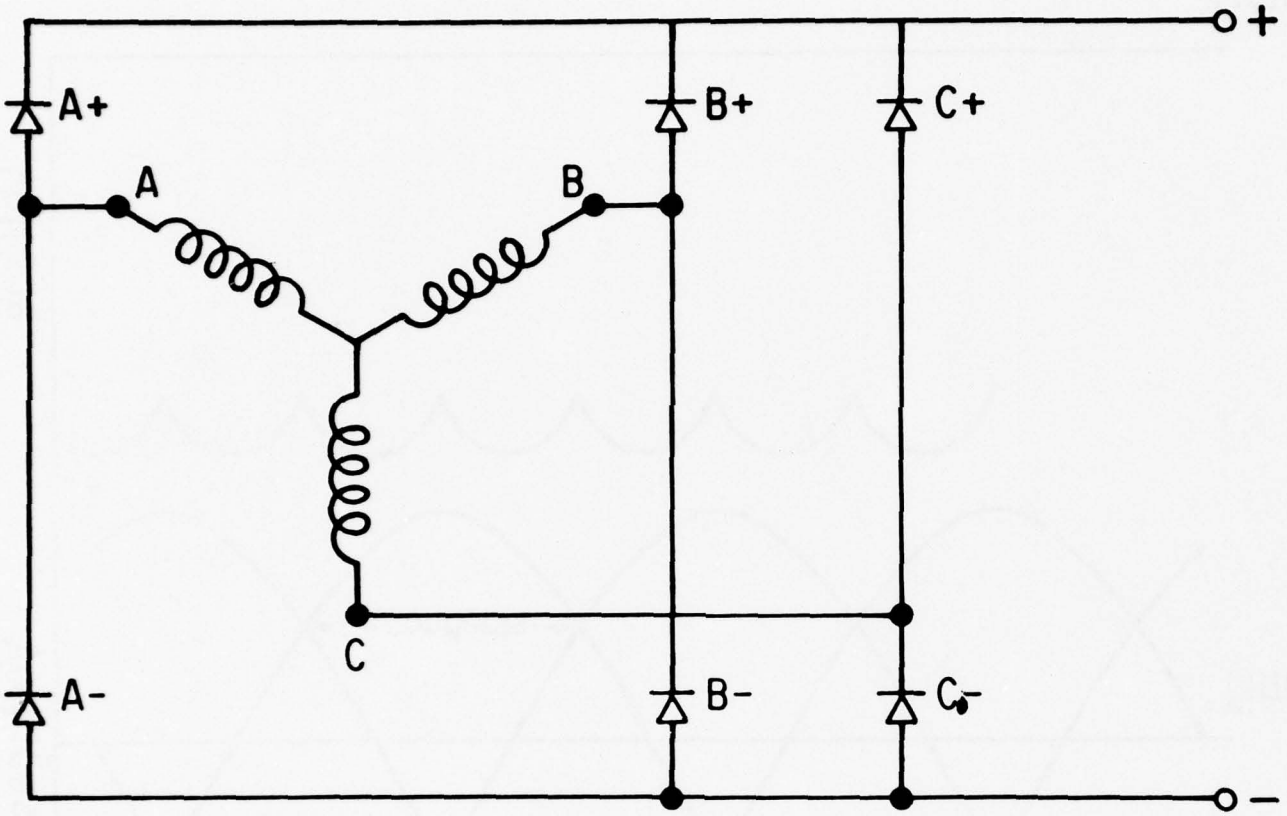


Figure 1. Three phase full wave rectifier

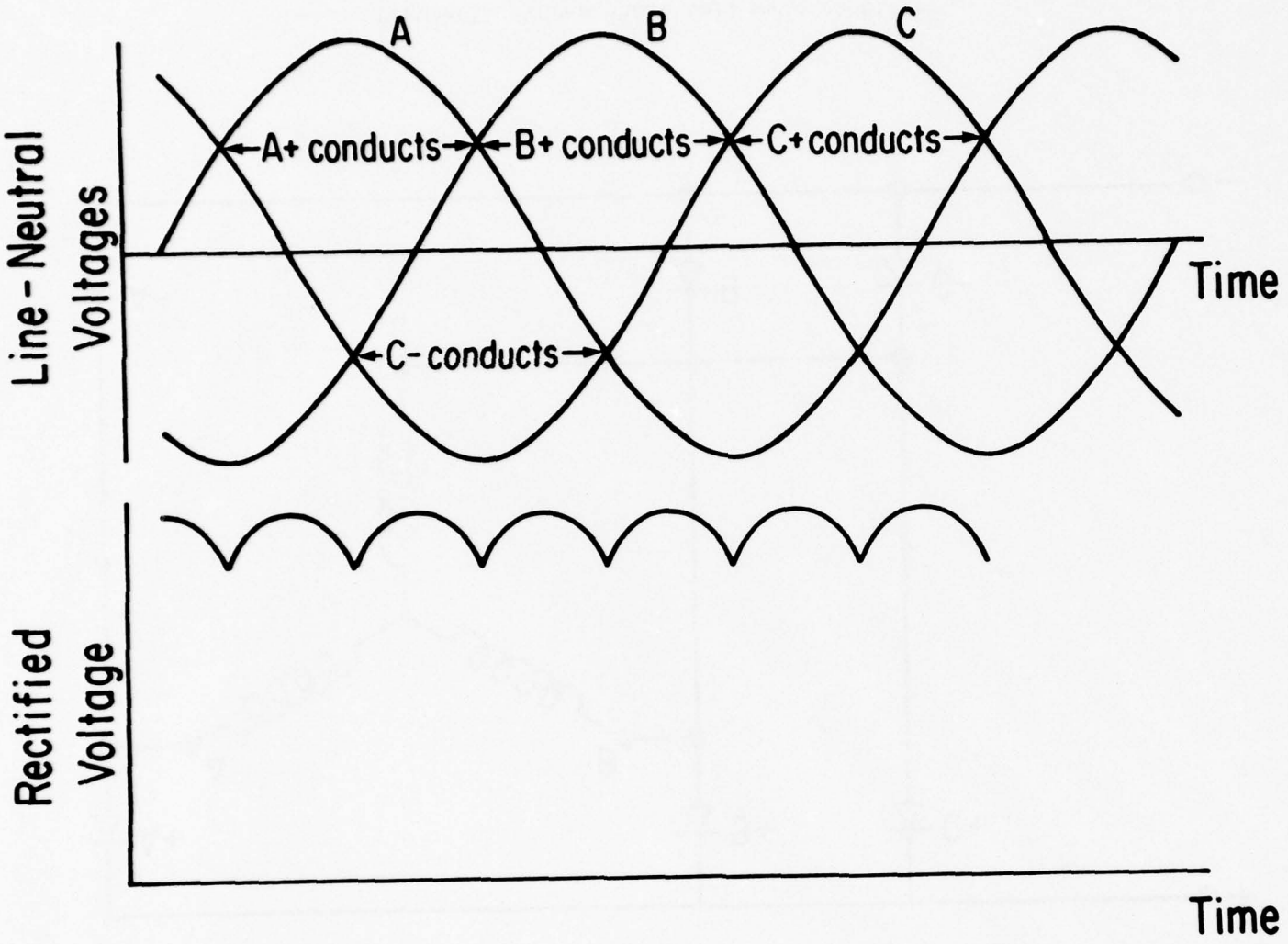


Figure 2. Line to neutral voltages and rectified voltage for the three phase full wave rectifier operating from a low reactance alternator or alternator/transformer package.

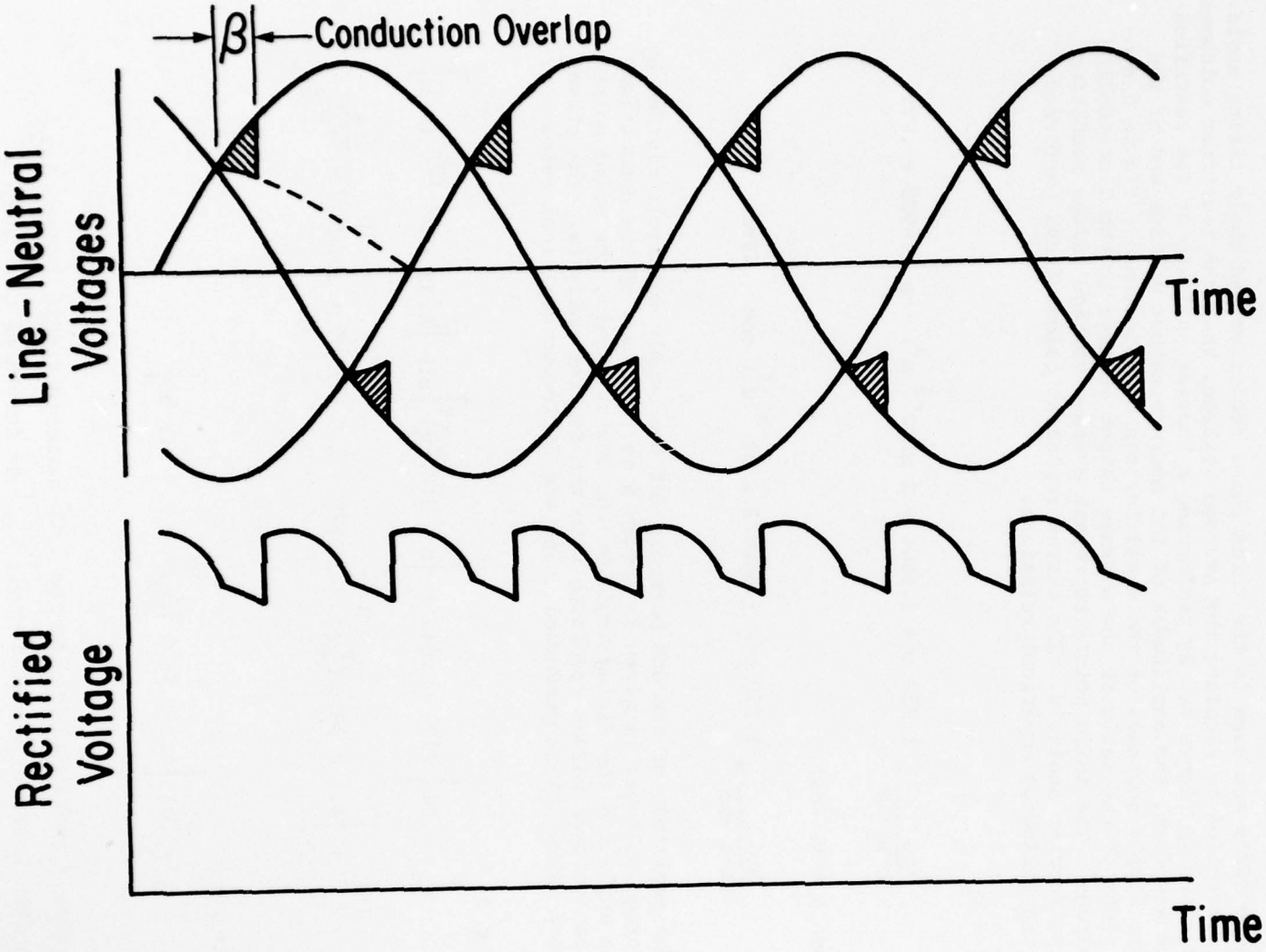


Figure 3. Illustration of conduction overlap and its effect on rectified voltage for three phase full wave rectifier operating from a high reactance alternator or alternator/transformer package.

When SCR's are used in the three phase rectifier and their firing angle, α, is controlled to regulate the average voltage, then the rectifier voltages are as shown in Figure 4. By performing a Fourier analysis of the rectified voltage waveform, the amplitudes of the average output voltage and of the harmonic ripple voltages of the rectifier can be determined. Figure 5 contains plots of the ratio of the average output voltage to the line-to-line rms voltage. The solid points represent average voltage values resulting from the Fourier analysis. The curves represent calculations performed using the following empirical relations.

When $\alpha \leq \beta$

$$\frac{V_{AVG}}{V_{L-L\ rms}} = 1.350 \cos (.660\alpha + 2 \times 10^{-5}\ \alpha^3) \cos (.692\beta + .07\alpha)$$

and when $\alpha \geq \beta$, then

$$\frac{V_{AVG}}{V_{L-L\ rms}} = 1.350 \cos (.660\alpha\ 2 \times 10^{-5}\ \alpha^3) \cos (.699\alpha)$$

The amplitude of the 6th harmonic (of the supply voltage), divided by the average voltage, is given in Figure 6 as functions of the conduction overlap angle and the firing angle of the SCR's. Again, the solid points represent voltage values resulting from the Fourier analysis. The curves represent calculations performed using the following empirical relations.

When $\alpha < \beta$

$$r_6 = .01\left\{.217\beta - .04\alpha + \left[2 + 3.3\left(\frac{\alpha}{30}\right)^2\right]\sin\left[\left(6.32 + \alpha^{0.15}\right)\ (\beta-\alpha)\right]\right.$$
$$\left. + \left[4.1 + 38.8\left(\frac{\alpha}{60}\right)^2 - .217\beta + 1.5 \sin 5\beta + .04\alpha\right]e^{-\frac{\beta-\alpha}{\frac{8.5+\sqrt{\alpha}}{1.5}}}\right.$$

and when $\alpha \geq \beta$

$$r_6 = .01\left[4.1 + 38.8\left(\frac{\alpha}{60}\right)^2 + 1.5 \sin 5\alpha\right]$$

Figure 7 contains plots of the 12th harmonic ripple factor, r_{12}, and the 18th harmonic ripple factor, r_{18}, as functions of β and α.

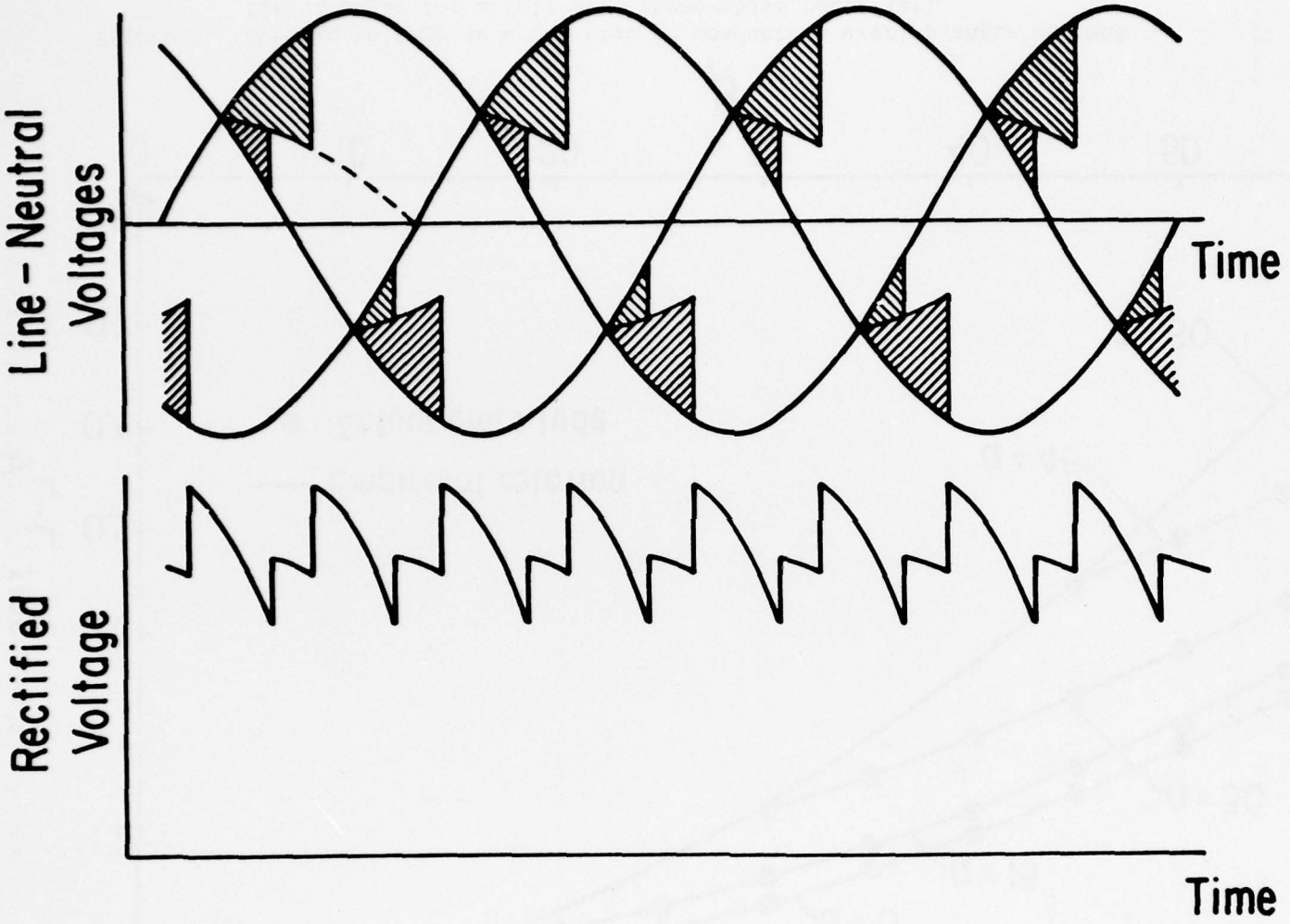


Figure 4. Illustration of effect of conduction overlap and SCR firing angle on rectified voltage for three-phase full-wave rectifier.

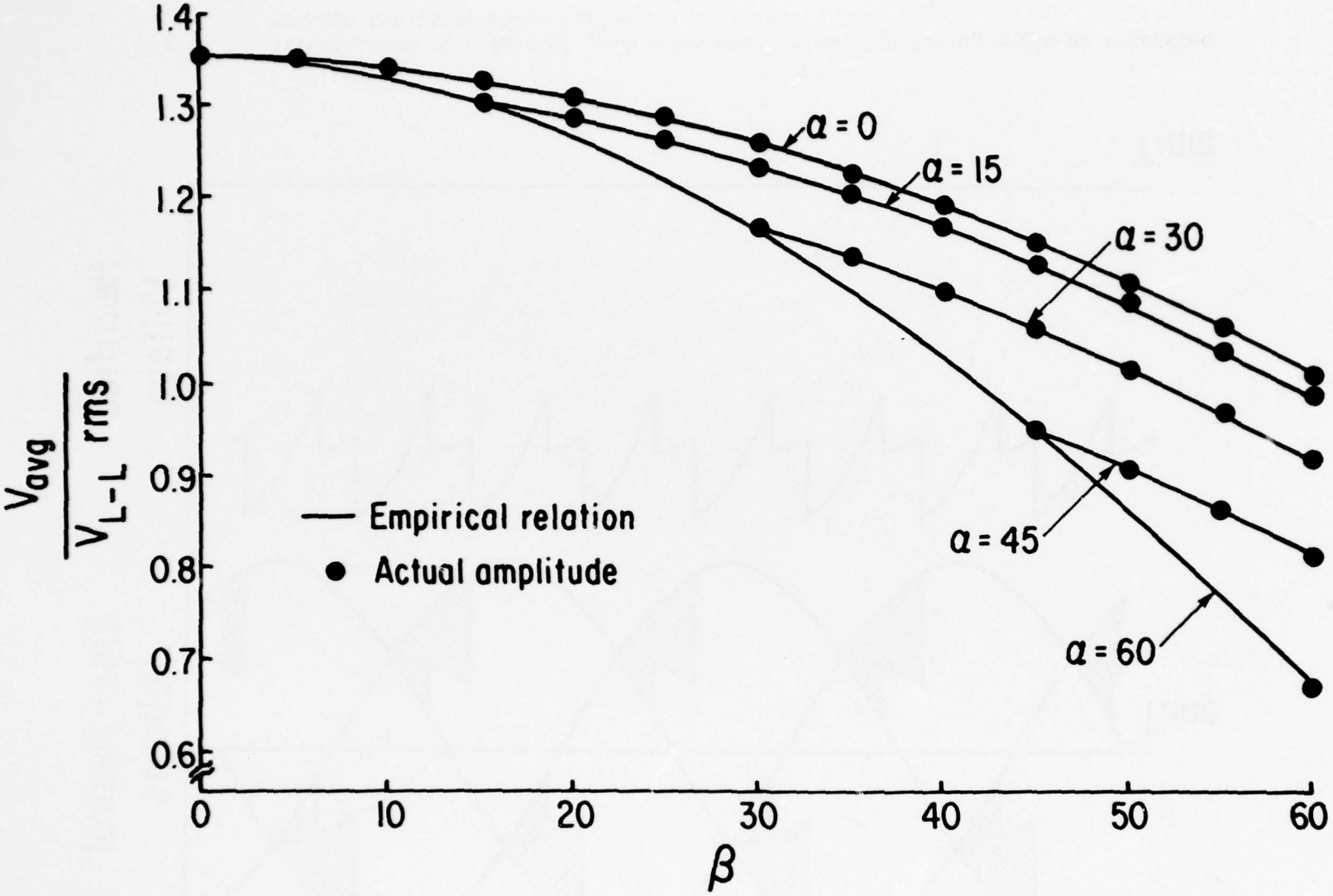


Figure 5. Average voltage as a function of conduction overlap angle and SCR firing angle for a full-wave three-phase rectifier.

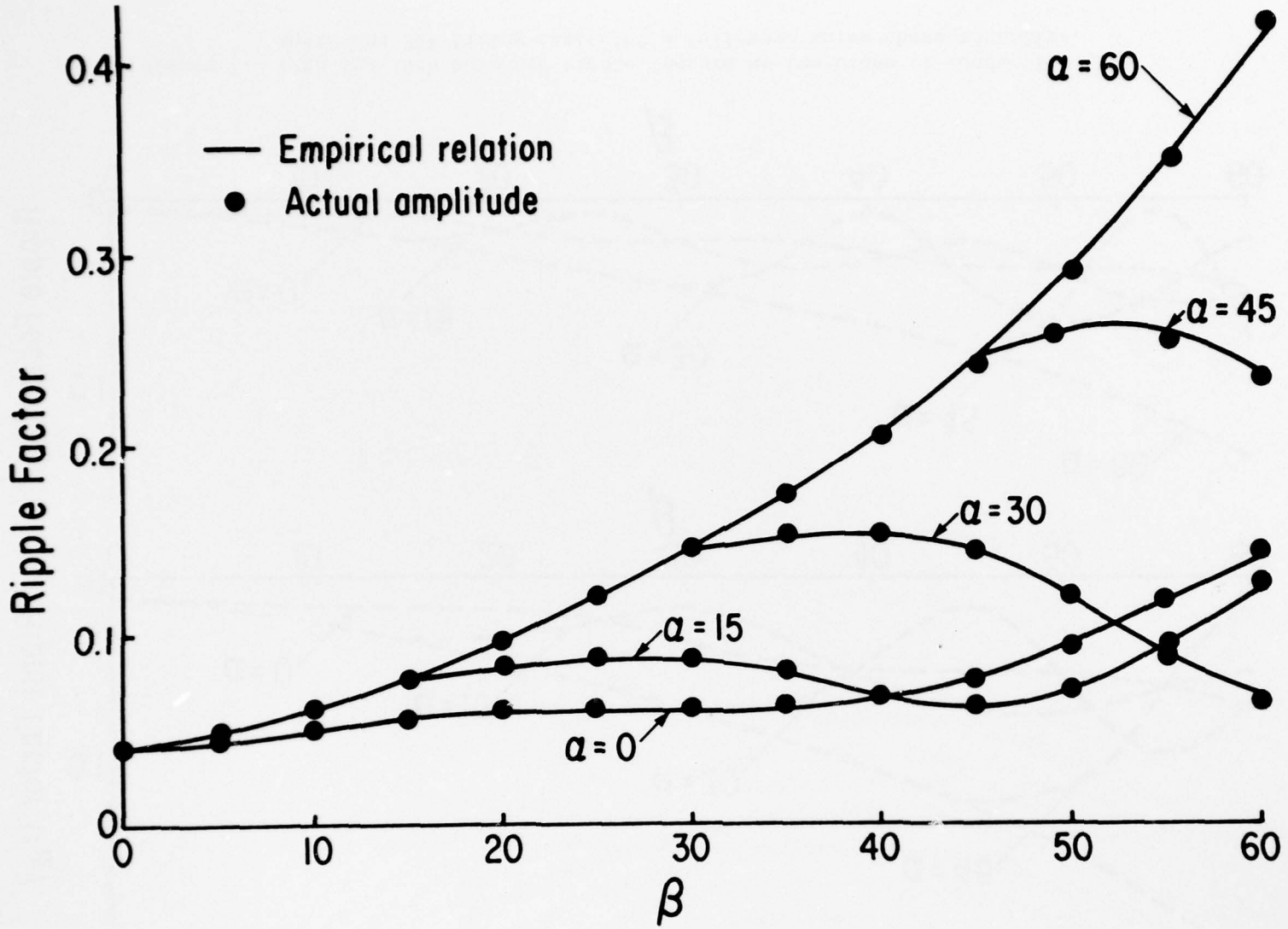


Figure 6. 6th harmonic ripple factor as a function of conduction overlap angle and SCR firing angle for a full-wave three-phase rectifier.

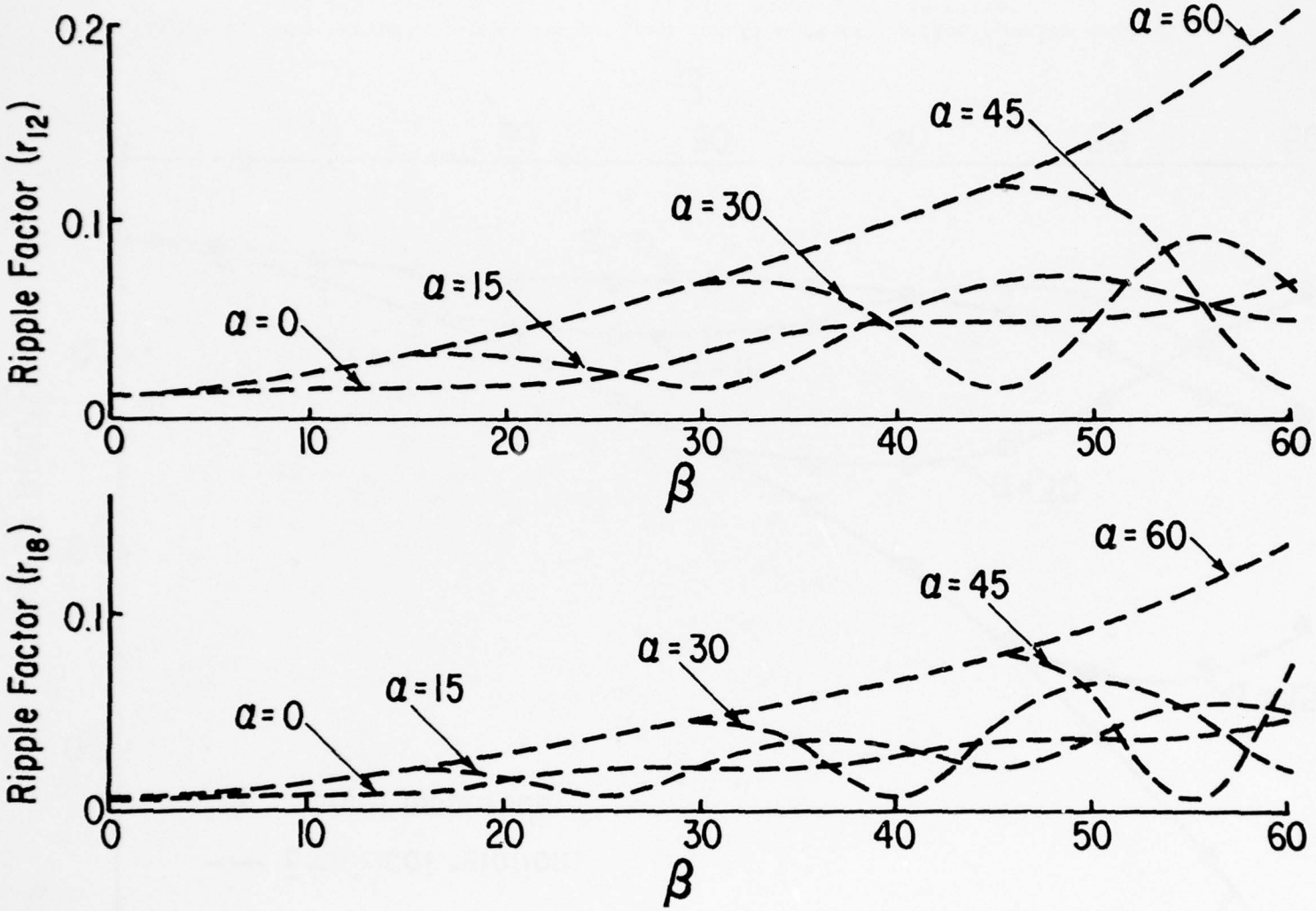


Figure 7. 12th and 18th harmonic ripple factors as functions of conduction angle and SCR firing angle for a full-wave three-phase rectifier.

APPENDIX D

THE INTERRUPTION OF VACUUM ARCS AT HIGH DC VOLTAGES

A. S. Gilmour, Jr. & D. L. Lockwood

The Interruption of Vacuum Arcs at High DC Voltages

ALEXANDER S. GILMOUR, JR., SENIOR MEMBER, IEEE, AND DAVID L. LOCKWOOD, SENIOR MEMBER, IEEE

Abstract—In 1967, it was observed by the authors that an axial magnetic field applied to a vacuum-arc discharge in a coaxial diode was capable of extinguishing the discharge. A continuing effort to develop a high-voltage dc arc interrupter has resulted in a simple, lightweight device capable of interrupting 800 A at 25 kV. Operation at higher levels was limited, not by the interrupter, but by the lack of availability of adequate power supplies. This device has been operated at repetition frequencies of several pulses per second. Successful operation at a frequency of 1 kHz has been achieved at lower power levels. The turn-on and turn-off times are, respectively, as short as one and two microseconds. The pulsewidth is continuously variable from a few microseconds to infinity (dc operation). It has been demonstrated that operation above 10 kV requires very pure materials and the use of ultra-high vacuum techniques. Among the many uses for the interrupter are those in high-power modulators and high-power inverters. An enticing future application is for switching in high-voltage dc power transmission systems.

I. INTRODUCTION

STARTING in the early 1960's, high-voltage switching studies employing laser-triggered vacuum arcs were performed by one of the authors [1]. Shortly thereafter, a search for arc-interruption techniques was started. Techniques other than the use of the laser were developed for triggering vacuum arcs and, in addition, an axial self-excited magnetic field [2] was used for collimating the plasma plume from the vacuum arc in a coaxial-electrode geometry. During these tests, the magnetic field was also used to control the impedance of the plasma. In 1967, a vacuum-arc switch with a coaxial electrode configuration was surrounded by a separately excited magnetic-field coil and it was demonstrated that a vacuum-arc discharge could be extinguished [3]. Since that time, there has been a continuing effort to develop a magnetically operated pulsed vacuum-arc interrupter. The purpose of this effort has been to improve the means of extinguishing a vacuum-arc discharge to permit the use of the discharge in a high-power interrupter. One of the uses for such a device would be to replace the pulse forming network and thyratron used in high-power radar modulators. Not only would the use of the interrupter make possible a continuously variable pulsewidth, but the size and weight of the modulator would be reduced. Other uses for the interrupter include high-power inverters, the generation of high-voltage pulses by interrupting the current in an inductive storage unit, and switching in high-voltage dc power transmission systems.

This paper is organized so that a basic description of the vacuum-arc interrupter is given first. This is followed by a description of the high-voltage tests that were performed to achieve an interruption capability of 25 kV. Next, the current capability and the turn-off time are discussed. Finally, the projected life of future interrupters is given.

II. BASIC DESCRIPTION OF INTERRUPTER

The operation of the high-voltage arc interrupter depends, to a large extent, on the characteristics of vacuum arcs. A vacuum arc is a plasma discharge established between two electrodes in a vacuum [4]. The constituent material of the negative electrode is vaporized and ionized by the arc spots to provide the conducting medium [5].

Manuscript received December 15, 1973; revised November 26, 1974. This work was supported by the Rome Air Development Center, Air Force Systems Command.

The authors are at the State University of New York at Buffalo, Buffalo, N. Y.

Copyright ©1975 by The Institute of Electrical and Electronics Engineers, Inc.
Printed in U.S.A. Annals No. 504EO003

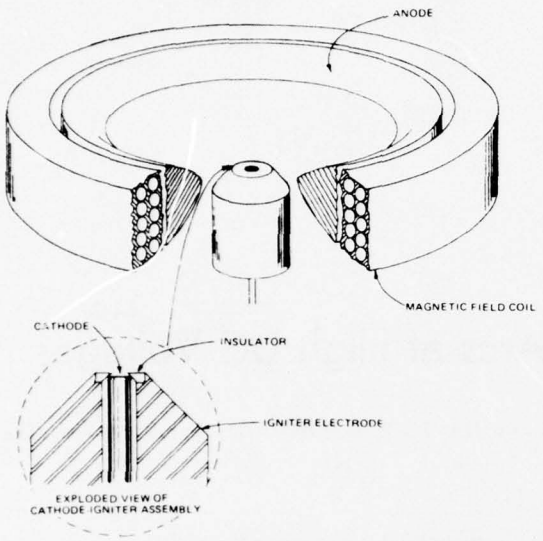


Fig. 1. Configuration of high-voltage arc interrupter.

A vacuum arc discharge is an almost ideal medium for use in switching [6], [7] because it makes possible a high-vacuum device having excellent insulation properties when nonconducting and it becomes a plasma discharge device with a very low-voltage drop during conduction.

Shown in Fig. 1 is a drawing of a high-voltage arc interrupter, the configuration of which is typical of those used for arc-interruption experiments. A vacuum-arc discharge between the cathode and anode is initiated by the use of a third electrode called an igniter [2]. The igniter electrode is separated from the cathode by an insulator on which the metallic vapor from the arc can deposit forming a conductive thin film. To ignite the arc, a current pulse is passed through this film causing a portion of it to vaporize. The resulting plasma burst quickly fills the interelectrode space allowing the main arc current to pass between the anode and cathode with a rise time on the order of 1 μs. During the ensuing discharge, the metallic film is regenerated, preparing the system for the next ignition pulse.

For arc interruption to occur, the electrodes must be of a coaxial geometry [8]. The cathode is a small electrode placed on the axis and the anode is an annulus surrounding the cathode. The arc is extinguished by applying a coaxial magnetic field to the device in such a way that the field lines are essentially perpendicular to the paths of the electron current from the cathode to the anode. The effect of the field is to increase the voltage drop across the arc and thereby decrease the discharge current. This is shown for a switch operating at 5 kV in Fig. 2. The form of the curve in Fig. 2, is very nearly

$$\frac{I_r}{I_0} = \frac{1}{1 + KB_z^2}$$

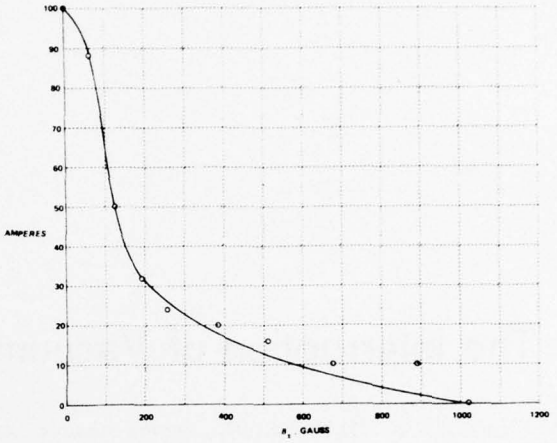


Fig. 2. Arc current vs. axial field strength for switch at 5 kV.

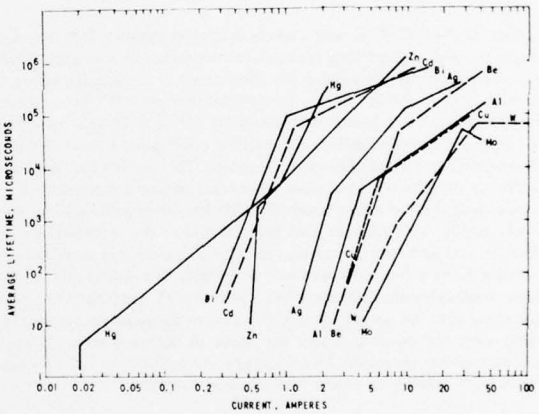


Fig. 3. Average arc lifetime as a function of current for pure electrode materials (from [9]).

where

B_z magnetic flux density
I_0 arc current for $B_z = 0$
I_r arc current for $B_z > 0$
K constant.

The arc is extinguished when the current is reduced to a value where the average lifetime [9] of the arc becomes very short compared to the duration of the magnetic field pulse. Average arc lifetimes as a function of current are shown for several metals in Fig. 3. Notice, for example, that if the current through a zinc arc is reduced to a value below 0.5 A, the average lifetime of the arc will be below 10 μs. Therefore, if a magnetic-field pulse with a length of 10 μs is used and if the arc current is reduced to 0.5 A, on the average, the arc should be extinguished 50 percent of the time. In practice, the duration and amplitude of the magnetic field are increased sufficiently to ensure arc extinction. When conduction ceases, metallic

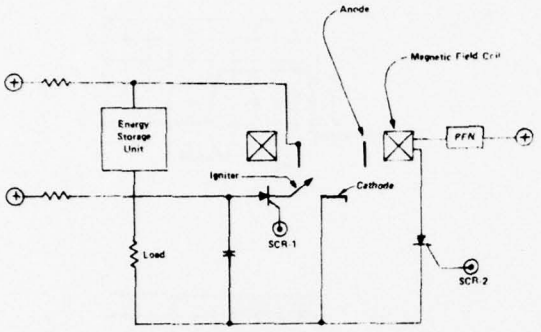


Fig. 4. Arc-interruption test circuit.

vapor is no longer emitted by the cathode. The vapor in the interelectrode space rapidly condenses and the interrupter returns to the high-vacuum state and remains off when the magnetic field is removed.

The circuit for testing the interrupter is shown in Fig. 4. Arc ignition is accomplished by triggering SCR-1 and arc extinction results from energizing the magnetic field coil by triggering SCR-2. During conduction, electron current flows from the energy storage unit through the load, through the interrupter and back to the energy storage unit.

III. HIGH-VOLTAGE ARC INTERRUPTION STUDIES

The capability to interrupt a direct current of 800 A at 25 kV has resulted largely from the gradual refinement, through experimentation, of a series of interrupters. There have been four major milestones in the development of the present interrupter. The first was the demonstration that dc arc interruption could be achieved. The second was the increase of the voltage of operation from a few hundred volts to a few kilovolts by significantly reducing the area of the anode and by shielding the magnetic-field coil. The third major milestone was the increase of the voltage of operation from a few kilovolts to 15 kV. This was accomplished by shaping the anode so that it concentrated the magnetic flux lines of a magnetic-field coil that was quite large in diameter and was, therefore, removed from close proximity to the plasma. The fourth major improvement resulted from the fabrication of the interrupter from extremely pure high-vacuum materials and then from operating the interrupter in an ultra-high vacuum system. Operation at 25 kV and 800 A was achieved and was limited, not by the interrupter, but by the electronic equipment associated with the interrupter (the power supplies, the capacitors, etc). In the paragraphs that follow, the experiments that were performed in achieving each of the four milestones are described.

A. Demonstration of Arc Interruption

The interrupter configurations used for the initial demonstration of dc arc interruption and for subsequent low-voltage tests were similar to that shown in Fig. 5(a). The

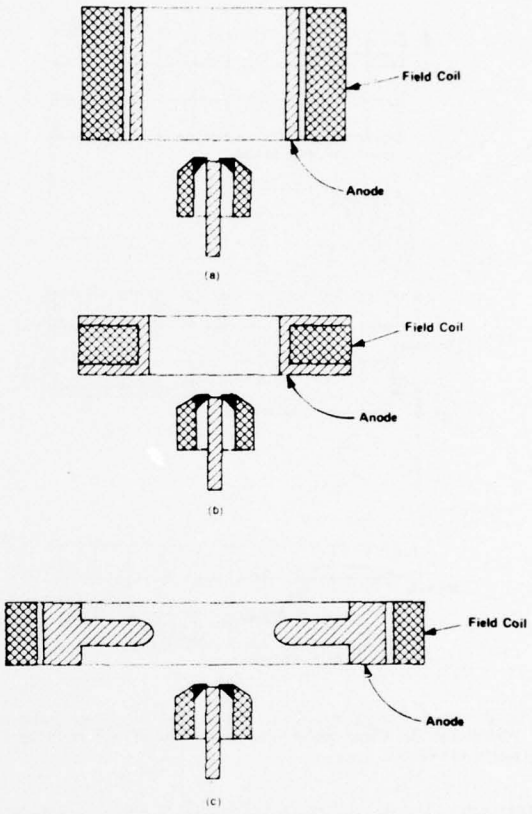


Fig. 5. (a) Configuration used to demonstrate arc interruption. (b) Configuration used to achieve 3-kV operation. (c) Configuration used to achieve 15-kV operation.

cathode-igniter assembly was similar to that described in the previous section. The cathode diameter was 0.125 in (0.317 cm), the outer diameter of the insulator was 0.250 in (0.635 cm), and the outer diameter of the igniter electrode was 0.5 in (1.27 cm). The anode was 1.5 in (3.8 cm) in diameter and 1 in (2.54 cm) long. The magnetic-field coil was in the form of a short solenoid surrounding the anode. Shown in Fig. 6 are oscillograms of the load voltage resulting from operation of the interrupter. The magnetic field pulses used in obtaining the results shown in Fig. 6(a), (b), and (c) were identical. Fig. 6(a) shows a reasonably clean load voltage pulse with a duration of about 50 μs. The amplitude of the pulse was only about 500 V, however, interruption of the arc *was* accomplished. Fig. 6(b) shows the load voltage in a case when extinction occurred, however, the arc failed to turn off immediately upon application of the magnetic field. Fig. 6(c) shows a case where arc interruption failed to occur. If the sweep rate on the oscilloscope had been reduced, the oscillogram would show that the interrupter returned to the fully conducting state at the end of the magnetic-field pulse and stayed on until the energy storage unit was discharged.

Attempts to operate devices with the configuration of

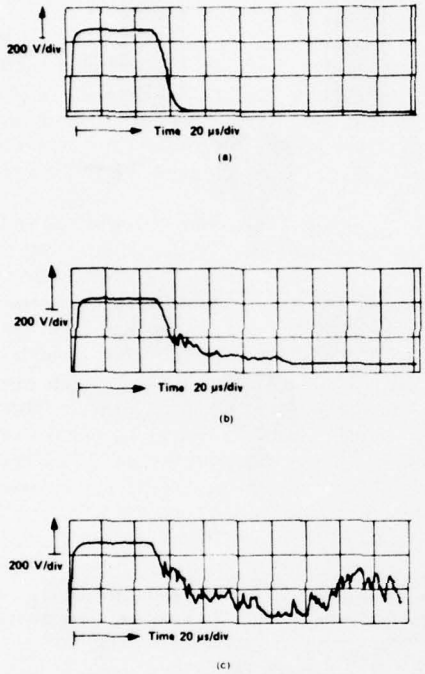


Fig. 6. Load voltage waveforms during first arc interruption experiments. (a) Clean pulse. (b) Slow turn-off. (c) Interruption failed to occur.

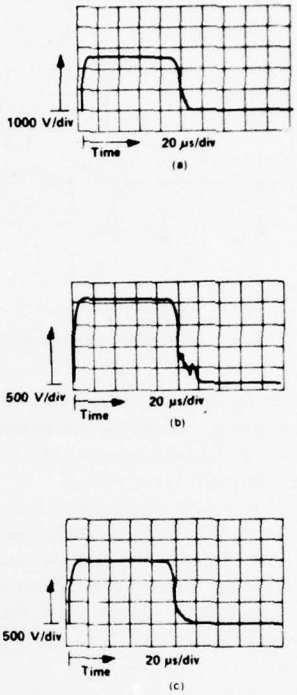


Fig. 7. Voltage waveform across load with improved anode and field coil configuration for the following voltages. (a) 2500 V. (b) 2000 V. (c) 1500 V.

Fig. 5(a) at voltages much higher than 500 V resulted in failure to extinguish the arc on nearly every pulse. In experimenting with various configurations of the anode, significant reductions in the rate at which the interrupter failed to turn off occurred when the length of the anode was reduced. Also, the failure rate was reduced when insulating surfaces were shielded so that the plasma plume did not impinge on them.

B. Arc Interruption at 3 kV

As a result of the knowledge gained with the configuration shown in Fig. 5(a), the new interrupter was designed as is shown in Fig. 5(b). The testing circuit was that shown in Fig. 4. The anode, which had the same inside diameter as that shown in Fig. 5(a) but which was only 0.625 in (1.56 cm) high, surrounded the magnetic field winding on the three sides where most of the exposure to the plasma occurred. This arrangement effectively removed all exposed insulating surfaces from the arcing region. These changes resulted in a marked improvement in performance, as is shown by the oscillograms of the load voltage in Fig. 7. Fig. 7(a) shows the interrupter performance at 1500 V, Fig. 7(b) at 2000 V, and Fig. 7(c) at 2500 V. All data were taken with a 20-Ω load so that the peak power was 312.5 kW at 2500 V. At 2500 V, the interrupter failed to turn off on approximately one out of every 20 pulses. At higher voltages, the failure rate increased rapidly and the highest voltage at which the interrupter could be operated at all was 3000 V. While it was very difficult to identify the mechanisms which prevented arc interruption, discharges were frequently observed on the exposed surfaces of the magnetic-field coil and on the leads to the coil. Attempts to improve the shielding of the coil were not successful.

C. Arc Interruption at 15 kV

The third milestone in the improvement of the interrupter was the employment of the configuration shown in Fig. 5(c). The anode was fabricated from solid copper and was used to concentrate the flux lines from a relatively large diameter magnetic-field coil into the interaction region between the cathode and the anode. This concentration of flux lines, which is sketched in Fig. 8, results from the relatively slow diffusion of the rapidly varying magnetic flux lines through the anode [10].

Measurements of field concentration were made with an electrode geometry similar to that shown in Fig. 8. Several anodes were fabricated having an outside diameter of 3 in (7.62 cm) and having inside diameters that ranged from 0.25 in (0.64 cm) to 2.5 in (6.35 cm). A coil form was fitted to the outside of the anode and was wound with solid copper wire. The magnetic flux density was measured at a peak current of 800 A from a 100-μF capacitor for numbers of turns on the field coil from one to ten and for each of the anodes. The normalized flux density is plotted

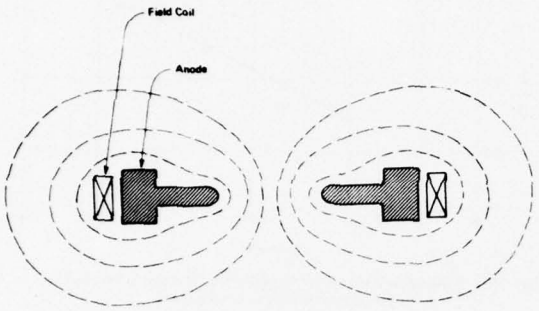


Fig. 8. Concentration of magnetic flux lines by anode for time varying magnetic field.

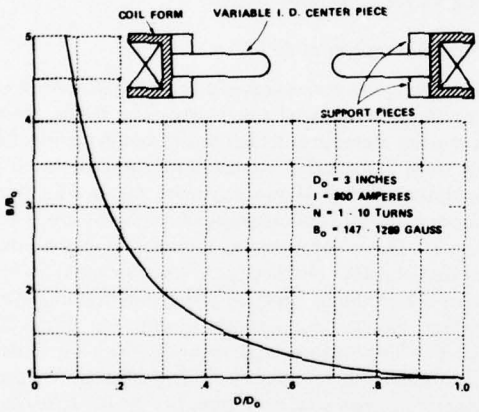


Fig. 9. Normalized axial field vs. normalized anode aperture.

against normalized anode aperture in Fig. 9. The magnetic flux density, B_0 was measured with the anode removed. Note that the peak flux density was increased by a factor of up to 5 by the anode.

The advantages (beyond the obvious one of enhancing turn-off) of using the anode to concentrate the magnetic flux were as follows:

1) The diameter of the magnetic field coil could be increased considerably so as to move the surfaces of the coil away from the plasma discharge. It might be possible to put the coil outside the vacuum envelope.

2) The inner diameter of the anode could be reduced thus decreasing the turn-on time. The turn-on time for large aperture anodes is limited by the rate at which the charge density can build up in the interelectrode space. This is proportional to the volume and, therefore, reducing the aperture diameter reduces turn-on time.

3) The rise time of the magnetic field and the turn-off time of the interrupter were decreased.

The electric circuit for the high-voltage interrupter was basically the same as was shown in Fig. 4. The components used in the circuit, however, were rated for high-voltage operation. The power supply for charging the energy storage unit was rated at 25 kV and 0.6 A. The energy storage unit was a 9-μF capacitor rated at 30 kV and designed for pulsed operation. The charging resistor was capable of dissipating the full 15-kW output of the power supply so that tests could be performed on interrupters with high failure rates. The load resistor was also rated for high-power operation and could be varied from 30 to 400 Ω.

The enlargement of the magnetic-field coil and use of the anode as a magnetic flux concentrator resulted in a tremendous improvement in the high-voltage interruption capability of the interrupter. The performance of the interrupter at 10 kV and 200 A was quite good with failure of the device to interrupt the arc occurring on one pulse in 20. At 15 kV and 300 A, the failure rate of this interrupter was quite high and, at higher voltages, interruption did not occur. It should be pointed out that, while the interrupter failed to turn off at voltages above 15 kV, the current through the arc was depressed very nearly to zero by the pulsed magnetic field.

Several problems occurred almost simultaneously in the voltage range from 12 to 15 kV, any one of which could have been responsible for the failure of the interrupter to operate properly. These problems and recommendations for eliminating them are as follows:

1) Anode spots were frequently observed and were *always* observed when the interrupter failed to turn off. It is not clear whether the anode spots were the cause or the result of the failure to turn off, however, it is possible to argue that they may have been the cause. The cathode material being used in the high-voltage tests was titanium. This material was selected for its gettering properties, which are expected to be important to maintain a high vacuum in interrupters that are not continuously evacuated by external pumps. When titanium collected on the anode during operation of the interrupter, it may have combined chemically with gas atoms in the vacuum chamber to form an insulating layer. (It should be pointed out here that a diffusion pumped vacuum chamber was used for these interrupter tests. Oil molecules may also have been combined with the titanium on the anode.) The insulating layer resulted in the formation of anode spots when electrical breakdown occurred during subsequent plasma pulses. This anode spot problem should be alleviated by using cleaner vacuum systems and also, possibly, by using cathode materials other than titanium.

2) Plastics, which were used for the sake of expediency, continued to cause problems at the high voltages. For example, the form for the magnetic field coil, which was fabricated from teflon, seemed to emit bursts of plasma. The obvious solution to this problem is to use only ceramics as insulating materials.

3) Electrical breakdown occurred on the surfaces of the high-voltage vacuum feedthrough used for the anode connection. While this feedthrough might normally operate above 15 kV, in the presence of charged particles from the plasma discharge, breakdown frequently occurred at

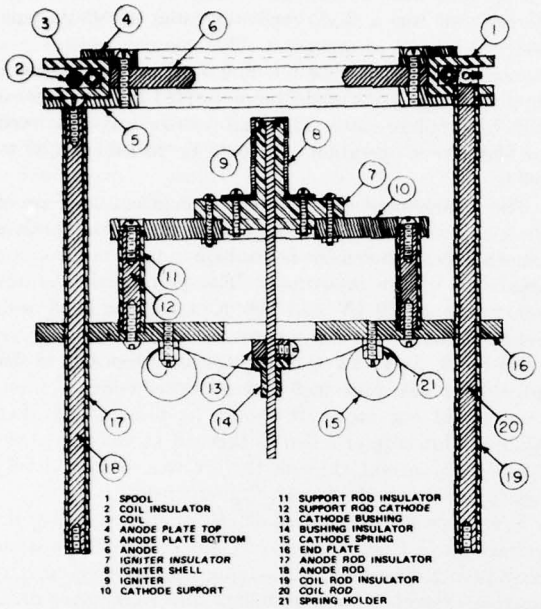


Fig. 10. Sketch showing major components of the high-voltage interrupter.

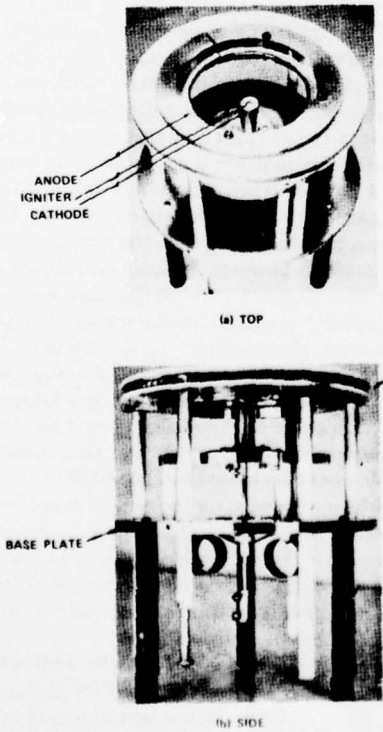


Fig. 11. Laboratory model of 25-kV interrupter.

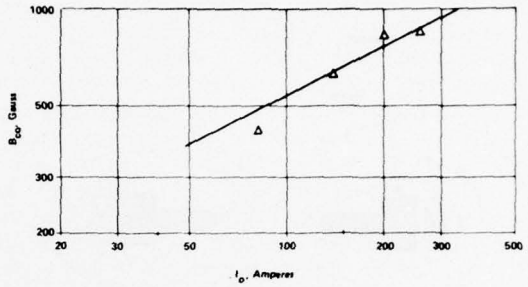


Fig. 12. Magnetic flux density required for arc interruption as a function of initial arc current.

12 kV. Clearly, the solution to this problem are to provide better shielding of the insulators and to use insulators having longer breakdown paths.

D. Arc Interruption at 25 kV

An interrupter was designed taking cognizance of all of the problems mentioned previously. The insulators were high-density alumina and high-purity boron nitride. Metal parts were high-purity copper and stainless steel. The interrupter which is shown schematically in Fig. 10 used a copper cathode. A photograph of the hardware is shown in Fig. 11. The interrupter was mounted in an ion-pumped ultra-high vacuum chamber and was subjected to an extensive conditioning process. After conditioning, the interrupter operated successfully at currents up to 800 A at 25 kV. The turn-on and turn-off times were, respectively, as short as one and two microseconds. The rate of change of current was, therefore, nearly 10^9 A/s. Clearly, to prevent the interrupter from causing electromagnetic interference problems, it must be used in conjunction with properly designed circuits.

IV. TURN-OFF CHARACTERISTICS OF INTERRUPTER

It was deduced from Fig. 2 that the arc current is inversely proportional to the square of the magnetic flux density plus a constant. The relation between the arc current in the absence of the magnetic field, I_0, and the magnetic flux density required for arc interruption, B_{c0}, can be determined by letting the current in the presence of the magnetic field, I_r, equal the cutoff current of the arc, I_{c0} (that value of current at which the arc life is short compared to the duration of the magnetic-field pulse). Since I_{c0} will normally be very small compared to I_0, it is readily found that

$$B_{c0} \propto I_0^{1/2}.$$

In Fig. 12, B_{c0} is plotted as a function of I_0 on log–log coordinates for one of the interrupter geometries that was studied. A line with a slope of one half is drawn through the data points to show that the aforementioned relation is obeyed. If the half-power relation between flux density and current holds at higher current levels, then currents

a flux density of a few thousand gauss (assuming that other phenomena such as the formation of anode spots do not come into play).

The proportionality constant in the half-power relation between cutoff flux density and initial current has been found to be relatively independent of voltage of operation of the interrupter. However, this constant was dependent on the geometry of the interrupter. In general, if the length of the anode was increased, the flux density required to interrupt a given current was decreased. It was pointed out in the previous section, however, that the voltage capability of the interrupter decreased as the anode length was increased. For a given magnetic-field level, therefore, a tradeoff between the current and the voltage capabilities of the interrupter is required.

The magnetic field required for arc interruption is dependent, primarily, on the current rather than the voltage of operation of the interrupter. The overall gain of the interrupter (the ratio of the energy controlled to the energy required for control) is, therefore, proportional to the pulsewidth and voltage at which the interrupter operates. The amount of energy required to drive the magnetic-field coil was typically about 3 J when the current through the interrupter was 300 A. At an operating voltage of 15 kV and a pulsewidth of 30 μs, the energy controlled by the interrupter was 135 J and so the gain of the interrupter was over 40. The energy loss in the interrupter during conduction was less than 1 J and the ignition energy was a small fraction of a joule. The overall efficiency of the interrupter was, therefore, over 97 percent.

The critical information required for determining the turn-off time of the interrupter is contained in Fig. 2. In that figure, magnetic flux density was plotted along the abscissa. If the magnetic flux density applied to the interrupter is a linear function of time, then a plot of the arc current as a function of time during arc extinction should have the same shape as Fig. 2. In the experiments that were performed, the current for driving the field coil was derived from either a capacitor or a pulse forming network. In either case, the time dependence of the current and, therefore, of the magnetic field was very nearly linear during arc extinction. As a result, the turn-off characteristics shown in Figs. 6(a) and 7 are all similar in shape to the curve shown in Fig. 2. It is clear that the shape of the turn-off characteristics could easily be controlled by shaping the current pulse to the magnetic-field coil. Control of the current pulse shape was demonstrated [8], by placing the magnetic field winding in series with the arc current circuit.

The maximum current handling capability and the turn-off time of the interrupter were limited by the SCR's [11] used to drive the magnetic-field coil. The reasons for this are pointed out in the following discussion of the characteristics of the SCR's which are important in the design of high-power pulse generators.

1) *Forward breakover voltage* under static conditions is important for two reasons. The first is that the SCR is subjected to a high voltage in the forward direction during most of its operating lifetime. The second is that the peak magnetic field can be increased and the overall weight of the PFN can be reduced by increasing the voltage.

2) The maximum forward leakage current must be low to prevent the PFN from discharging during the interpulse period.

3) The rate of application of current to the field coil is a critical parameter because it controls the rate of rise of the magnetic-field pulse, which, in turn, controls the turn-off time of the interrupter. In general, the rate of application of current to the field coil must be maximized to minimize the interrupter turn-off time. The rate of rise of current through the SCR is limited by the rate at which the gate region becomes activated.

4) The forward voltage application rate, dv/dt, must not exceed a value that will induce triggering in the gate region.

The SCR's used for the experiments described in this report had the following characteristics:

V_{fwd}	1400 V
di/dt	200 A/μs
dv/dt	200 V/μs
I_{pk}	1000 A
I_f	<1 A.

These SCR's were chosen as being the most rugged available for laboratory use while still exhibiting a range of characteristics which would permit operation at high enough field levels to interrupt a 1000-A discharge. The interrupter turn-off time that was possible with these SCR's was 2 μs.

There are SCR's which have much higher switching speeds (up to 5000 A/μs) and which would greatly reduce the turn-off time of the interrupter.

It should be noted that in some applications, the interrupter could be used in a hybrid circuit in parallel with a conventional "closing" switch (a switching device that can be closed to cause current to flow but which cannot be opened to interrupt the flow of current). The "closing" switch would carry the circuit current until interruption of the circuit is required. During an interruption event, the interrupter would be turned on, the circuit current would be commutated to the interrupter, the "closing" switch would be opened, and, finally, the interrupter would be opened. By using this hybrid circuit technique, depending on the application of the interrupter, the life could be substantially increased.

V. PROJECTED LIFE OF INTERRUPTER

The rate of consumption of the cathode has been shown to be about 10^{-7} kg/C of charge passed through the arc [12]. The time rate of use of cathode material, $\dot{M}$, is then

$$\dot{M} = I_{avg} \quad 10^{-7}$$

where I_{avg} is the average current through the interrupter. The life of the interrupter in hours is then simply

$$T = \frac{M_t}{3600\dot{M}} = 2.78 \times 10^3 \frac{M_t}{I_{avg}}$$

where M_t is the total mass in kilograms of the cathode that is consumed.

Relatively simple automatic feed mechanisms have been developed [13] to supply as much as several kilograms of cathode material to the arc. Lifetimes of several thousands of hours are projected for the interrupter when the average cathode current is less than a few amperes.

The pulsewidth of the interrupter has been varied from about two to several hundred microseconds (and, in theory, dc operation could be achieved with proper cooling). In the high-voltage interruption studies, the pulse repetititon frequency was limited to several pulses per second. In the lower voltage studies, however, up to 1000 pulses per second have been achieved. It is clear, therefore, that the range of duty cycles (pulsewidth times pulse repetition frequency) over which the interrupter is capable of operating is very broad. Unlike most electron devices, these factors along with the peak current of operation must be given careful consideration when the life of the interrupter in a particular application is of importance.

During operation of the interrupter, most of the material emitted by the cathode passes through the aperture in the anode and impinges in a metallic collector that is maintained at cathode potential. This material does not interfere with the operation of the interrupter. In fact, through the use of the proper materials, continuous evacuation of the interrupter can be achieved. A small fraction of the emitted material is deposited on the anode and on the field-coil structure. However, this has not impaired the operation of the interrupter. It has been necessary to shield insulators such as anode supports to prevent electrical breakdown along the surfaces.

VI. CONCLUSION

The major accomplishment described in this paper was the demonstration of switching at voltages up to 25 kV and at currents up to 800 A. Operation at this level at repetition frequencies of several pulses per second was demonstrated. At lower power levels, operation at a frequency of 1 kHz was achieved. It has been shown that the pulsewidth can be continuously varied from about 2 μs to infinity (dc operation). Turn-on and turn-off times in the microsecond range are possible. Operation at voltage levels above 25 kV was limited, not by the interrupter, but by the power supplies and other apparatus used for testing the interrupter. Immediate applications for the interrupter are in high-power modulators and inverters. With further development, the interruption of high-voltage dc transmission systems should be possible.

REFERENCES

[1] A. S. Gilmour, Jr., and R. J. Clark, Jr., "Studies on a laser-triggered, high-voltage, high-vacuum switch tube," *Proc. 3rd. Int. Symp. Discharge and Electrical Insulation in Vacuum*, pp. 367–372, Sept. 1968.
[2] A. S. Gilmour, Jr., R. J. Clark, Jr., and H. Veron, "Pulsed vacuum-arc microthrustors," AIAA Paper 67-737.
[3] D. L. Lockwood, H. Veron, R. J. Clark, Jr., and A. S. Gilmour, Jr., "Magnetically modulated vacuum-arc diode," Patent pending, 49473, 1967.
[4] G. A. Farrall, "Vacuum arcs and switching," *Proc. IEEE*, vol. 61, pp. 1113, Aug. 1973.
[5] A. E. Gile, "Arc electrode phenomena," *Proc. Inst. Elec. Eng.* vol. 118, pp. 1131–1154, Sept. 1971.
[6] A. Selzer, "Switching in vacuum: A review," *IEEE Spectrum*, vol. 8, pp. 26–37, June 1971.
[7] M. P. Reece, "The vacuum switch," *Proc. Inst. Elec. Eng.*, vol. 110, pp. 793–811, Apr. 1963.
[8] A. S. Gilmour, Jr. and D. L. Lockwood, "Pulsed metallic-plasma generators," *Proc. IEEE*, vol. 60, pp. 977–991, Aug. 1972.
[9] J. B. Cobine and G. A. Farrall, "Experimental study of arc stability—I," *J. Appl. Phys.*, vol. 31, pp. 2296–2304, Dec. 1960.
[10] H. Knoepfel, *Pulsed High Magnetic Fields*. Amsterdam, The Netherlands: North Holland Publishing Co., 1970.
[11] F. E. Gentry, F. W. Gutzwiller, Nick Holonyak, Jr., and E. E. Von Zastrow, *Semiconductor Controlled Rectifiers*. Englewood Cliffs, N. J.: Prentice-Hall, 1964.
[12] C. W. Kimblin, "Erosion and ionization in the cathode spot region of vacuum arcs," *J. Appl. Phys.*, vol. 44, no. 7, pp. 3074–3081, July 1973.
[13] A. S. Gilmour, Jr., J. R. Graham, D. L. Lockwood, R. J. Clark, Jr., and H. Veron, "Recent progress in pulsed vacuum-arc microthrustor research," AIAA Paper 68-555.

☆ U. S. GOVERNMENT PRINTING OFFICE: 1977 — 757-001/247